TECHNISCHE UNIVERSITÄT DARMSTADT

GEORG SPEYER HAUS
INSTITUT FÜR TUMORBIOLOGIE
UND EXPERIMENTELLE THERAPIE

Investigating the Oncogenic Function of FUBP1 in Glioblastoma Cell Lines

Von Fachbereich Biologie der Technischen Universität Darmstadt

Zur Erlangung des akademischen Grades

eines Doctor rerum naturalium

genehmigte Dissertation von

M.Sc. Venkatesh Kolluru

aus Visakhapatnam, India

1. Referent/ Referentin: Prof. Dr. B. Süß

2. Referent/Referentin: Prof. Dr. M. Zörnig

3. Referent/Referentin: Prof. Dr. A. Bertl

Tag der Einreichung: 11-02-15

Tag der mündlichen Prüfung: 23-03-15

Darmstadt 2015

D 17

Contents

Summary

Data obtained in our laboratory established FUBP1 (Fuse Binding Protein 1) as an important oncoprotein overexpressed in HCC (Hepatocellular Carcinoma) that induces tumor propagation through direct or indirect repression of cell cycle inhibitors and pro-apoptotic target genes. However, Prof. Kinzler's laboratory (Ludwig Center for Cancer Genetics and Howard Hughes Medical Institutions, USA) found that inactivating mutations in the genes *CIC* and *FUBP1* contribute to human oligodendroglioma. Their study enhanced our interest in investigating the expression levels of FUBP1 in different glioma cells. We detected low expression of FUBP1 in astrocytes and demonstrated elevated levels of FUBP1 in glioblastoma, the most common malignant brain tumor in humans. Among the challenges in the treatment of glioblastoma are the frequency of recurrence, the aggressiveness and the infiltrative behavior of the tumor. In contrast to oligodendroglioma, glioblastoma seem to require significant FUBP1 levels.

The glioblastoma cell lines LNT229 and U87-MG were used to explore the oncogenic function of FUBP1 in glioblastoma, and further functional assays were performed. The results from the proliferation and apoptosis assays revealed less proliferation and more apoptosis in LNT229 *FUBP1* knockdown cells, which co-relates with results obtained with HCC cell lines. In contrast to LNT229, U87-MG cells showed more proliferation and less apoptosis upon *FUBP1* knockdown. Interestingly, *FUBP1*-deficient U87-MG cells showed enhanced xenograft tumor growth. Affymetrix array results revealed a significant upregulation of pro-apoptotic genes in *FUBP1* knockdown LNT229 cells in contrast to *FUBP1* knockdown U87-MG cells. In the latter, pro-proliferative and pro-angiogenic genes were significantly upregulated. qRT-PCR analysis showed a significant increase in *TGFβ-1*, *MMP2* and *AKT* in U87-MG *FUBP1*-deficient cells while these genes were downregulated in LNT229 FUBP1-deficient cells. Interestingly, the knockdown of *MMP2* in U87-MG cells led to a significant increase in FUBP1 protein levels. Further, *APAF-1* mRNA levels were investigated in LNT229 and U87-MG cells. To our surprise, *APAF1* levels were high in *FUBP1*-deficient LNT229 cells compared to control LNT229 cells. However, we detected no change in *APAF1* levels between control and *FUBP1*-deficient U87-MG cells. We speculate that different signaling pathways are activated in LNT229 and U87-MG cells upon *FUBP1* knockdown. Therefore, we hypothesize that FUBP1 might fulfill a special important function as an oncogene in glioblastomas which might differ from its role in HCC.

Zusammenfassung

Das Far Upstream Binding Protein 1 (FUBP1) wurde in unserer Arbeitsgruppe als ein wichtiges Onkoprotein im Hepatozellulären Karzinom (HCC) identifiziert. Es konnte gezeigt werden, dass es in über 90% aller HCCs überexprimiert wird und die Tumorentwicklung durch direkte und indirekte Regulierung von Zellzyklus-Inhibitoren sowie pro-apoptotischen Zielgenen positiv beeinflusst. Die Gruppe von Prof. Kinzler (Ludwig Center for Cancer Genetics and Howard Hughes Medical Institutions, USA) hat interessanteweise herausgefunden, dass die Gene *CIC* und *FUBP1* in Oligodendrogliomen durch geringe Mutationen inaktiviert sindwasauf eine Tumor-suppressor-function von FUBP1 in dieser Tumor-entität hinweisen könnte. Bei der Untersuchung von Gliomzellen konnten wir eine geringe Expression von FUBP1 in Astrozyten feststellen und ein hohes FUBP1-Level in Glioblastomzellen. Das Glioblastom ist ein sehr aggressiver Hirntumor mit einer sehr hohen Rückfallquote, der vor allem durch sein infiltratives Wachstum charakterisiert wird. Im Vergleich zu dem weniger aggressiven Oligodendrogliom scheint im Glioblastom eine höhre FUBP1-Expression benötigt zu werden.

In dieser Arbeit sollte die onkogene Funktion von FUBP1 in den beiden Glioblastom-Zelllinien LNT229 und U87-MG untersucht werden. Proliferations- und Apoptose-Analysen in LNT229 *FUBP1*-knockdown Zellen zeigten eine verringerte Proliferations- und eine erhöhte Apoptoserate, was mit den Ergebnissen im HCC korreliert. Im Gegensatz dazu wurde in den U87-MG Zellen eine erhöhte Proliferationsrate und eine erhöhte Apoptoseresistenz nach der Herrunter-Regulation von FUBP1 beobachtet. Zusätzlich zeigte sich in einem Maus-Xenograft Experiment mit FUBP1-defizienten U87-MG Zellen ein stärkeres Tumorwachstum im Vergleich zu U87-MG Kontrollzellen mit normaler FUBP1-Expression. Eine genomweite Expressionsanalyse der Zellen ergab, dass durch die Inhibierung von FUBP1 in den LNT229 Zellen pro-apoptotische Gene hochreguliert werden, während bei den FUBP1-defizienten U87-MG Zellen pro-proliferative und pro-angiogenetische Gene signifikant erhöht waren. Die mRNA Analyse mittels qRT-PCR zeigte einen signifikanten Anstieg an *TGFβ-1*, *MMP2* und *AKT* in U87-MG FUBP1-defizienten Zellen, während diese Gene in LNT229 *FUBP1*-defizienten Zellen herunterreguliert waren. Des Weiteren konnte der Anstieg von FUBP1 nach Herunterregulation von MMP2 in U87-MG Zellen gezeigt werden. Zusätzlich wurde beobachtet, dass das pro-apoptotische Adapterprotein APAF-1 in FUBP1-defizienten LNT229 Zellen im Vergleich zu LNT229-

Kontrollzellen hoch expremiert wurde, während es keinen Unterschied zwischen FUBP1-defizienten U87-MG und Kontrollzellen gab.

Demzufolge nehmen wir an, dass die Inhibierung von FUBP1 in diesen beiden Zelllinien zur Aktivierung unterschiedlicher Signalwege führt, und dass FUBP1 in Gehirntumoren eine Rolle spielen könnte, die sich von der im HCC unterscheidet

1. Introduction

1.1 Far Upstream Element (FUSE) Binding Protein 1

The far upstream element (FUSE) binding protein 1 (FUBP1) was originally found to bind to the approx. 40 base pair long DNA sequence motif *FUSE*, which is located for example 1.5 kb upstream of the transcriptional start site of the *c-myc* p2 promoter. Experiments revealed that the transcriptional regulator FUBP1 enhances *c-myc* promoter activity (Duncan, Bazar et al. 1994). Furthermore, the activity of the *c-myc* promoter was reduced upon mutations in the *FUSE* element (Avigan, Strober et al. 1990).

1.1.1 FUBP family members and their domain structure

The human *FUBP1* gene encodes a 644-amino acid protein, with a molecular mass of 67.5 kDa, which consist of three domains (Figure 1): the N-terminal repression domain (1-106 aa), the C-terminal transactivation domain (with tyrosin-rich motifs) and the central DNA binding domain (107-447 aa), built of four conserved K-homology (KH) motifs (Duncan, Bazar et al. 1994, Davis-Smyth, Duncan et al. 1996). The KH motifs were first identified within the heterogenous nuclear ribonucleoprotein K (hnRNPK) (Valverde, Edwards et al. 2008), and they assist in the binding to single stranded DNA. In an inactive state, the C-terminal transactivation domain of FUBP1 is repressed by the N-terminal domain (Davis-Smyth, Duncan et al. 1996). The mechanism of activation, leading to conformational changes of FUBP1 and thereby dissolving the enclosed conformation of the inactive protein, is not well studied (Zhang and Chen 2013). However, in the active state, the C-terminal transactivation domain is responsible for the function of FUBP1 as a transcriptional regulator (Davis-Smyth, Duncan et al. 1996). The interaction between FUBP1 and the transcription factor TFIIH (consisting of 9 different proteins) is aided by the three tyrosine rich-motifs of the C-terminal transactivation domain (Liu, Akoulitchev et al. 2001). Three nuclear localization signals (NLS) ensure the nuclear localization of the protein.

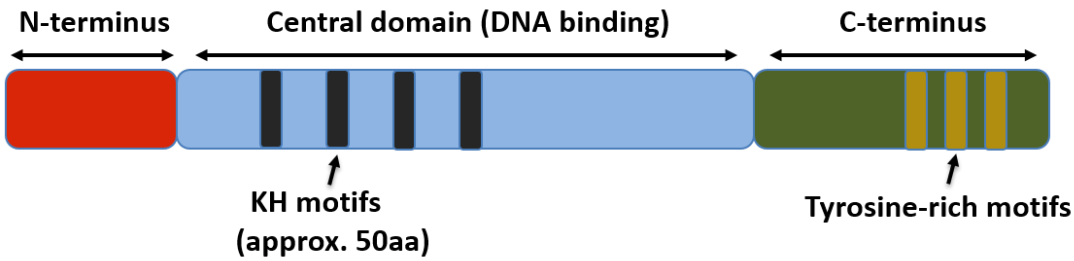

Figure 1: Structure of the FUBP1 protein

FUBP1 is structured into three domains: an N-terminal repression domain, a central single stranded nucleotide binding domain (consisting of four KH motifs) and a C-terminal transactivation domain (containing three tyrosine-rich motifs) (Michelotti, Michelotti et al. 1996).

Two genes (*FUBP2* and *FUBP3*) with high similarity to *FUBP1* were identified. FUBP2 is also known as K-homology splicing regulator protein (KHSRP). The overall amino acid sequence of FUBP1 shows a homology of 63.6% with FUBP2 and 56.6% with FUBP3. Moreover, the highest conservation (~80%) is observed in the central binding domain (Davis-Smyth, Duncan et al. 1996). Nevertheless, *FUBP2* and *FUBP3* are localized on different chromosomes (Chr. 19 and 9, respectively) compared to *FUBP1* (Bouchireb and Clark 1999). The role of FUBP2 in stabilization, degradation, splicing and trafficking of mRNA is well studied (Gherzi, Lee et al. 2004). The activation potential of the C-terminal transactivation domain is strongest in FUBP3, moderate in FUBP1 and weakest in FUBP2. The functional differences in the N-terminal repression domain influence the interaction of FUBP1/2/3 with the antagonistic FUBP-interacting repressor (FIR). FUBP3 is not capable to interact with FIR, in contrast to FUBP1 and FUBP2 (Chung, Liu et al. 2006).

1.1.2 Functions of FUBP1

FUBP1 is known to transcriptionally activate the *c-myc*-promoter. c-Myc is involved in cell cycle progression and apoptosis, subsequently implying a potential role of FUBP1 in the above mentioned processes. Different studies state and have confirmed the potential role of FUBP1 in diverse cell fate decisions. Upon *FUBP1* knockdown, decreased cell proliferation in U2OS and Saos-2 osteosarcoma cell lines (He, Weber et al. 2000) was observed due to reduced *c-myc* expression. Furthermore, upon induction of differentiation in HL-60 and U937 leukemia cells, FUBP1 levels were decreased and c-Myc expression vanished (Avigan, Strober et al. 1990).

All FUBP family members possess the KH domains, which are important for the binding of single stranded DNA or RNA (Valverde, Edwards et al. 2008). Although the underlying mechanism is not well studied, FUBP1 seems to be involved in the regulation of neuronal differentiation, viral replication, cell growth and cell cycle progression. It was also observed that FUBP1 influences the hematopoietic stem cell self-renewal during definitive hematopoiesis, most certainly by regulating cellular proliferation and apoptosis (Katharina Gerlach, AG Zörnig; un-published data).

1.1.3 Molecular function of FUBP1

"Traditional" transcription factors commonly bind to double-stranded rather than single-stranded DNA. The basal transcription of the *c-myc* gene is hardly influenced by FUBP1; instead, FUBP1 promotes the maximum level of *c-myc* transcription, as described in the following passage. Upon serum addition, basal transcription of *c-myc* starts, leading to torsional stress and unwinding of DNA. Due to melting of the double-stranded DNA, the AT-rich *FUSE* element is exposed in its single stranded conformation (Duncan, Bazar et al. 1994), thereby enabling the binding of FUBP1. However, FUBP1 substitutes FUBP3 by an unknown mechanism, and *c-Myc* mRNA expression increase exponentially. FUBP1 causes the looping of DNA in the promoter region and interacts with the common transcription factor TFIIH, thereby enhancing its helicase activity. TFIIH is important for promoter clearance by RNA Polymerase II (Maxon, Goodrich et al. 1994), and upon FUBP1 binding increases its activity on the *c-myc* promoter, allowing full scale *c-myc* transcription (Michelotti, Michelotti et al. 1996). Two hours after serum addition, a maximum of *c-myc* transcription is observed. Upon binding of the antagonist FIR, a triple complex consisting of *FUSE*, FIR and FUBP1 is formed. Eventually, FIR replaces FUBP1, and *c-myc* peak expression is reduced to basal levels. The important interplay between FUBP1, *FUSE*, FIR and TFIIH (Figure 2), as well as TFIIH, allows the precise control of the *c-myc* promoter and the exponential increase and decrease of c-myc mRNA expression in the G1 phase of the cell cycle.

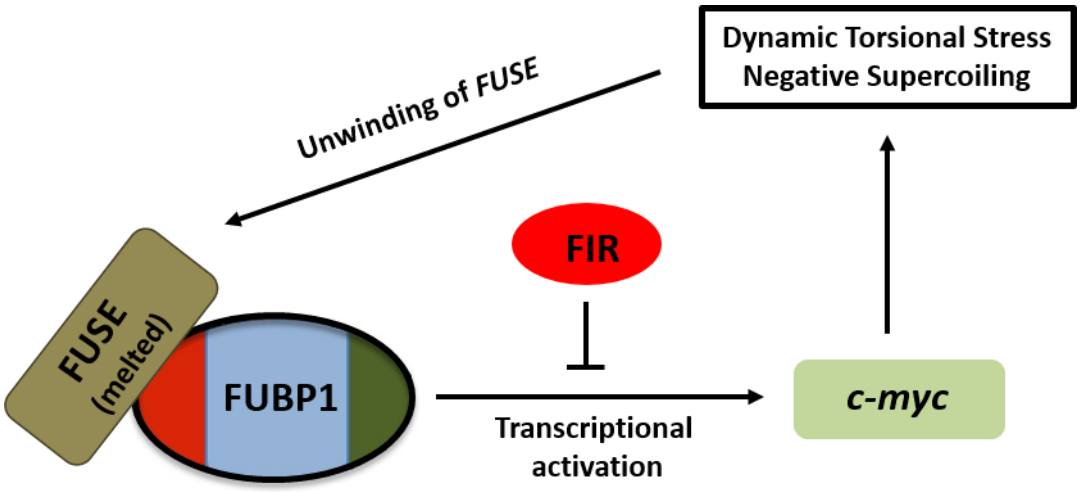

Figure 2: Schematic overview of the interplay between *FUSE*, FUBP1 and FIR during regulation of *c-myc* transcription

Basal transcription at the c-myc promotor leads to negative supercoiling of the DNA upstream of the promoter region. Melted *FUSE* sequence facilitates the binding of FUBP1 protein, which mediates a steep increase in c-myc transcription. Eventually, binding of FIR to *FUSE* and FUBP1 leads to termination of *c-myc* expression back to basal levels (Hsiao, Nath et al. 2010).

1.1.4 FUBP1 as a Cancer Biomarker

Because FUBP1 upregulates *c-myc* mRNA expression and facilitates pro-oncogenic functions, its expression is increased in many cancer types (see Table 1, (Zhang and Chen 2013)). As another suggested mode of oncogenic action, FUBP1 promotes the replication of HCV, a virus which causes hepatocellular carcinoma (Zhang, Harris et al. 2008).

In colorectal cancer patients, a splicing variant of FIR was found, which lacked the N-terminus and was therefore unable to inhibit FUBP1 activity. This splicing variant exhibits dominant negative effects compared to functional wildtype FIR and is only found in colorectal cancer tissue, indicating a potential role in colorectal carcinogenesis (Matsushita, Tomonaga et al. 2006, Matsushita, Kajiwara et al. 2009).

Studies in clear cell renal cell carcinoma (ccRCC) showed a correlation between elevated FUBP1 and *c-myc* levels, indicating that FUBP1 facilitates oncogenic functions (Weber, Kristiansen et al. 2008). The high/over expression of FUBP1 in cancer cells compared to normal tissue suggest FUBP1 as a potent onco-protien and cancer biomarker.

Table 1: FUBP1 expression in different cancers entities (Zhang and Chen 2013)

Malignancy	Alterations	Downstream Target	Reference
Oligodendrioglioma	FUBP1 mutational inactivation	NA	(Bettegowda, Agrawal et al. 2011)
Non-small lung cancer	FUBP1 ↑	*Stathmin 1* ↑	(Singer, Malz et al. 2009)
Breast	FUBP1 ↑	NA	(Lasserre, Fack et al. 2009, Xu, Yan et al. 2010)
Clear cell renal cancer	FUBP1 ↑	*c-myc* ↑	(Weber, Kristiansen et al. 2008)
Liver	FUBP1 ↑	*p21* ↑, *p15* ↑, *Cyclin D2* ↑	(Zubaidah, Tan et al. 2008, Rabenhorst, Beinoraviciute-Kellner et al. 2009)
Liver	FUBP1 ↑	*Stathmin 1* ↑	(Zubaidah, Tan et al. 2008, Malz, Weber et al. 2009)
Bladder	FUBP1 ↑	NA	(Weber, Kristiansen et al. 2008)
Prostate	FUBP1 ↑	NA	(Weber, Kristiansen et al. 2008)
Colon	FIR truncation	*c-myc* ↑	(Matsushita, Tomonaga et al. 2006, Matsushita, Kajiwara et al. 2009)

NA: not available

1.2 Role of FUBP1 in Gliomas

Gliomas denote the most frequent cancer of the central nervous system (CNS), accounting for about 80 % of all malignant primary brain and CNS tumors (Hinsdale 2011). Gliomas are defined as tumors derived from glial cells and include tumors of astrocytic, oligodendrial, ependymal, or mixed origin. Based on histological appearance, the World Health Organization (WHO) classifies the different types of gliomas into prognostic grades ranging from I to IV (Louis, Ohgaki et al. 2007). The most malignant astrocytic glioma, glioblastoma multiforme (WHO grade IV), constitutes more than 50 % of all gliomas and is the most common malignant primary brain tumor (Hinsdale 2011). Even though glioblastoma multiforme is a quite rare tumor with a global incidence rate of only 3.17 per 100,000 (Hinsdale 2010), it significantly impacts the life of the affected patients due to its poor prognosis with a median survival time of only 12-15 months from the time of diagnosis (Stupp, Mason et al. 2005).

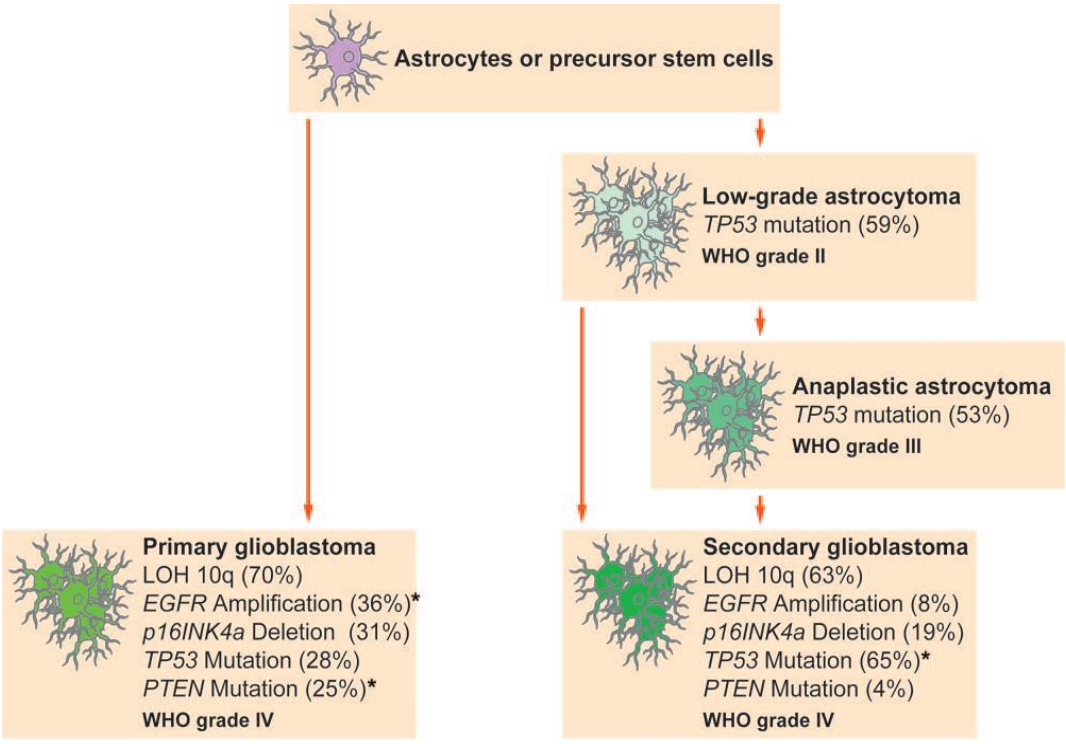

Figure 3: De novo vs Secondary GBM genetic pathways.

A classification of brain tumors that is based on their cell-of-origin according to WHO grade. The molecular and genetic changes along the percentages of their possible occurrence for the onset of the disease is being described (Ohgaki and Kleihues 2007).

1.2.1 Astrocytomas

Diffuse astrocytomas are comprised of tumor cells with histological characteristics of astrocytes and they present the most common type of all gliomas. They account for 60% of all primary brain tumors. The subtypes according to malignancy are diffuse astrocytomas (AII, WHO grade II), anaplastic astrocytomas (AA, WHO grade III) and glioblastoma multiforme (GBM, WHO grade IV), whereby glioblastomas are the most common astrocytoma subtype (Figure 3) (Louis, Ohgaki et al. 2007). Diagnosis of astrocytomas is based upon histological findings of fibrillary or gemistocytic neoplastic astrocytes with specific nuclear characteristics, surrounded by a loosely structured tumor matrix. The astrocytic nucleus is elongated and often has a distinct nucleolus. Astrocytes have more extensive cellular processes than oligodendrocytes. In addition, increased cellularity and the presence of significant mitotic activity upgrades the tumor to an anaplastic astrocytoma grade III. Anaplastic astrocytomas can progress from a diffuse astrocytoma grade II but may also arise *de novo*, i.e. without a less malignant precursor lesion. Additional features such as cellular pleomorphism, vascular thrombosis, microvascular proliferation and/or necrosis are diagnostic for a glioblastoma, grade IV. Most glioblastomas (>90%) arise rapidly *de novo* and are called primary glioblastomas. Secondary glioblastomas develop from a previously diagnosed diffuse astrocytoma grade II or anaplastic astrocytoma grade III. It is believed that the progression from a low grade to a high-grade tumor is associated with cumulative genetic alterations.

1.2.2 Oligodendroglioma

Oligodendrogliomas are composed of tumor cells with histological characteristics of oligodendrocytes. The two subtypes described in the literature are oligodendroglioma (OII, WHO grade II) and anaplastic oligodendroglioma (AO, WHO grade III). Mostly middle-aged adults are diagnosed with oligodendroglioma. In general, oligodendroglioma are slowly dividing, with relatively long survival times for the patients. Oligodendrogliomas classified as grade II are well differentiated and slowly dividing rounded cells consisting of homogenous slightly enlarged nuclei with increased chromatin density.

Recently, novel somatic mutations have been identified in oligodendroglioma which represents the second most common primary neuro-epithelial human brain

tumor (Bettegowda, Agrawal et al. 2011). Several mutations are located in the *FUBP1* gene and have been detected in 10-15% of all oligodendroglioma patients. In contrast to other mutations associated with oligodendroglioma such as *IDH1*, no hot-spot codon for FUBP1 mutations has been identified (Hartmann, Meyer et al. 2009, Sahm, Koelsche et al. 2012). Genetic analysis revealed that all the mutations result in inactivation of the encoded protein, as the mutations result in either deletions or nonsense sequences (Bettegowda, Agrawal et al. 2011). However, the function of the FUBP1 protein in the normal and neoplastic human brain is poorly understood.

1.2.3 Glioblastoma

Glioblastoma (GBM) is the most common primary brain tumor and accounts for over fifty-one percent of all gliomas (Adamson, Kanu et al. 2009). Over 13,000 deaths are recognised to gliomas annually, and approximately 18,000 new cases are diagnosed each year (Schwartzbaum, Fisher et al. 2006). As with many types of cancer, increasing age correlates with incidence; the average age of incidence of primary GBM is 62 years (Adamson, Kanu et al. 2009). GBM rarely affects children and only accounts for 8.8 percent of childhood brain tumors. Glioblastoma occurs in both men and women, however, primary GBM occurs more frequently in males while secondary GBM occurs more frequently in females (Schwartzbaum, Fisher et al. 2006). Although there are several treatments available for GBM including surgical resection, chemotherapy, and radiation, prognosis remains depressing. The average survival time following diagnosis of GBM patients is only 14 months (adapted from American Brain Tumor Association) and the five-year survival rate of GBM is only ten percent. For comparison, another aggressive cancer, small cell lung carcinoma, has a median survival of twenty months and a five-year survival of twenty percent (adapted from National Cancer Institute). Current research in GBM concentrates on the development of new, targeted therapies for potential cure. As with all cancers, assessing possible risk factors remains a major focus of disease prevention.

The World Health Organization (WHO) characterizes GBM as a grade IV tumor (Kelly, Kirkwood et al. 1984). GBM can present as either a primary or a secondary tumor, when the primary GBM has spread to another part of the brain. Primary tumors are more aggressive with lower survival rates than secondary tumors (American Brain Tumor Association).

Common pathologic characteristics of GBM include hyper-chromatic nuclei and the presence of necrotic tissue (Adamson, Kanu et al. 2009). Diffuse margins and microvascular proliferation allow GBMs to easily grow and metastasize. Tumors with diffuse margins more readily invade surrounding cerebral tissue which makes complete surgical resection difficult.

The pathology of GBM is intrinsically linked to the molecular basis of this deadly disease. Many different molecular pathway mutations and genetic abnormalities can lead to gliomagenesis. The combination of several different onco-genomic events contributes to GBM development and therefore, the exact molecular cause of GBM is difficult to decode. The most common and frequent mutations and molecular causes of GBM are listed in Table 2.

Table 2: Molecular causes and genetic changes for GBM occurrence (Kanu, Hughes et al. 2009).

Molecular causes of GBM	
CAUSE	**% INCIDANCE**
Deletion of chromosome 10	70%
EGFR amplification	40%-60%
P16INK4a deletion	30%
P14ARF mutation	30%
P53 mutation	30%
PTEN mutation	25%
RB1 methylated	15%
MGMT methylated	36%

Standard treatment for GBM patients includes surgical resection, chemotherapy, and radiation therapy. Surgical resection is performed with the intent for a complete removal of the GBM tumor. If a complete resection is impossible due to the location of the tumor, a partial resection may be performed; however, partial resection is associated with significantly lower survival rates. While there are many different chemotherapeutic agents available for the treatment of GBM, the current standard chemotherapy used is Temozolomide, or Temodar. Temozolomide is an oral alkylating agent, and inhibits DNA repair mechanisms in tumor cells (American Brain Tumor Association).

1.3 Extracellular matrix proteins

The extracellular matrix (ECM) is the non-cellular component present in all tissues and organs, and provides essential support for the cellular constituents. Additionally, it also initiates crucial biochemical and biomechanical help which is required for tissue morphogenesis, differentiation and homeostasis (Jarvelainen, Sainio et al. 2009). Fundamentally, the ECM is composed of water, proteins and polysaccharides, each tissue has an ECM with a unique composition and topology that is generated during tissue development through a dynamic and reciprocal, biochemical and biophysical exchange between the various cellular components (e.g. epithelial, fibroblast, adipocyte, endothelial elements) and the evolving cellular and protein microenvironment. Cell adhesion to the ECM is mediated by ECM receptors, such as integrins, discoidin domain receptors and syndecans (Leitinger and Hohenester 2007, Harburger and Calderwood 2009). Adhesion mediates cytoskeletal coupling to the ECM and is involved in cell migration through the ECM (Schmidt and Friedl 2010).

The ECM is composed of two main classes of macromolecules: proteoglycans (PGs) and fibrous proteins (Table 3). The main fibrous ECM proteins are collagens, elastins, fibronectins and laminins (Hoglund, Odelius et al. 2007). PGs have a wide variety of functions that reflect their unique buffering, hydration, binding and force-resistance properties.

Collagen is the most abundant fibrous protein within the interstitial ECM and constitutes up to 30% of the total protein mass of a multicellular animal. Collagens, which constitute the main structural element of the ECM, provide tensile strength, regulate cell adhesion, support chemotaxis and migration, and direct tissue development (Rozario and DeSimone 2010).

Fibronectin (FN) is intimately involved in directing the organization of the interstitial ECM and, additionally, has a crucial role in mediating cell attachment and function. FN is also important for cell migration during development and has been implicated in cardiovascular disease and tumor metastasis (Rozario and DeSimone 2010, Tsang, Cheung et al. 2010).

Matrix metalloproteinases (MMPs) are a large family of calcium-dependent zinc-containing endopeptidases, which are responsible for the tissue remodeling and degradation of the extracellular matrix (ECM), including collagens, elastins, gelatin, matrix glycoproteins, and proteoglycan. MMPs are usually minimally expressed in normal physiological conditions and thus homeostasis is maintained. Over-

expression of MMPs results in an imbalance between the activity of MMPs and TIMPs that can lead to a variety of pathological disorders (Aranapakam, Grosu et al. 2003, Venkatesan, Davis et al. 2004, Raspollini, Castiglione et al. 2005). MMPs have now been considered as a promising target for cancer therapy and a large number of synthetic and natural MMP inhibitors (MMPIs) have been identified as cytostatic and anti-angiogenic agents, and have begun to undergo clinical trials in view of their specific implication in malignant tissues.

There are 25 known MMP genes in humans, and many of these are involved in cancer (Rao 2003). MMP expression is induced by cytokines, growth factors, tumor promoters, physical stress, oncogenic transformation, and cell-matrix and cell-cell interaction (Rao 2003). They are regulated in a variety of ways including gene expression, pro-enzyme activation, and inhibition through specific tissue inhibitors (TIMPs) (Brew, Dinakarpandian et al. 2000). MMPs are responsible for tumor invasion by degrading ECM proteins and releasing the growth factors to activate signal transduction cascades which promote migration (McCawley and Matrisian 2001). MMP-2 and MMP-9 are predominantly involved in glioblastoma, and their mRNA and protein expression levels are higher in GBM patient biopsy tissue (Rao, Steck et al. 1993). Both of these MMPs are involved in GBM proliferation and migration through the activation of transforming growth factor beta- 1 (TGFβ-1). MMP-9 and MMP-2 promote GBM invasion in vitro and in xenograft models (McCawley and Matrisian 2001, Bellail, Hunter et al. 2004) and their inhibition dramatically reduces the invasive phenotype.

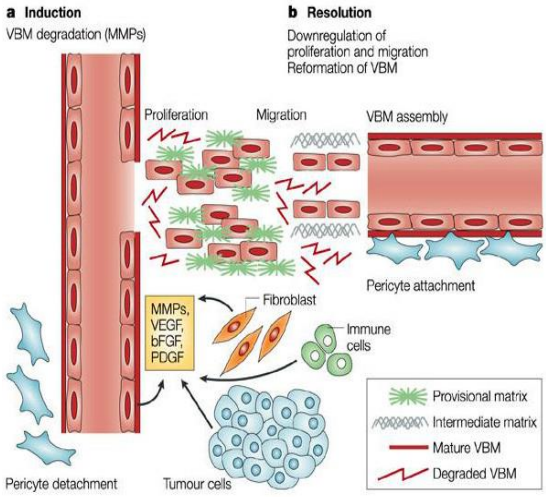

Figure 4: Schematic representation of MMPs and their role in proliferation and migration of the tumor cells.

The proteolytic degradation of the vascular basement membrane (VBM) is mediated by proteases, such as the matrix metalloproteases (MMPs), secreted by tumor and stromal cells. MMPs play an important role in human brain tumor invasion, migration and proliferation (Uhm, Dooley et al. 1997).

The developing fetal brain shows characteristics similar to that of the GBM, defined by elevated levels of fibrous ECM proteins. This is in contrast to the mature adult brain, which shows significantly lower expression of the same ECM proteins (Ruoslahti 1996). The fetal brain ECM contains elevated levels of the fibrous proteins, fibronectin, laminin, vitronectin and collagen (Mahesparan, Read et al. 2003). The most abundant brain protein hyaluronan (HA) has also been shown to be elevated in the matrices of gliomas, similar to what is seen for the embryonic brain matrix (Ulrich, de Juan Pardo et al. 2009).

Table 3: Expression of ECM proteins/molecules in normal brain and gliomas (Delpech, Maingonnat et al. 1993, Tysnes, Mahesparan et al. 1999).

Molecules	Abundance		Function
	Normal Brain	**Glioma**	
Hyaluronic Acid (HA) Proteoglycan (PG)	↑ ↑	↑↑↑ ↑↑↑	**HA**: space filling molecule, regulates cell proliferation, adhesion and motility. **PG**: HA binding proteins
Fibrous Proteins ▪ Vitronectin ▪ Fibronectin ▪ Laminin ▪ Collagen IV	Found in trace amounts along brain vasculature and basement membrane.	 ↑↑↑ ↑↑↑ ↑↑↑ ↑↑↑	**Fibrous Proteins:** structural elements of the connective tissue in the basement membrane of blood vessels of the normal brain and gliomas, in high grade gliomas they are also expressed and secreted by glioma cells.
Matrix metalloproteinase (MMPs)	↑	↑↑↑	**MMPs**: Molecules that aid in the breakdown of the basement membrane during the ECM remodelling; MMP2, MMP9

1.4 MicroRNA synthesis and functions

MicroRNAs (miRNAs) are 20–22 nucleotides long noncoding RNAs that are important regulators of gene expression and were first described in 1993 (Lee, Feinbaum et al. 1993). MiRNAs play an important role in diverse cellular processes including development, immunity, cell-cycle control, metabolism, viral or bacterial disease, stem-cell differentiation, and oncogenesis (Ambros 2004, Bala, Marcos et al. 2009). In general, miRNAs are transcribed from RNA polymerase II or III in the nucleus and transported to the cytoplasm, where they are processed into mature miRNAs (Bartel 2009). Mature miRNAs can target hundreds of genes by

either binding to the 3' or 5' untranslated (UTR) region of mRNA (Bartel 2009). Pri-miRNAs are cleaved into precursor miRNAs (pre-miRNAs) of about 50-150 nucleotides by Drosha, an endoribonuclease III (RNAse III), and its cofactor RNA-binding protein pasha (DGCR8). These pre-miRNAs are then exported to the cytoplasm by exportin 5. This is further excised to double-stranded duplexes of 20–23 nucleotides by Dicer, an RNAse III enzyme. The miRNA duplex later separates into single-stranded mature miRNA, and incorporates into the RNA-induced silencing complex (RISC), which is composed of Argonaute proteins. This complex further binds to the 3′-untranslated region (3′-UTR) of its target transcript and negatively regulates protein translation by a mechanism that depends on the complementarity between the miRNA and target messenger RNA. Partial complementarity results in translational repression, while complete complementarity triggers mRNA degradation (Figure 5).

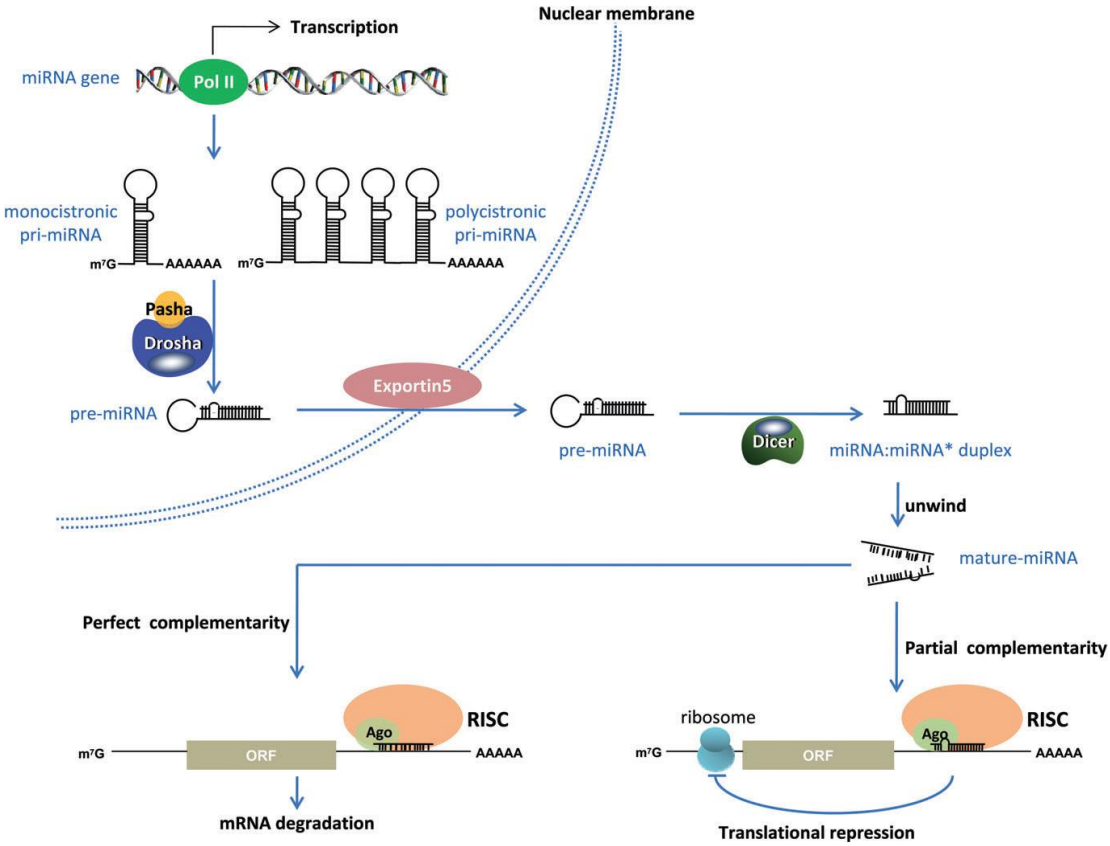

Figure 5: Schematic representation of Micro-RNA Biogenesis.

In the nucleus, miRNAs are transcribed by Pol II. Pri-miRNAs are cleaved by Drosha and Pasha to pre-miRNAs that are exported to the cytoplasm by exportin 5. In the cytoplasam, pre-miRNAs are excised from a double-stranded miRNA: miRNA* duplex of 20-23 nucleotides by Dicer. The miRNA duplex unwinds to single-stranded mature miRNA and is incorporated into the RISC complex, which is composed of Argonaute proteins. The miRNA/RISC complex binds to the 3'-UTR of target cellular gene and negatively regulates gene expression. Perfect complementarity triggers mRNA degradation, while partial complementarity results in translational repression (Law and Wong 2011).

Studies suggest that miRNAs not only target mRNAs but are also capable of modulating transcription and methylation processes (Sinkkonen, Hugenschmidt et al. 2008, Sato, Tsuchiya et al. 2011). An important feature of miRNAs is that a single miRNA can regulate multiple target mRNAs. This property of miRNAs enables them to exert a wide control on a network of genes. Previous studies state that overexpression of a single miRNA can downregulate over 100 mRNAs (Lim, Lau et al. 2005). Therefore, it is not surprising that miRNAs are involved in diverse physiological and developmental processes. In a short time, miRNA research has received tremendous attention due to the fine-tuning roles of miRNAs in most biological pathways. Moreover, disease-specific tissue miRNA signatures have been identified in various diseases such as hepatocellular carcinoma (HCC), hepatitis C virus (HCV), hepatitis B virus (HBV), cardiac disease, neuro-inflammation, rheumatic arthritis (RA), and various cancers (Budhu, Jia et al. 2008, Bala, Marcos et al. 2009, Maes, Chertkow et al. 2009, Nakasa, Nagata et al. 2011, Qu, Zhang et al. 2011).

1.4.1 Role of miRNAs in HCC

Hepatocellular carcinoma (HCC) is the sixth most common malignancy and the third-leading cause of cancer-related death in the world (Forner, Llovet et al. 2012). The frequency of HCC is increasing in many parts of the world. The overall survival rate is 5–9% from the time of clinical diagnosis of HCC, and the prognosis is largely caused by late detection of the tumors (Poon and Fan 2004, Schwartz, Roayaie et al. 2007). Although the 5-year survival is better for patients who undergo curative resection if the tumor is detected early, these patients still have a high rate of recurrence (Yuen, Cheng et al. 2000, Fukuda, Itamoto et al. 2005). Hepato-carcinogenesis is closely associated with chronic hepatitis B virus (HBV) and hepatitis C virus (HCV) infections (Yu and Chen 1994, Hung, Chen et al. 2013). More than 90% of HCC cases develop in chronically inflamed liver as a result of viral hepatitis and alcohol abuse and in increasing incidence in patients with non-alcoholic fatty liver disease (Welzel, Graubard et al. 2011). Still the underlying molecular pathogenesis is not completely understood.

HCC is pathologically and clinically a heterogeneous disease. The prognosis depends on the aggressiveness of the HCC and residual liver function (Bruix, Sherman et al. 2011). The progression of HCC is thought to involve the

deregulation of genes that are critical to cellular processes such as cell cycle control, cell growth, apoptosis, and cell migration and spreading. Previous studies have focused on investigating the genes and proteins essential for the development of HCC (Aravalli, Steer et al. 2008, Huang and He 2011). Recent reports identify microRNAs that are implicated in HCC development and progression. Various miRNAs were deregulated or aberrantly expressed in human HCC (Table 4) (Otsuka, Kishikawa et al. 2014). In most cases, HCC originates on a background of cirrhosis, a chronic and diffuse hepatic disease that results from continuous liver injury and regeneration, due to different factors. Different etiologies of HCC play a role in the different miRNA expression profiles.

Table 4: miRNAs regulated in HCC (Otsuka, Kishikawa et al. 2014).

miRNAs	Molecular alteration	Targets	Characteristics
miR-10a	Upregulated	EphA4, CADM1	EMT, metastasis
miR-17-5p	Upregulated	p38 pathway	Multiple tumor nodules, vein invasion, shortened overall survival
miR-18a	Upregulated	ER1a	Poor prognosis, poor differentiation, proliferation
miR-18b	Upregulated	TIMP3	Cell growth; tumorigenesis; metastasis
miR-21	Upregulated	C/EBPb, RhoB, PDCD4, PTEN	Drugresistance, metastasis
miR-23a	Upregulated	PGC-1a,G6PC	Gluconeogenesis
miR-143	Upregulated	FNDC3B	Metastasis
miR-155	Upregulated	SOCS1, DKK1, APC, PTEN	High recurrence and poor prognosis following OLT, proliferation, tumorigenesis
miR-210	Upregulated	VMP1, AIFM3	Metastasis; apoptosis; proliferation

let-7 a,b,c,d,f,g	Downregulated	STAT3	Apoptosis, proliferation, earlyrecurrence
miR-1	Downregulated	ET1	Proliferation
miR-7a	Downregulated	PIK3CD, Caspase-3, HMGA2, C-myc, BCL-Xl	Proliferation, apoptosis, tumorigenesis, metastasis
miR-26a/b	Downregulated	IL-6, CyclinD2, E2	Poor survival
miR-199a/b-3p	Downregulated	PAK4, c-Met, mTOR, DDR1, caveolin-2	Reduced time to recurrence, poor overall survival and progression-free survival rates, proliferation, autophagy, metastasis
miR-200a	Downregulated	HDAC4	Proliferation, metastasis

miRNAs represent promising diagnostic markers of HCC. In fact, miRNAs are stable in human serum/plasma once they are released from cancer cells. Studies have shown that circulating miRNAs are resistant to RNAse activity and extreme pH and temperature (Chen, Ba et al. 2008, Mitchell, Parkin et al. 2008). However, even though a number of HCC-associated miRNAs have been identified, only few of them are validated to assist in diagnosis of HCC. Inhibiting or overexpressing miRNAs have been considered as novel strategy in cancer therapy for HCC. In fact, the discovery of miRNAs as an important player in the development and progression of HCC has implied that miRNAs can be used as therapeutic targets.

The complexity of miRNA biology offers novel mechanisms of action for therapeutics but at the same time poses unique challenges for the development of therapeutic drugs. The therapeutic application of miRNAs involves two strategies. The first aims to inhibit oncogenic miRNAs by using miRNA antagonists, such as antimiRs, locked nucleic acids (LNAs) or antagomiRs (Krutzfeldt, Kuwajima et al. 2007). MicroRNA antagonists are single-stranded RNA molecules, approximately 21–23 nt long, that act through complementary base-pairing with miRNAs. To achieve effective pharmacological inhibition of disease-associated miRNAs, miRNA antagonists contain chemical modifications to enhance binding affinity,

confer nuclease resistance, and facilitate cellular uptake (Krutzfeldt, Kuwajima et al. 2007).

The second strategy, miRNA replacement, involves the reintroduction of a tumor suppressor miRNA mimetic to restore a loss of function (Bader, Brown et al. 2010). miRNA mimetics represent an additional level of complexity compared with antimiRs. This strategy involves the risk to induce unwanted effects when novel miRNAs are introduced into a cell, but currently, *in vivo* evidence for toxicity induced by miRNA mimetics is still lacking.

1.5 Aim of the project

The aim of this thesis was to evaluate the oncogenic function of FUBP1 in glioblastoma.

At the beginning of the study, it was known that FUBP1 is highly deregulated in several cancerous tissues. In our group, we could show that FUBP1 is strongly overexpressed in hepatocellular carcinoma compared to normal liver tissue. Furthermore, a stable knockdown of *FUBP1* in the human HCC cell Hep3B led to impaired tumor growth in a xenograft transplantation model (Rabenhorst, Beinoraviciute-Kellner et al. 2009). Interestingly, when FUBP1 was overexpressed using adenovirus, a significant increase in FUBP1 mRNA levels was observed but protein levels failed to show an equivalent increase. So, I speculated about the involvement of miRNAs in regulating the expression level of FUBP1 in HCC cell lines.

Our group detected low expression of FUBP1 in astrocytes and demonstrated elevated levels of FUBP1 in glioblastoma, the most common malignant brain tumor in humans. In addition, Prof. Kinzler's group found that inactivating mutations in the genes *CIC* and *FUBP1* contribute to human oligodendroglioma (Bettegowda, Agrawal et al. 2011).

Based on these findings, the goal of the projects was:

(i) to investigate the role of FUBP1 in glioblastoma cell lines.

(ii) to identify miRNAs which are regulated by FUBP1 in HCC cell lines.

For this purpose, the following issues were addressed:

1. The expression analysis of FUBP1 in different glioblastoma cell lines
2. The functional role (apoptosis, proliferation, migration, invasion) of FUBP1 in glioblastoma cell lines
3. Studying the consequences of *FUBP1* knockdown in glioblastoma cell lines in *in vivo* mouse model
4. Identification of potential molecular candidates that could explain the differential role of FUBP1 in different glioblastoma cell lines
5. Identifying miRNAs that are regulated by FUBP1 in HCC cell lines using miRNA microarrays
6. Validating the identified miRNAs by luciferase assays

2. Materials and Methods

2.1 Materials

2.1.1 Plasmid and shRNA constructs

Table 5: List of plasmids used

Plasmid name	Plasmid description	Reference
pGIPZ	Ampicillin resistance; puromycin selectable marker; GFP marker to detect shRNA expression	Open Biosystems, Huntsville
pMD2.G	Expression plasmid for vesicular stomatitis virus glycoproteins (vsv-g)	Addgene Inc., Cambridge, UK M. Grez, GSH, Frankfurt.
pCMV-dR8.91	Encapsidation plasmid for lentivirus production	Addgene Inc., Cambridge, UK. M.Grez, GSH, Frankfurt.

2.1.2 qRT-PCR Oligonucleotides

Table 6: qRT-PCR oligonucleotides

Name	Gene	Sequence (5'→3')
qRT PCR huTGFβ-1 for	*TGFβ-1*	tggcgatacctcagcaacc
qRT PCR huTGFβ-1 rev	*TGFβ-1*	ctcgtggatccacttccag
qRT PCR huGAPDH-for	GAPDH	aatggaaatcccatcaccatct
qRT PCR huGAPDH-rev	*GAPDH*	cgccccacttgattttgg
qRT PCR huMMP2-for	*MMP2*	gcggcggtcacagctactt
qRT PCR huMMP2-rev	*MMP2*	cacgctcttcagactttggttct
qRT PCR huMMP9-for	*MMP9*	tgggggcaactcggc
qRT PCR huMMP9-rev	*MMP9*	ggaatgatctaagcccag
qRT PCR huIGF-II-for	*IGF-II*	ccgtgcttccggacaact
qRT PCR huMMP9-rev	*IGF-II*	ctgcttccaggtgtcatattgg

2.1.3 Competent E.coli strain

Table 7: *E.coli* strains used for DNA cloning experiments

Strain	Genotype	Manufacturer
DH5α	*sup*E44 lacU169 (80lacZM15) *hsd*R17 *rec*A1 *end*A1 *gyr*A96 *thi*-1 *rel*A1	*Clontech Laboratories Inc.*, Mountain View, CA, USA
One Shot® TOP10	F-mcrAΔ (mrr-hsdRMS-mcrBC) ϕ80 *lacZΔM15*ΔlacX74 *recA1 araD139Δ(ara-leu)7697 galU galK rpsL(StrR) endA1 nupG*	*Invitrogen GmbH*, Darmstadt

2.1.4 Enzymes

Table 8: Enzymes used for molecular biology methods

Enzyme	Concentration [U/ml-1]	Manufacturer
DNAse I	5,000000*	*Sigma Aldrich Chemie*, Taufkirchen
RNAse A	100 mg / ml^{-1}	*Roche*, Mannheim
Taq Polymerase	5,000	*Invitrogen GmbH*, Darmstadt
T4 DNA Ligase	200,000	*NEBiolab*, Schwalbach
Omniscript Reverse Transcriptase	4	*Qiagen GmbH*, Hilden

*Was used in lyophilized form, concentration in [U/mg^{-1}]

2.1.5 Cell culture materials

2.1.5.1 Cell culture disposables

Name	Manufacturer
6 well plates Corning	Sarstedt, Nümbrecht; Greiner, Frickenhausen
24 well plates Corning	Sarstedt, Nümbrecht; Greiner, Frickenhausen
96 well plates Corning	Sarstedt, Nümbrecht; Greiner, Frickenhausen
Cover slips	VWR Supplier Partnership, Langenfeld
Culture dishes (10-15 cm)	Greiner, Frickenhausen
Object slides	VWR Supplier Partnership, Langenfeld
Pipettes (5, 10, 25 ml)	BD Falcon, Heidelberg

Sterile filter (Millex-GP, 0.45 µm)	Millipore, Eschborn
Sterile syringes	Codan, Lensahn
T25 flasks	Greiner, Frickenhausen
T75 flasks	Greiner, Frickenhausen

2.1.5.2 Cell lines

Table 9: Cell lines used for functional studies

Cell line	Description	Reference
HEK 293 T	human epithelial kidney cells derived from the HEK-293 cell line, which was transformed with the SV40 "larg T"-antigen.	ATCC (CRL-11268)
Hep3B	Human hepatocellular carcinoma cells, positive for HepB viral DNA sequences, S1	ATCC (HB-8064™)
LNT229	Human glioblastoma cell line	ATCC (CRL-2611™)
U-87 MG	Human glioblastoma cell line, classified as grade IV	ATCC (HTB-14™)

2.1.6 Buffers and solutions

Table 10: Media for bacteria

Medium	Components for 1L	Preparation
LB-medium	5 g yeast extract 10 g peptone 10 g NaCl	MQ-water (ddH_2O) ad 1L, adjust to pH 7.2, autoclave for 30 minutes
LB-Ampmedium	5 g yeast extract 10 g peptone 10 g NaCl 15 g agar-agar	MQ-water (ddH_2O) ad 1L, adjust to pH 7.2, for selective LB-agar plates allow media to cool down to 50°C before adding selective antibiotic(s)

Table 11: Supplements

Media	Ingredients for 1 L / Concentration	Preparation
Kanamycin	25 mg/ml^{-1}	Dissolve in ddH_2O, filter sterilize (0.2 µm), store at -20°C (1 ml Aliquots)
Ampicillin	100 mg/ml^{-1}	Dissolve in ddH_2O, filter sterilize (0.2 µm), store at -20°C (1 ml Aliquots)

Table 12: Buffer for plasmid DNA preparations

Buffer	Ingredients / Concentration
GTE buffer	50 mM Glucose 25 ml Tris-HCl pH 8.0 10 mM EDTA
Lysis buffer	200 mM NaOH 1% SDS
Neutralization buffer	3 M KoAc, pH 5,2

Table 13: Buffer for Annexin-V staining

Name	Description
1x binding buffer	10 mM HEPES/NaOH pH 7.4, 140 mM NaCl, 2.5 mM $CaCl_2$

Table 14: Buffer for agarose gel electrophoresis

Buffer	Ingredients / Concentration
Running buffer (0.5x TBE)	44.5 mM Tris 44.5 mM boric acid 1 mM EDTA, pH 8.0
DNA loading buffer	100 mM EDTA 1% SDS 0.25% (w/v) bromphenol blue 0.25% (w/v) xylenecylanol 20% (w/v) glycerol

Table 15: Buffers for SDS-PAGE gel electrophoresis

Buffer	Ingredients / Concentration
SDS sample buffer	62.5 mM Tris-HCl, pH 6.8 2% (w/v) SDS 20% (w/v) glycerol 0.1% (w/v) bromphenol blue 50 mM DTT
SDS-PAGE running buffer	50 mM Tris 200 mM glycine 0.15% (w/v) SDS

Table 16: Comassie staining buffer

Buffer	Ingredients / Concentration
Quick Coomassie staining solution	MQ-water (ddH_2O) ad 1L 0.3% HCl conc. Coomassie blue R-250, 80 mg / 1L solution
Coomassie gel stain	MQ-water (ddH_2O) ad 1L 45% (v/v) methanol 1% glacial acetic acid Coomassie blue R-250, 1 g / 1L solution
Coomassie gel destain	MQ-water (ddH_2O) ad 1L 10% methanol 10% glacial acetic acid

Table 17: Lysis buffer

Buffer	Ingredients / Concentration
Bacterial lysis buffer	50 mM MES, pH 6.5 50 mM NaCl 1 tablet *Complete* EDTA-free Protease Inhibitor Cocktail ad 50 ml solution
RIPA buffer	10 mM Tris-HCl, pH 7.4 20 mM KCl 1.5 mM MgCl2 0.5% SDS 1.3 mM PMSF 1 tablet Complete EDTA free Protease Inhibitor Cocktail ad 50 ml solution

Table 18: Western blot analysis buffer

Buffer	Ingredients / Concentration
Blotting buffer	48 mM Tris, pH 7.5 39 mM glycine 20% (v/v) methanol
TBS-T	25 mM Tris, pH 8.1 150 mM NaCl 0.1% Tween20
Blocking buffer	3% non-fat milk powder in TBS-T

Table 19: Solutions for DH5α cells preparation

Medium	Components
Solution A	100mM RbCl2; 50mM MnCl2; 30mM KAc; 10mM CaCl2; 13% glycerin; pH 5.8, sterile filtered.
Solution B	10mM MOPS, 10mM RbCl2; 75mM CaCl2; 13% glycerin; pH 7,0, sterile filtered.

Table 20: Media and solutions for cell culture

Name	Description	Manufacturer
DMEM	Dulbecc's modified eagle medium	Gibco BRL, Eggenstein
AdvancedMEM	modified eagle medium	Gibco BRL, Eggenstein
FBS	Fetal bovine serum	PAA Laboratories, Pasching
L-Glutamine	200 mM solution	PAA Laboratories, Pasching
Penicillin	10,000 U/ml	PAA Laboratories, Pasching
Streptomycin	10,000 µg /ml	PAA Laboratories, Pasching
Trypsin-EDTA	0,02% Trypsin; 0.05% EDTA	Gibco, Eggenstein
DMSO	Dimethylsulfoxide, highly purified	Merck, Darmstadt
DPBS	Phosphate buffered Saline	PAA Laboratories, Pasching

2.1.7 Kits

Table 21: Kits used for molecular techniques

Name	Manufacturer
Plasmid Maxi Kit	*Qiagen GmbH*, Hilden
Qiaquick® Gel Extraktion Kit	*Qiagen GmbH*, Hilden
Omniscript® Reverse Transcription	*Qiagen GmbH*, Hilden
Amersham ECL Western Blotting Detection	*GE Healthcare*, Munich

2.1.8 *Antibodies*

Table 22: Primary antibodies for Western blotting

Name	Isolated from	Dilution factor	Lot number	Manufacturer
Anti-human β-Actin	Goat	1:2000	E1013	Santa Cruz Biotechnology, Inc, Europe.
Anti-human FUBP1	Goat	1:1000	K0905	Santa Cruz Biotechnology, Inc, Europe.
Anti-human MMP2	Rabbit	1:1000	Sc-10736	Santa Cruz Biotechnology, Inc, Europe.
Anti-human APAF1	Mouse	1:1000	611365	BD Biosciences, Europe.

Table 23: Secondary antibodies for western blotting

Name	Isolated from	Dilution factor	Manufacturer
Anti-goat HRP	Rabbit	1:5000	Invitrogen, Karlsruhe, Germany
Anti-mouse HRP	Sheep	1:2000	GE Healthcare, Munich, Germany
Anti-rabbit HRP	Donkey	1:2000	GE Healthcare, Munich, Germany

Table 24: Benchmark™ Prestainend Protein ladder

Band No.	Apparent molecular weight [kDa]
1	181.8
2	115.5
3	82.2
4	64.2
5	48.8
6	37.1
7	25.9
8	19.4
9	14.8
10	6.0

2.1.9 Chemotherapeutics and Small Molecule Compounds

Table 25: Chemotherapeutics and small molecules

Name	Concentration	Preparation	Manufacturer
mitomycin C	0.4 mg/ml	Dissolved in ddH_2O steril / methanol (4:1)	*Roche*, Mannheim

2.1.10 Laboratory Equipment

Table 26: Centrifuges

Name	Manufacturer
Beckman J2-HS	*Beckman*, Munich
Biocentrifuge, J2-21M/E with JA-10 and JA-20 rotors	*Beckman*, Munich
Cold-Centrifuge Megafuge 1.0R	*Heraeus*, Hanau
Cold-Centrifuge Minifuge GL	*Heraeus*, Hanau
Desk-Centrifuge Biofuge pico	*Heraeus*, Hanau

Table 27: Incubators

Name	Manufacturer
Bacterial Incubator Function Line	*Heraus,* Hanau
Bacterial-Shaker-Incubator Multitron model	*Infors AG*, Bottmingen (Switzerland)
Cell Culture Incubator MCO 17 AI	*Sanyo Component Europe GmbH,* Ingolstadt

Table 28: Heat Blocks and Water bath

Name	Manufacturer
Cooling-Thermomixer MKR 13	*HLC Biotech*, Bovenden
Dri.Block DB-2D	*Techne Dexford*, Cambridge (England)
Thermomixer Compact for 1.5ml Tubes	*Eppendorf AG*, Hamburg
Water-Bath	*GFL*, Burgwedel

Table 29: Electrophoresis

Name	Manufacturer
BioRad Power Pac 300	*BioRad Laboratories*, Munich
DNA Mini-Subcell for Agarose Gels	*BioRad Laboratories*, Munich
Electrophoresis Power Supply EPS 301	*Amersham Pharmacia Biotech*
Gel-Chamber Model Hoefer HE 33 for Mini Gels	*Amersham Pharmacia Biotech*
Mini-Protean® 3 Cell Gel Chamber	*BioRad Laboratories*, Munich
Semidry Blotting Unit Semiphor Transphor Unit	*Hoefer Pharmacia Biotech*

Table 30: Others

Name	Manufacturer
Autoclave Tuttnauer Systec 2540 EL	*Systec*, Wettenberg
Bunsen Burner Model 1230/1	*Carl Friedrich Usbeck KG*, Radevormwald
CryoPure tubes 1.8 ml	*Sarstedt,* Nümbrecht
Fluorescence Microscope Nikon Eclipse Te300	*Nikon*, Düsseldorf
Freezer (-20°C)	*Liebherr*, Ochsenhausen
Freezer CFC Free (-80°C)	*Sanyo*, Wiesbaden
Freezing container	*Qualilab*, France
Gene Amp® PCR System 9700	*PE Applied Biosystems*
Hypercassette	*Amersham*, Buckinghamshire (England)
Integra Pipetboy	*Integra Biosciences*, Fernwald
Laminar Air Flow (NSF 49 BS 5726 DIN (1-4))	*Clean Air*, Woerden (Netherlands)
Magnetic-Stirrer Model IKA-Combimag RCH	*IKA Labortechnik*, Staufen
Microscope for Cell Culture	*Helmut Hund GmbH*, Wetzlar
Mircowave Sharp R-3V10	*Sharp Corp*.
NanoDrop™ 1000 Spectrophotometer	*Thermo Fischer Scientific*, Bonn
Neubauer Improved Hemocytometer	*Marienfeld Superior*, Darmstadt
pH-Meter Model PHM 83 autocal	*Radiometer*, Copenhagen (Denmark)
Refrigerator (4°C)	*Bosch*
Roller RM5 Assistant 348	*Karl Hechst GmbH&Co.KG*, Sondheim
Rotate roller	*Gerlinde Kister*, Mühlhausen
UV-Transluminator with video camera and -printer	*UVP Inc.*, San Gabriel (USA)
vacuum pump	*KNF Neuberger LABOPORT*, Freiburg
Vortex Genie 2	*Scientific Industries*, New York (USA)

2.1.11 Chemicals and Reagents

Table 31: Reagents

Name	Manufacturer
Acrylamide Solution (Rotiphorese Gel 30)	*Carl Roth GmbH&Co.KG*, Karlsruhe
Agarose UltraPure (TM) Agarose	*Invitrogen GmbH*, Darmstadt
Ampicillin	*AppliChem GmbH*, Darmstadt
APS (10% in H2O)	*Sigma-Aldrich Chemie GmbH*, Steinheim
Boric Acid	*Carl Roth GmbH&Co.KG*, Karlsruhe
Bradford Reagent (Roti®-Quant)	*Carl Roth GmbH&Co.KG*, Karlsruhe
Bromphenol Blue	*Carl Roth GmbH&Co.KG*, Karlsruhe
Complete Mini Protease Inihibitor Cocktail	*Roche*, Mannheim
DTT	*Sigma-Aldrich Chemie GmbH*, Steinheim
EDTA	*Sigma-Aldrich Chemie GmbH*, Steinheim
EGTA	*Sigma-Aldrich Chemie GmbH*, Steinheim
EtBr	*Carl Roth GmbH&Co.KG*, Karlsruhe

EtOH	*Carl Roth GmbH&Co.KG*, Karlsruhe
Glucose	*Carl Roth GmbH&Co.KG*, Karlsruhe
Glycerol	*Carl Roth GmbH&Co.KG*, Karlsruhe
Glycine	*Carl Roth GmbH&Co.KG*, Karlsruhe
HEPES	*Carl Roth GmbH&Co.KG*, Karlsruhe
Illustra™ dNTP Set	*GE Healthcare Europe GmbH*, Munich
Isopropanol (2-Propanol)	*Carl Roth GmbH&Co.KG*, Karlsruhe
KCl	*Carl Roth GmbH&Co.KG*, Karlsruhe
$MgCl_2$	*Sigma-Aldrich Chemie GmbH*, Steinheim
Na-β-glycerophosphate	*Sigma-Aldrich Chemie GmbH*, Steinheim
Na-pyrophosphate	*Sigma-Aldrich Chemie GmbH*, Steinheim
Na_2HPO_4	*Carl Roth GmbH&Co.KG*, Karlsruhe
NaAc	*Carl Roth GmbH&Co.KG*, Karlsruhe
NaCl	*Carl Roth GmbH&Co.KG*, Karlsruhe
NaF (Natriumfluorid)	*Sigma-Aldrich Chemie GmbH*, Steinheim
NaOH	*AppliChem GmbH*, Darmstadt
Nonfat dried milk powder	*AppliChem GmbH*, Darmstadt
PMSF	*Carl Roth GmbH&Co.KG*, Karlsruhe
Ponceau S Solution	*Sigma-Aldrich Chemie GmbH*, Steinheim
Roti®-Quant	*Carl Roth GmbH&Co.KG*, Karlsruhe
SDS	*Carl Roth GmbH&Co.KG*, Karlsruhe
Sodium Chlorid	*Roth*, Karlsruhe
Sucrose	*Carl Roth GmbH&Co.KG*, Karlsruhe
TEMED	*Carl Roth GmbH&Co.KG*, Karlsruhe
Tris	*Carl Roth GmbH&Co.KG*, Karlsruhe
TrisBase	*Roth*, Karlsruhe
Triton-X-100	*Fluka*, Buchs (Switzerland)
Tween-20	*Carl Roth GmbH&Co.KG*, Karlsruhe

2.2 Methods

2.2.1 Bacteria culture

2.2.1.1 Generation of chemo-competent *Escherichia coli* (DH5α) cells

Competence is the ability of bacterial cells to take up DNA from the environment which can be artificially achieved by exposure to high concentrations of calcium ions, causing permeabilization of the bacterial cell membrane. 5 ml LB medium was inoculated with a single colony of *E.coli*. The bacteria were grown overnight at 37°C with shaking at 250 rpm. The following day, the culture was further expanded in 300 ml LB medium untill OD of 0.5 was reached. The LB medium was collected, incubated on ice for 20 min and was centrifuged at 4°C at a speed of

4,000 x g for 10 min. The supernatant was discarded, and the bacterial pellet was resuspended in 200 ml ice-cold solution A (Table 19). After incubation on ice for 1-2 hours, bacteria were centrifuged for 10 min, and the bacterial pellet was resuspended in 15 ml ice-cold solution B (Table 19). The resulting competent bacterial cells were divided in 200 µl aliquots, frozen in liquid nitrogen and stored at -80°C.

2.2.1.2 Transformation of *E.coli* (DH5α) by heat shock

The introduction of foreign DNA into competent bacteria is called “transformation”. Chemo-competent *E.coli* bacteria (DH5α) were thawed on ice, and 50 µl of cells were mixed with 10-100 ng of plasmid DNA. After incubation on ice for 20 min, cells and DNA were subjected to a heat shock at 42°C for 90 sec, after which they were incubated on ice for 2 min. 500 µl of LB medium without antibiotics was added, and the bacterial culture was incubated at 37°C for 40 min at 250 rpm. Bacteria were then centrifuged at 4,000 x g for 1 min. The supernatant was discarded, and the pellet was resuspended in 100 µl LB medium. The resulting transformed bacteria were streaked on LB-ampicillin agar plates and incubated overnight at 37°C.

2.2.1.3 Storage of transformed bacteria

For long-term storage, 0.5 ml overnight culture-containing transformed bacteria were mixed with 0.5 ml sterile 100% glycerol and immediately frozen at -80°C.

2.2.2 DNA isolation and analysis

2.2.2.1 Plasmid DNA isolation (Mini-prep)

For small scale isolation of plasmid DNA from bacterial cells, alkaline lysis of bacteria in NaOH-SDS buffer was performed. NaOH causes denaturation of chromosomal and plasmid DNA, while SDS denatures proteins. Neutralization with potassium acetate leads to precipitation of SDS and formation of large complexes containing denatured proteins, chromosomal DNA and cellular debris. After removal of these complexes by centrifugation, plasmid DNA in the supernatant was concentrated by ethanol precipitation, and RNA was degraded by RNAse-A treatment. 3 ml LB medium (containing 100 µg/ml ampicillin) was inoculated with one single colony of transformed *E.coli* bacteria (DH5α) and incubated overnight at 37°C while shaking at 250 rpm. 1.5 ml of this culture was centrifuged at 12,000

x g for 2 min, the supernatant was discarded and the bacterial pellet was resuspended in 100 µl GTE solution by vortexing. After addition of 200 µl NaOH-SDS, the solution was mixed by inverting the tubes (5 times) and incubated at room temperature for 5 min. For precipitation of proteins and genomic DNA, 150 µl 5M KOAc was added and mixed carefully by inversion, followed by incubation on ice for 5 min. The samples were centrifuged at 12,000 x g for 5 min, the supernatant was transferred to a new Eppendorf tube, and the DNA was precipitated with 1 ml 100% ethanol (centrifugation at 12,000 x g, 10 min). The pellet was washed with 70% ethanol, and after centrifugation, the DNA was air-dried and resuspended in 30 µl sterile deionized H_2O containing 0.2 mg/ml RNAse A (*Roche*, Mannheim). The isolated plasmid DNA was stored at –20°C.

2.2.2.2 Isolation of plasmid DNA for large-scale preparations (Maxi-prep)

For the amplification of large amount of plasmid DNA, the plasmid of interest was transformed into competent *E.coli* bacteria (DH5α) and the resulting ampicillin-resistant bacteria were grown overnight at 37°C with shaking at 170 rpm in 250 ml LB medium containing 100 µg/ml ampicillin. Bacterial cells were harvested by centrifugation at 6,000 x g for 15 min at 4°C, and plasmid DNA was isolated using a commercially available kit (*Qiagen* and *Macherey-Nagel*).
Purification of plasmid DNA was performed according to the manufacturer´s instructions. In brief, bacterial cells were lysed, and plasmid DNA was immobilized on an anion-exchange column, washed and eluted using a buffer with high salt concentrations. After precipitating with isopropanol and washing with 70% ethanol, the DNA was air dried and dissolved in sterile deionized water.

2.2.2.3 DNA concentration measurement

The DNA concentration was determined using a “Nanodrop” device. 2µL of purified plasmid preparation was spotted on the lower pedestal, and the absorption at a wavelength of 260 nm (caused by de-localized π-electrons of purin or pyrimidine bases) was measured. To determine the purity of the DNA sample, the absorption at a wavelength of 280 nm (absorption by aromatic amino acid side chains) was measured.
A sufficient purity should be indicated with an absorption ratio of A260 / A280: 1.7 - 2

2.2.2.4 Agarose gel electrophoresis

Agarose gel electrophoresis is a method for the detection of DNA fragments and can be used to determine the size and the concentration of DNA molecules. Agarose forms a meshwork in which DNA can migrate, and application of an electric field causes movement of the negatively charged DNA towards the anode. During this process, DNA molecules are separated based on their size. Due to the addition of the intercalating dye ethidium bromide, DNA becomes visible upon UV light illumination. Plasmid DNA or PCR products were separated in 1-2% agarose 1 x TBE or TAE gels with 0.5 µg/ml ethidium bromide. Electrophoresis was performed in 0.5 x TBE or 1 x TAE buffer. DNA samples were mixed with 6 x DNA loading buffer, loaded onto agarose gels and separated at 10 V/cm gel length. A 1 kb DNA ladder or the 100 bp DNA ladder (*Fermentas*) was used as a marker.

2.2.3 Polymerase chain reaction (PCR)

The Polymerase chain reaction (PCR) is a method for the amplification of specific DNA sequences. Template DNA is incubated with the enzyme DNA polymerase in the presence of oligonucleotide primers, which possess a complementary sequence to the target DNA, and deoxyribonucleotide triphosphates (dATP, dCTP, dGTP, dTTP). The reaction is conducted in repeated thermal cycles that consist of three main steps: melting of template DNA (95°C), annealing of primers and template (52-60°C, depending on primer annealing temperatures), and DNA elongation (68-72°C, depending on the enzyme used). Heating to 95°C inactivates most DNA Polymerases and therefore, heat-stable enzymes like the *Thermus aquaticus* (Taq) Polymerase are commonly used. The annealing temperature of primers is calculated using the following equation (Rychlik *et al.*, 1990):

Annealing temperature = (number of G and C) x 4°C + (number of A and T) x 2°C

The time of elongation depended on the length of the sequence to be amplified, in general 1 min for 1 kb was used. PCR reactions for cloning of the amplified sequence were performed with *Pfx* polymerase (5 u/µl, *Roche*, Mannheim). The reaction mixtures were prepared and kept on ice until the thermocycler temperature reached 94°C (simplified hot start).

Template DNA	**10 ng - 100 ng**
dNTP-mix (2.5mM each)	6 µl
Primer 1 and 2 (10µM)	1.5 µl each
MgSO4 (25mM)	2 µl
10 x Pfx amplification buffer	5 µl
Pfx polymerase	0.8 µl
H_2O	ad 50 µl

For cloning PCR reactions, the following PCR protocol was used (annealing temperatures and elongation times were adapted for each specific reaction):

Denaturation	**94°C**	**3 min**
Amplification (35 cycles)	94°C	1 min
	58°C	1 min
	68°C	3 min
Final Elongation	68°C	10 min
Cooling	4°C	∞

The amplification of DNA fragments was performed in a *GeneAmp*® 9700 thermocycler (*Perkin Elmer*, Weiterstadt). PCR products were separated by agarose gel electrophoresis, isolated with the *QIAquick* gel extraction kit (*Qiagen*, Hilden) and either used directly for further cloning or stored at –20°C.

2.2.4 RNA isolation and analysis

2.2.4.1 RNA isolation

For RNA isolation, cells were washed with PBS, trypsinyzed and collected with DMEM in a Falcon tube. After centrifugation (5 min, 400 x g, 4°C), cells were used immediately for RNA isolation. Purification of total RNA was performed using the *RNeasy Mini Kit* (*Qiagen*, Hilden) according to the manufacturer´s instructions.
In brief, cells were lysed using *QIA shredder* columns (*Qiagen*, Hilden), and RNA was immobilized on silica-membrane columns. On-column DNAse I digestion was performed to remove contaminating DNA, and after washing, RNA was eluted using RNAse-free water.

2.2.4.2 Quantification of RNA concentration

RNA concentration was determined using a *NanoDrop 1000* Spectrophotometer (*Thermo Scientific*) by measurement of the absorption at a wavelength of 260 nm. 260/280 and 260/230 absorption ratios were determined to assess RNA purity. The 260/280 ratio should be in the range of 1.8- 2.0, and the 260/230 ratio should be between 2.0 and 2.2 for clean RNA preparations (280 nm: absorption by contaminating proteins, 230 nm: absorption by different contaminating organic compounds).

2.2.4.3 Reverse transcription

RNA was converted into cDNA using *Omniscript RT* kit (*Qiagen*) according to the manufacturer´s instructions. In brief, 1 µg of RNA was added to a 20 µl reaction mix containing RT reaction buffer, oligo (dT), random hexamer primer, dNTPs, RNAse inhibitor (*RiboLock, Fermentas*) and Reverse Transcriptase (RT). Control reactions were performed without Reverse Transcriptase (RT control).

2.2.4.4 Quantitative real time PCR (qPCR)

The copy number of RNA or DNA molecules in cells (e.g. cultivated cells or tissue samples) can be determined by quantitative real time PCR, whereas isolated DNA can directly be used as a template for qPCR analysis. A reverse transcription reaction has to be performed for the analysis of RNA, and the obtained cDNA is further used in qPCR analysis.

In principle, qPCR is a method based on a conventional PCR reaction. It is performed in the presence of a fluorescent agent whose amount bound to amplified DNA is determined during the course of the reaction as an indicator of the amount of amplified target sequence. Quantification of the fluorescent signal allows to monitor target amplification not only at the end of the reaction as in a conventional PCR but throughout all PCR cycles. Two different kinds of fluorescent dyes are commonly used for qPCR: non-specific dyes that intercalate into DNA double-strands (eg. *SYBR Green*) and/or specific DNA probes (oligonucleotides labeled with a fluorescent reporter) that bind to the amplified target sequence. Specificity of qPCR assays based on dyes like SYBR Green can be ensured by the combination of melting curve and agarose gel analysis together with sequencing of the reaction product. For quantification of the target sequence, the acquired fluorescence is plotted against the number of PCR cycles. A fluorescence

background threshold is defined, and the cycle at which the measured signal crosses this threshold (the cycle threshold or Ct value) is determined for each sample.

2.2.4.5 qPCR analysis using SYBR Green-based assays

The expression levels of mRNAs in murine cells were analyzed by SYBR Green-based qPCR assays. For this purpose, RNA was isolated, and a reverse transcription was performed as described in sections 2.1.5.1 and 2.1.5.3. For each sample, qPCR reactions were performed in triplicates in a reaction volume of 24 µl. The reaction mix contained 1 x *ABsolute^{TM} QPCR SYBR Green* mix (*Thermo Scientific*), gene-specific primers (500nM each) and 30 ng cDNA per reaction. To ensure the absence of DNA contamination, reactions with water or cDNA samples without RT were performed. Assays were carried out on a LightCycler®480 (Roche) with white *LightCycler®480 Multiwell plates 96*, and the following PCR-protocol was applied:

Denaturation	**95°C**	**15 min**
Amplification (40 cycles)	95°C	20 sec
	58°C	30 sec
	72°C	30 sec
Melting Curve	50°C	10 sec
	+2.2°C	10 sec
	... 95°C	target temperature

2.2.5 Protein biochemistry

2.2.5.1 Immunoblotting of proteins („Western blot analysis“)

2.2.5.1.1 Protein extraction from mammalian cells

For extraction of proteins, cultured mammalian cells were washed with PBS and either scraped from the culture plates with a rubber-policeman or trypsinized and collected with DMEM in a Falcon tube. After harvesting by centrifugation (5 min; 1,500 rpm; 4°C), cell pellets were resuspended in 1 ml PBS and transferred into a 1.5 ml Eppendorf tube. Cells were again pelleted by centrifugation (5 min; 1,500 rpm) and resuspended in 150-500 µl freshly prepared lysis buffer (depending on cell numbers e.g. 150 µl for 1x10^6 cells). Lysis of cells was performed by incubation

on ice for 20 min followed by sonification (*Sonifier 250, Branson*; Duty Cycle 30%, Output 3, 20 pulses).

2.2.5.1.2 Measurement of protein concentration according to the Bradford protocol

The protein concentration of cell lysates was determined by the Bradford assay. The basic principle of this assay uses the absorbance maximum shift of acidic *Coomassie Brilliant Blue G-250* solution from 465 nm to 595 nm that occurs after binding of the dye to proteins. This change in colour is caused by the stabilization of the anionic form of the dye by hydrophobic and ionic interactions between dye and protein. Protein concentrations were determined according to the manufacturer´s instructions (*Roti*®*-Quant, Carl Roth,* Karlsruhe). In brief, 2 µl of cell lysate were diluted in 800 µl water and 200 µl Bradford solution and incubated for 5 min at room temperature. The protein concentration was measured at 595 nm with a spectrophotometer and calculated using a BSA standard curve.

2.2.5.1.3 SDS- polyacrylamide-gel electrophoresis (PAGE)

SDS-PAGE is a method by which proteins can be separated depending on their molecular weight. Gels are formed by polymerization of acrylamide solution which results in the formation of a meshwork of polyacrylamide. The size of the pores in the gel depends on the percentage of acrylamide used. Higher concentrations of acrylamide are used for the separation of smaller proteins. Proteins migrate in the gel after application of an electric field. As the proteins are denatured by the negatively charged detergent sodium dodecyl sulfate (SDS) and reduced by ß-mercaptoethanol, which breaks S-S linkages, they migrate towards the anode, and the velocity of their migration is determined by the molecular weight of the protein. Protein samples are applied onto the stacking gel which has a low percentage of SDS and polyacrylamide, and the proteins migrate into the gel due to the electric field. At the boundary between stacking and separating gel, movement of the proteins is decelerated and a sharp frontline of the migrating samples is formed. In the separating gel, proteins with lower molecular weight move faster than proteins with high a molecular weight. SDS-gels were produced with the following compositions:

Protein samples were denatured for 5 min at 95°C in 5 x sample buffer, and separation by SDS PAGE was performed in 1 x SDS-PAGE buffer using the Mini-

Protean II system (BioRad, Munich). Electrophoresis was performed at 80 V for the stacking gel and 120 V for the running gel. The protein marker *BenchMark™ Prestained Protein Ladder* (*Invitrogen,* Karlsruhe) was used to determine the size of the protein run. Subsequently, proteins were detected by immunoblotting (Western blot analysis).

2.2.5.1.4 Protein transfer onto nitrocellulose membranes

For the detection of proteins by specific antibodies, protein transfer onto nitrocellulose membranes was performed after SDS-PAGE. Nitrocellulose transfer membranes (*Schleicher & Schuell BioScience*, Dassel) and Whatman papers were soaked in 1 x blotting buffer. The SDS gel was placed on the nitrocellulose membrane and was sandwiched between 3 layers of Whatman papers on top of the anode of a semi-dry blotting chamber (*Keutz*, Reiskirchen) and again 3 Whatman papers on the cathode of the blotting chamber. Protein transfer was performed at 50 V and 55 mA for 2 h. After blotting, membranes were stained with Ponceau S solution to confirm equal transfer of proteins from the gel.

2.2.5.1.5 Immunodetection of blotted proteins

Following protein transfer, unspecific protein binding sites of the nitrocellulose membranes were blocked by incubation in blocking buffer (5% non-fat milk and 0.1% Tween in 1 x PBS for ECL detection or *Odyssey Blocking Buffer* for detection using the *Odyssey* system) for at least 2 hours at room temperature or at 4°C overnight. For specific protein detection, the respective antibodies were diluted in blocking buffer, and membranes were incubated for 1 hour at room temperature or at 4°C overnight. Membranes were then washed 3 x 10 min with PBS-T (1 x PBS + 0.1% Tween) to remove unbound antibody. Membranes were then incubated with the corresponding secondary antibody diluted in blocking buffer. The secondary antibody was either coupled to Horseradish Peroxidase (HRP) for ECL detection or to IR (Infrared) dyes for detection with the *Odyssey* system. After incubation for 1 hour at room temperature, membranes were washed for 3 x 10 min with PBS-T. Secondary antibody signals were then measured by ECL chemo-luminescence or with the *Odyssey* system.

Detection of proteins by ECL (Luminiscence assay)

Secondary antibodies coupled to the enzyme Horseradish Peroxidase (HRP) are commonly used for specific detection of proteins. This enzyme converts the substrate luminol into 3-aminophthalate which then emits light with a wavelength of around 428 nm. Addition of chemicals like modified phenols to the solution leads to enhanced chemiluminiscence (ECL).
In this work, the *ECL™* Western blot reagents (*GE Healthcare*, Munich) were used for detection of proteins by Western blot Analysis. After incubation of nitrocellulose membranes with ECL, a sensitive film (*SuperRX, Fujifilm*) was exposed onto the membrane and developed using an *Optimax X-Ray Film Processor* (*Protec-Medizintechnik*, Oberstenfeld).

Detection of proteins using the *Odyssey* system

An alternative method to the use of HRP-coupled secondary antibodies is the use of antibodies coupled to fluorescent dyes that can be detected by corresponding scanners. In this work, the *Odyssey infrared imaging system* (*Li-Cor*, Bad Homburg) was used. Secondary antibodies for this system were coupled to infrared dyes that emit light at a wavelength of either 800 or 680 nm.

2.2.6 Luciferase reporter assay

The ability of miRNA's to influence the activity of the *FUBP1* 3'UTR was tested in Luciferase reporter assays. For this purpose, the 3'UTR of the Luciferase-containing *pISO* reporter construct (Addgene, Cambridge, USA) was cloned with 3'UTR of human *FUBP1*. The predicted miRNA binding sites were mutated by base pair changes using *Dpn*I mediated site-directed mutagenesis. Hep3B cells were co-transfected with wild type or mutated *FUBP1* 3'UTR plasmid, Renilla normalization plasmid (pGL 4.74) and pcDNA vector to level out DNA amounts using the transfection reagent Attractene (QIAGEN, Hilden, Germany). Transfected cells were harvested after 48 hours and lysed in 1 x *Passive Lysis Buffer* (*Promega*, Mannheim). Lysates were analyzed using the *Dual-Luciferase™ Reporter Assay System* (*Promega*, Mannheim) according to the manufacturer´s instructions. Luciferase activity was quantified using a *LUMI Star Galaxy Luminometer* (*BMG Labtech*, Offenburg).

2.2.7 Mammalian cell culture

2.2.7.1 Culture of mammalian cells

Cells were cultured in a BBD-6220 incubator at 37°C with 5% CO2 in a humidified atmosphere. Cells were grown in DMEM medium (Dulbecco´s modified Eagles medium) containing 10% v/v fetal bovine serum (FBS), 1% v/v L-Glutamin (100mM) and 1% v/v Penicillin/Streptomycin (10 µg/ml). For inactivation of the complement system, FBS was incubated at 56°C for 30 min before use.
Cells were usually passaged twice a week to prevent them from becoming confluent. After the removal of the medium by aspiration, cells were carefully washed with DPBS and treated with Trypsin for 5 - 10 minutes to detach cells from the culture dish. Afterwards, cells were resuspended in appropriate cell culture medium and 1/3 to 1/14 of the cells were transferred to a new culture plate with fresh medium.

2.2.7.2 Freezing and thawing of cells

For long-term storage, cells were frozen in FBS containing 10% dimethyl sulfoxide (DMSO). This organic solvent reduces the formation of ice crystals that can damage the cell membrane during the freezing process. Cells were washed and trypsinized as for passaging, resuspended in fresh medium and transferred to a Falcon tube (*Becton Dickinson Biosciences*, Heidelberg). The cells were harvested by centrifugation (5 min, 400 x g, 4°C), resuspended in FBS plus 10% DMSO and transferred into a cryo tube (*Nunc*, Wiesbaden). These tubes were stored in a freezing container (*Cryo1°C*, *Nalgene*, Roskilde, Denmark) in the -80°C refrigerator overnight and then moved to the liquid nitrogen storage tank.

For thawing, cells were kept under the sterile hood at room temperature until they defrosted and were then resuspended in cell culture medium and harvested by centrifugation (5 min, 400 x g, 4°C). The medium was aspirated to remove residual DMSO, cells were resuspended in fresh medium and transferred into cell culture dishes.

2.2.7.3 Determination of cell numbers using a hemacytometer

For quantification of cell numbers, 10 µl of a cell solution was transferred into a Neubauer hematocytometer (*Baxter Scientific*), and cells in 16 squares were

counted under the microscope in a 100x magnification. The cell number was calculated using the following equation:
Counted cell number x 10^4 = cell number/ml

2.2.7.4 Transfection of mammalian cells

Foreign DNA can be introduced into mammalian cells by transfection. DNA can be integrated in larger complexes that are taken up by cells by endocytosis or phagocytosis. Also, pores in the cell membrane can be generated by electroporation which leads to uptake of DNA from the cell culture medium. Depending on the cell type, different methods show different efficiencies. Therefore, transfection protocols have to be adapted for each individual cell line.

2.2.7.5 Polyethyleneimine (PEI)-mediated transfection

For transfection, a 10mM working solution of PEI (*Sigma*) was used. PEI transfection is most efficient when the ratio between postively charged amine nitrogens in PEI and negatively charged phosphates of the DNA backbone lies in the range of 9-13.5 (Boussif *et al.*, 1995).
1 µg of DNA and 2.7 µl of 10mM PEI were diluted in 150 µl DPBS in separate Eppendorf tubes. Both solutions were then mixed by vortexing and incubated at room temperature for 15 min. Cells were washed, and serum-free medium was added. After 4 hours, medium was aspirated and replaced by medium containing serum, glutamine and penicillin streptomycin.

2.2.7.6 *LipofectamineTM 2000*-mediated transfection

Lipofecatine™ 2000 was used according to the manufacturer´s instructions. Transfection was performed in medium without antibiotics. 2.5 µl Lipofectamine were used for the transfection of 1 µg DNA. DNA and Lipofectamine were diluted in 50 µl Opti-MEM reduced serum medium in separate tubes. Both solutions were mixed by pipetting and incubated at room temperature for 15-20 min before adding the mixture to the cells. After 4 hours, medium was aspired and replaced by fresh medium.

2.2.7.7 Lentiviral transduction of mammalian cells

2.2.7.7.1 Lentivirus production in HEK-293T cells

For lentivirus production, HEK-293T cells were transfected with the respective lentiviral construct and two packaging plasmids (*pCMV-dR8.91 & pMD2.G*) containing structural virus proteins. $3x10^6$ HEK-293T cells were seeded per 10 cm dish and transfected with 10 µg of total DNA (1.75 µg *pMD2.G*, 3.25 µg *p8.91* and 5 µg expression vector) using PEI. 48 hours after transfection, virus supernatant was collected, filtered through a 0.45 µg syringe filter unit, centrifuged (20,000 rpm, 4^0C, 2:20 hrs) and aliquoted into PCR tubes (15 µL each)

2.2.7.7.2 Lentiviral transduction

For transduction, $1x10^5$ cells were seeded in 6 well plates 24 hours before transduction. Lentivirus-containing supernatant or concentrated virus aliquots was diluted with fresh medium to a total volume of 6 ml/well to achieve a multiplicity of infection (MOI) of 10. To achieve higher transduction efficiencies, polybrene was added to the medium to a final concentration of 8 µg/ml, and cells were centrifuged at 250 x g and 32°C for 50 min (spin infection).

2.2.8 Apoptosis assay

To test the sensitivity of different cells to apoptotic stimuli, cells were plated at $3x10^5$ in 6 well plates. For apoptosis induction, cells were treated with TRAIL or MG132 (proteosomal inhibitor). Concentrations and incubation times were modified according to the particular cell line. After incubation, cell culture supernatant was collected (to include apoptotic, detached cells in the analysis), and adherent cells were harvested using Trypsin. Cells were washed in PBS and fixed for flow cytometric analysis following the Nicoletti protocol.

2.2.8.1 Nicoletti assay

A typical feature of apoptosis is the fragmentation of genomic DNA which can be measured by different techniques to discriminate between living and apoptotic cells. Propidium iodide (PI) is a dye which specifically intercalates into nucleic acids which can be used to quantify DNA fragmentation by flow cytometry. For this purpose, cells were fixed with ethanol and stained with PI in the presence of RNAse-A. After RNA digestion, the PI signal intensity was comparatively equal to the DNA content of a cell hence, the cell cycle profile for all the cells could be

determined. As ethanol fixation permeabilizes the cell membranes, fragmented DNA is lost from apoptotic cells and therefore, apoptotic cells display a subG1 content of DNA (Riccardi and Nicoletti, 2006).

Cells were harvested and transferred to FACS tubes. After centrifugation (5 min, 400 x g, 4°C), they were washed with PBS and again pelleted. Cells were fixed by adding 1 ml ice-cold 70% ethanol and after thorough mixing, incubated at 4°C for at least 12 hours (up to two weeks). Before staining, cells were washed with 38mM Na-Citrate (pH 7.4), centrifuged (5 min, 400 x g, 4°C) and 200- 500 µl of staining solution were added. Staining was performed for 20 min at room temperature in the dark. Acqusition of cell cycle profiles was done on a *Becton Dickinson Biosciences FACS Calibur*. PI fluorescence was measured in the FL2 channel after activation of the doublet discrimination module (DDM), and data sets were analyzed using *Cell Quest-Pro* software (*Becton Dickinson Biosciences*, Heidelberg). At least 20,000 events were acquired for each sample. Staining solution: 38mM Na-Citrate (pH 7.4), 50 µg/ml propidium iodide, 5 µg/ml RNAse A

2.2.9 Proliferation assay

2.2.9.1 Click-iT™ EdU assay

$2x10^5$ Hep3B cells were seeded into 6 well plates in DMEM with 10% FBS. The next day, cells were incubated with 10µM 5-ethynyl-2'-deoxyuridine (EdU) for 1 hour. After harvesting of the cells using Trypsin, cells were washed with 1% BSA in PBS. Cells were fixed using Click-iT™ fixative solution provided in the kit and incubated in dark for 15 minutes. Cell were further washed with 1% BSA in PBS and permeabalized using Click-iT™ saponin-based permeabilization reagent for 15 minutes. Cells were further incubated in dark for 30 minutes with Click-iT™ reaction cocktail (PBS, $CuSO_4$, fluorescent dye azide and reaction buffer) and washed with Click-iT™ saponin-based permeabilization reagent. Cells were further stained with Alexa Fluro® 647 and analysed using flow cytometer.

2.2.10 miRNA quantification using qRT-PCR

To quantify miRNA levels, cDNA was reverse transcribed from total RNA samples using specific miRNA primers from the TaqMan MicroRNA Assays and reagents from the TaqMan MicroRNA Reverse Transcription kit (Applied Biosystems). The resulting cDNA was amplified by PCR using TaqMan MicroRNA Assay primers with the TaqMan Universal PCR Master Mix and analyzed with a 7500 ABI PRISM

Sequence Detector System according to the manufacturer's instructions (Applied Biosystems). The relative levels of miRNA expression were calculated from the relevant signals by the ΔΔCt method by normalization to the signal of RNU48.

2.2.11 miRNA target prediction

In order to identify the miRNAs that regulate *FUBP1*, the following software programme for analysis were used: TargetScan (http://www.targetscan.org/), PicTar (http://pictar.mdc-berlin.de/) and miRanda (http://www.microrna.org) were used. Only those miRNA target predictions that were found in at least two databases were accepted as reliable.

3. Results

3.1 Analysis of FUBP1 expression in glioblastoma cell lines

FUBP1 has been known to activate the proto-oncogene c-*myc* (Duncan, Bazar et al. 1994) and was shown to act as an onco-protien in HCC in Prof. Martin Zörnig's lab (Rabenhorst, Beinoraviciute-Kellner et al. 2009). In general, FUBP1 was found to be expressed in a broad range of normal tissues. An increased expression of FUBP1 was observed in glioblastoma cells when compared to normal oligodendrocytes and astrocytes (Rabenhorst U 2010). However, previous studies revealed that inactivating mutations in the genes *CIC* and *FUBP1* contribute to human oligiodendrogioma (Bettegowda, Agrawal et al. 2011). Therefore, the role of FUBP1 in glioblastoma was investigated in detail. The expression of FUBP1 in different glioblastoma cell lines was analysed by western blotting. The analysis revealed that FUBP1 is differentially expressed in a variety of glioblastoma cell lines. LN-308, SKMG-3 and U-138 MG cells showed higher expression of FUBP1 compared to LNT-229, LN-428 and U-373 MG (with moderate expression) and U-87 MG (showing the lowest expression) (Figure 6)

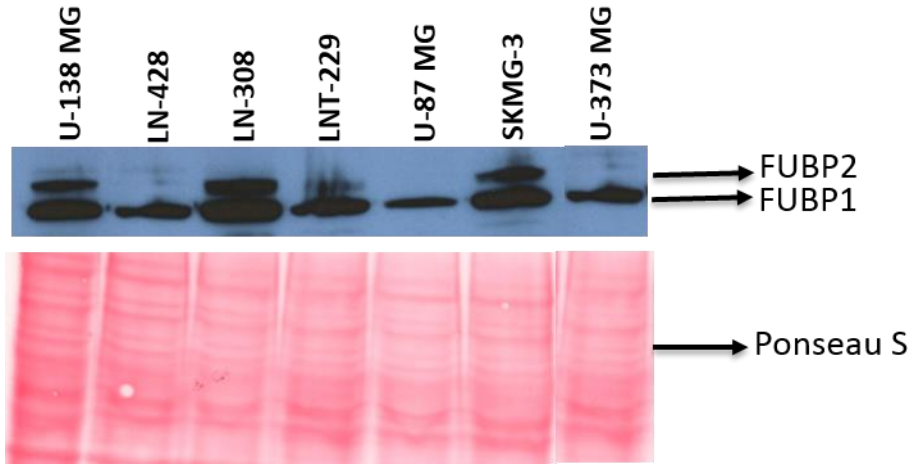

Figure 6: FUBP1 expression in different glioblastoma cell lines.

Seven different glioblastoma cell lines were cultured, and FUBP1 expression was tested by immunoblotting with a FUBP1-specific antibody. Immunoblotting analysis revealed differential expression of FUBP1 in a variety of cell lines. 80 µg of each cell lysate was loaded for Western blot analysis. Ponseau S staining was used as a loading control.

3.2 Functional analysis of FUBP1 in glioblastoma cell lines by gene silencing

To study whether FUBP1 overexpression plays a crucial role and is of functional relevance in glioblastoma, the consequences of *FUBP1* knockdown in the glioblastoma cell lines LNT-229, SKMG-3, LN-428, U-138 MG, U-87 MG and U-373 MG were analyzed. For this purpose, *FUBP1*-specific shRNAs were cloned into the lentiviral expression vector *pSEW*. Lentivirus was produced in HEK-293T cells and used for stable transduction of LNT-229, SKMG-3, LN-428, U-138 MG, U-87 MG and U-373 MG cells. In addition to vector-containing *FUBP1*-specific shRNA, the scrambled shRNA served as a control. *FUBP1*-specific shRNA led to a significant downregulation of FUBP1 protein levels in all the cell lines (Figure 7).

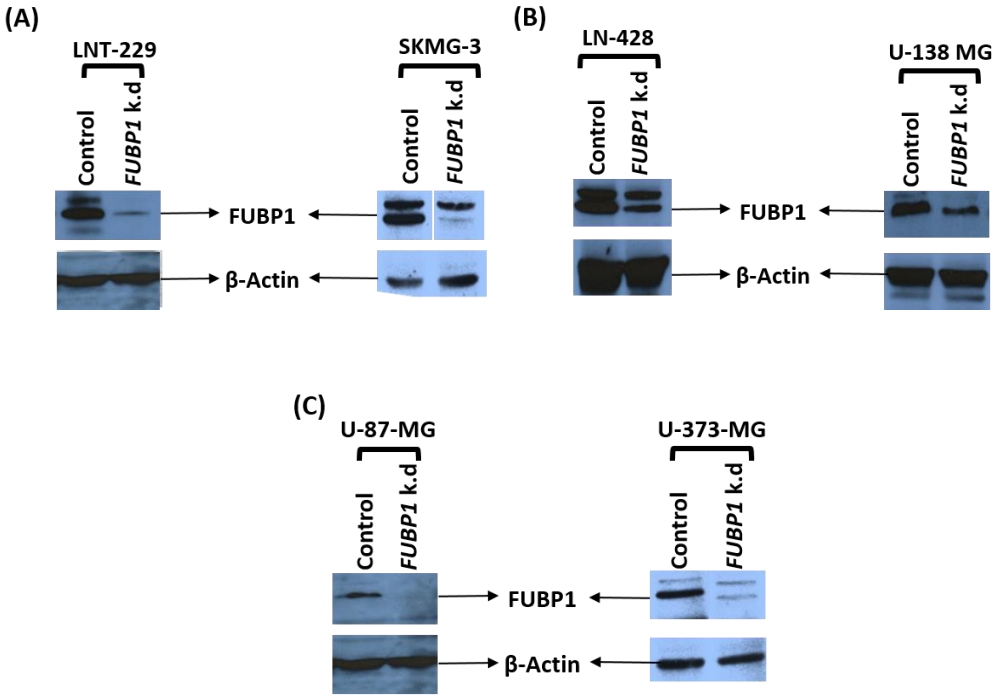

Figure 7: Knockdown of FUBP1 expression in the glioblastoma cell lines LNT-229, SKMG-3, LN-428, U-138 MG, U-87 MG and U-373 MG.

LNT-229, SKMG-3 (A), LN-428, U-138 MG (B), U-87 MG & U-373 MG (C) cells were transduced with lentiviral particles containing either empty *pSEW* vector or *pSEW-FUBP1* shRNA. Following two passages after transduction, the knockdown efficiency was tested by immunoblotting with a FUBP1-specific antibody. Transduction of *FUBP1*shRNA led to a strong downregulation of the FUBP1 protein. 80 µg of each cell lysate was loaded for Western blot analysis. β-Actin was visualized as a loading control.

3.3 Consequences of the *FUBP1* knockdown on apoptosis rates in the glioblastoma cell lines LNT-229, SKMG-3, LN-428, U-138 MG, U-87 MG and U-373 MG.

Inhibition of apoptosis is one of the major events contributing to cancer progression. The knockdown of *FUBP1* has already been shown to enhance apoptosis in HCC cells. Glioblastoma cells are resistant to many apoptotic stimuli. LNT-229, SKMG-3, LN-428, U-138 MG, U-87 MG and U-373 MG cells stably transduced with empty *pSEW* vector and *pSEW-sh2FUBP1* were treated with 250 ng/mL TRAIL and 2.5 µM MG132 for the induction of apoptosis. After incubation for 6-7 hours, cells were harvested and fixed with ethanol. The percentage of apoptotic cells was determined by propidium iodide staining followed by flow cytometric analysis. LNT-229, SKMG-3, LN-428, U-138 MG *FUBP1*- deficient cells displayed a significantly higher percentage of apoptotic cells compared to control cells (Figure 8 (A), (B), (C) & (D)). In contrast, U-87 MG and U-373 MG cells bearing the *FUBP1* knockdown were much more resistant to apoptotic stimuli compared to control cells (Figure 8 (E) & (F)). To some extent, untreated knockdown cells died to a greater extent than the untreated LNT-229, SKMG-3 and U-138 MG & LN-428 control cells (Figure 8 (A-D). This is not the case in U-87 MG and U-373 MG (Figure 8 (E-F))

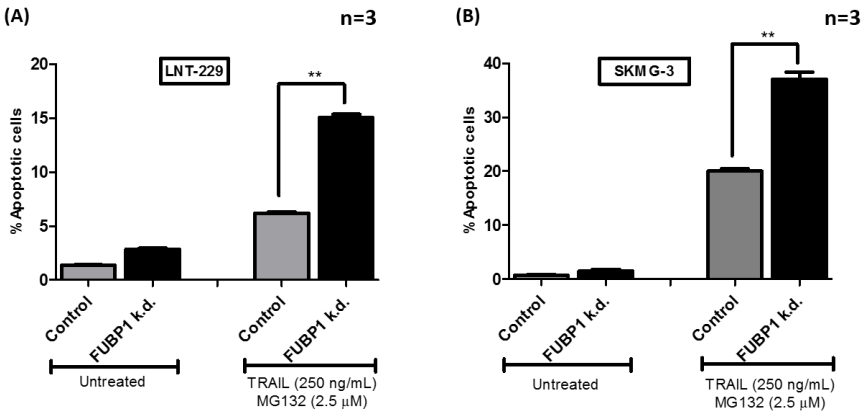

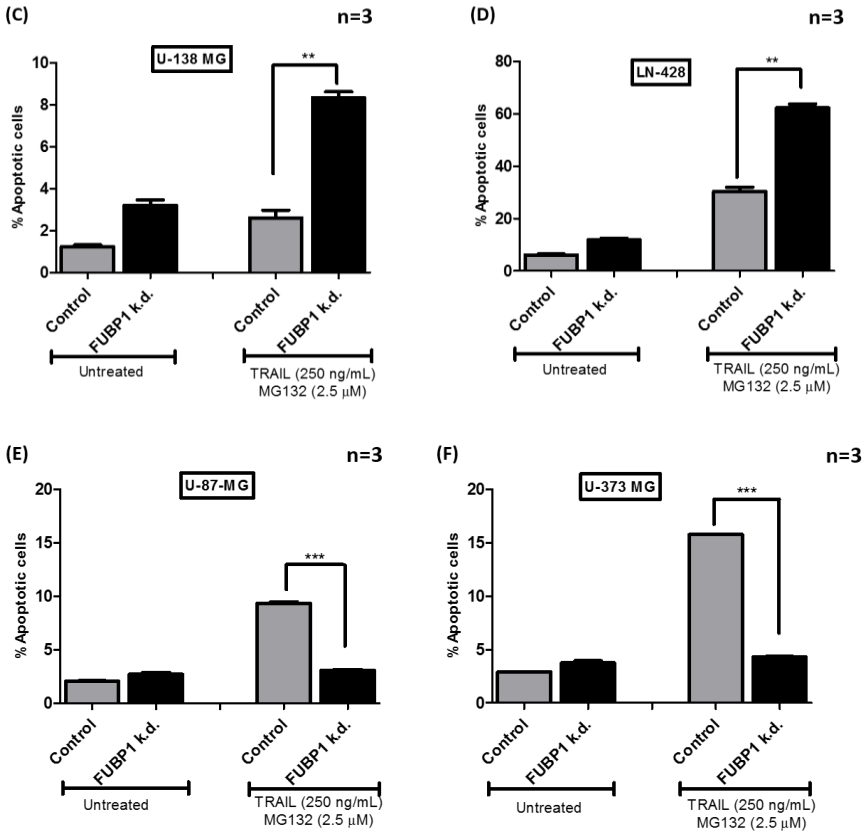

Figure 8: Influence of a *FUBP1* knockdown on apoptosis in LNT-229, SKMG-3, LN-428, U-138 MG, U-87 MG and U-373 MG

3x10^5 LNT-229, SKMG-3, LN-428, U-138 MG, U-87 MG and U-373 MG (*pSEW* vector or *pSEW-FUBP1* shRNA) cells were seeded into six-well plates. 24 hours later, apoptosis was induced by MG132 (2.5 µM) and recombinant TRAIL (250 ng/mL). Cells were harvested after incubation for six hours. Apoptotic cells were identified by staining with propidium iodide, and the dead cells were measured by FACS. Apoptotic cells display a subG1 DNA content. Mean and standard deviation are shown for three independent experiments.
**: p<0.01, ***: p<0.001.

3.4 Consequences of a *FUBP1* knockdown on cell proliferation in the glioblastoma cell lines LNT-229 and U-87 MG

Next, the importance of FUBP1 expression for glioblastoma cell proliferation was tested. LNT-229, LN-428, U-138, U-87 MG and U-373 MG cells stably transduced with empty *pSEW* vector or *pSEW-shFUBP1* were labelled with 10 µM EdU for 1 hour and subsequently fixed, washed, and incubated with Click-iT™ reaction cocktail 30 minutes. Further cells were stained with Alexa Fluro® 647 and analysed using flow cytometer. LNT-229 and LN-428 FUBP1-deficient cells contained significantly less EdU positive cells (corresponding to less cells in the S-phase of the cell cycle during incubation time with EdU) compared to control cells with normal FUBP1 levels. Surprisingly, U-87 MG and U-373 MG cells bearing a *FUBP1*

knockdown comprised more EdU positive cells compared to control cells (Figure 9). However, there was no change in the proliferation rates within control and *FUBP1* knockdown U-138 MG cells.

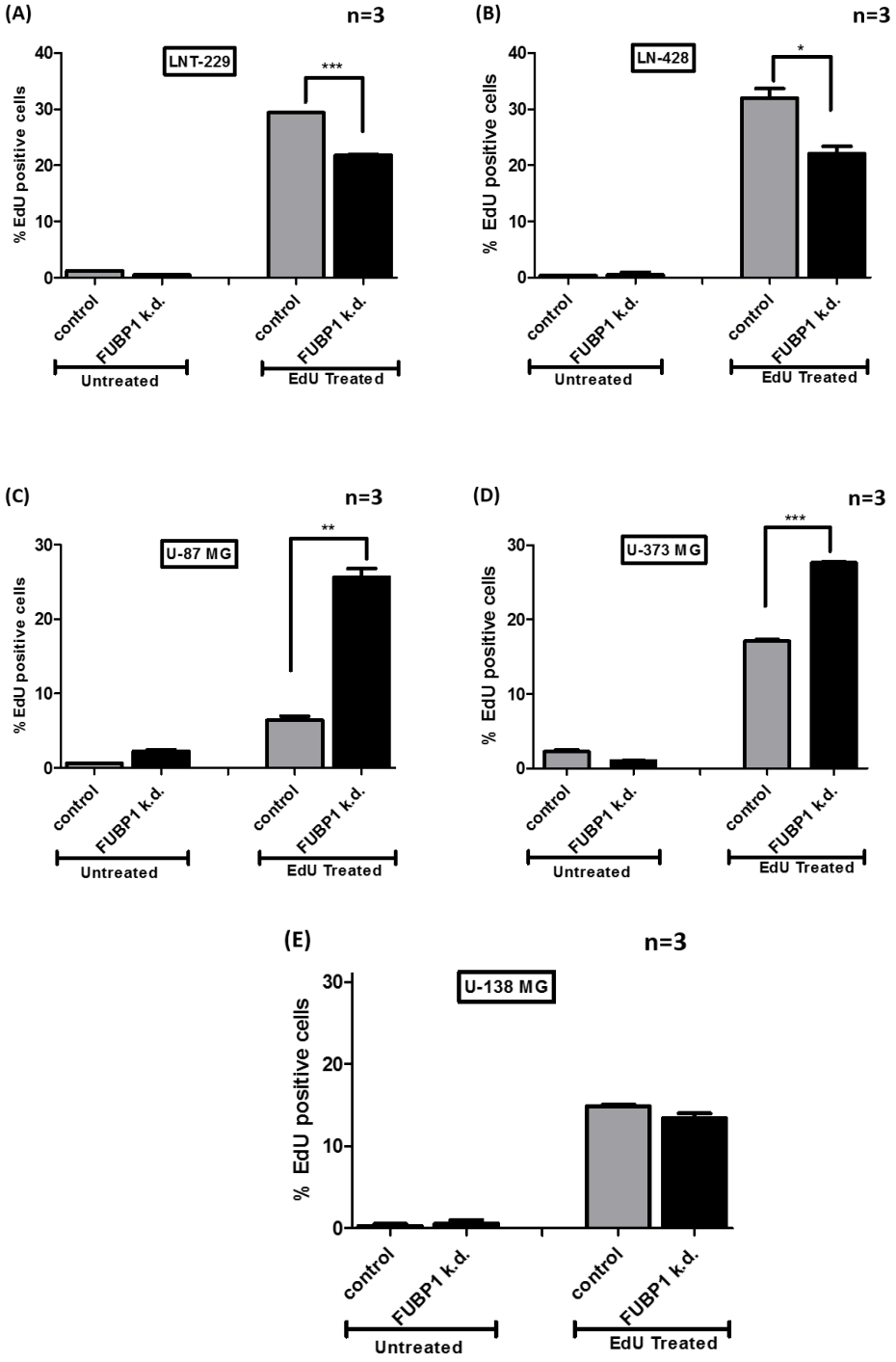

Figure 9: Influence of a *FUBP1* knockdown on cell proliferation in LNT-229 and U-87 MG

$3x10^5$ LNT-229, LN-428 and U-138 MG (*pSEW* vector and *pSEW-FUBP1* shRNA transduced (A, B and E)) and U-87 MG and U-373 MG (*pSEW* vector or *pSEW-FUBP1* shRNA transduced (C and D)) cells were seeded into six well plates. The next day, cells were treated with 10µM EdU for 2 hrs and stained with APC-labelled anti-EdU antibody as described by the manufacturer's protocol. EdU-positive cells were measured by flow cytometry. Mean and standard deviation are shown for three independent experiments. **: $p<0.01$, ***: $p<0.001$.

3.5 FUBP1-deficient U-87 MG cells displayed a higher vascular tube formation capacity compared to LNT-229 *FUBP1* knockdown cells

To investigate the capacity of U-87 MG and LNT-229 cells which had shown opposite effects in the apoptosis and proliferation assays, to undergo vasculogenesis *in cell culture*, I used a matrigel tube formation assay. U-87 MG FUBP1-deficient cells underwent a dramatic re-organization and formed an efficient vasculogenic network of tubular structures within two days. U-87 MG control cells were clustered in groups, and less vascular tube formation was observed as with the cells lacking FUBP1. In contrast, LNT-229 *FUBP1* knockdown cells formed hardly any structures, and all the cells died. LNT-229 control cells showed less events of tubular formation when compared to U-87 MG control cells. In addition, FUBP1- deficient U-87 MG cells, when cultured for a longer time period, formed a higher number of spheroids compared to U-87 MG control cells which might be due to an upregulation of pro-proliferative and/or angiogenic genes upon *FUBP1* knockdown (Figure 10).

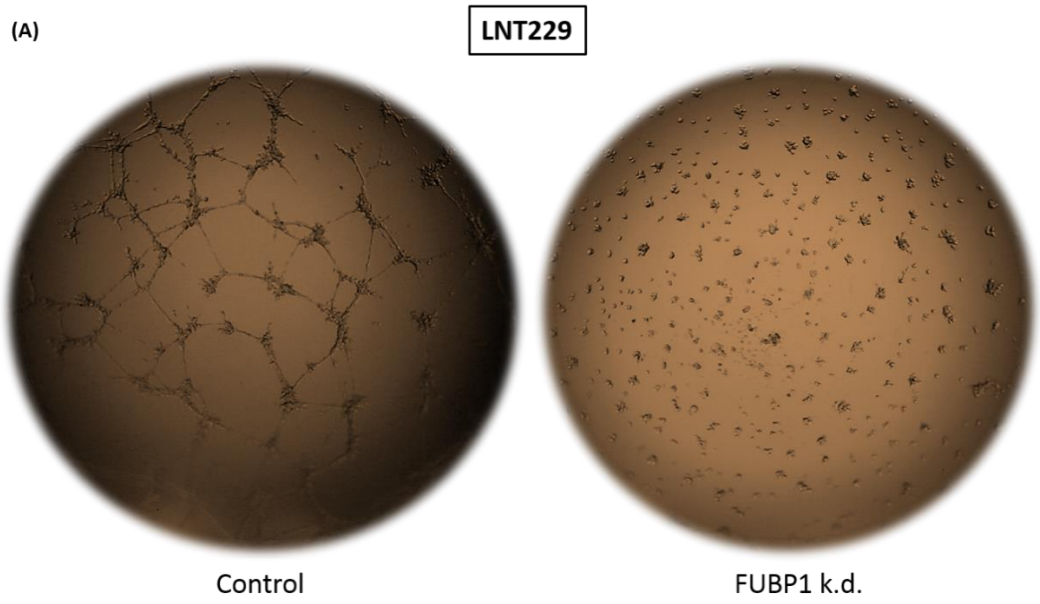

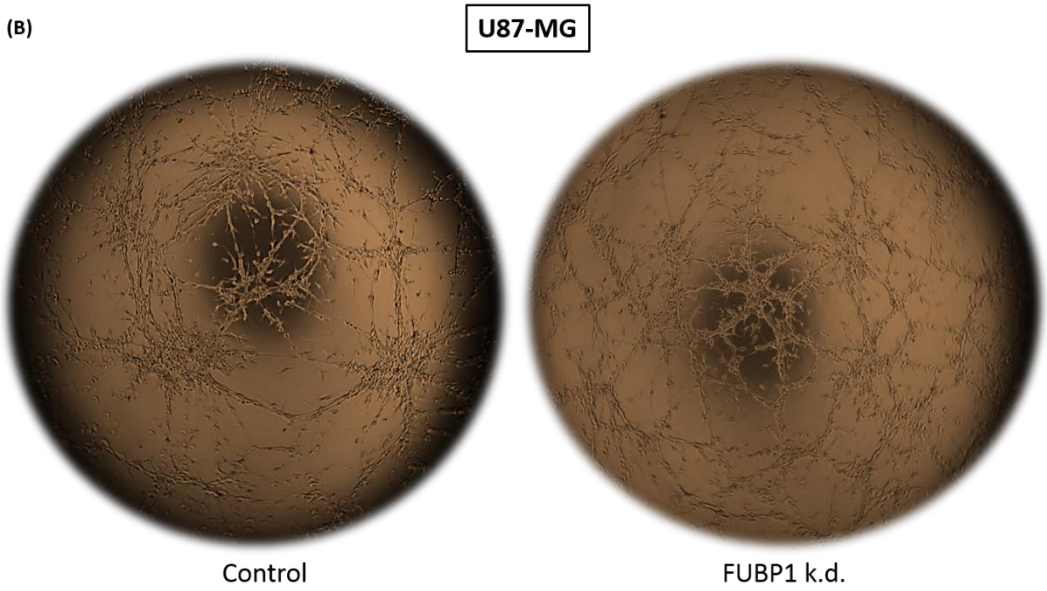

Figure 10: Influence of a *FUBP1* knockdown on vascular tube formation in LNT-229 and U-87 MG

Matrigel was layered on a well of a 24 well plate and incubated until it had become semi-solid. $3x10^5$ LNT-229 (*pSEW* vector or *pSEW-FUBP1* shRNA transduced (A)) or U-87 MG (*pSEW* vector and *pSEW-FUBP1* shRNA transduced (B)) cells were seeded on the matrigel and incubated for 24 hours in serum-free medium. Microscopic pictures were taken, and spheroids and vascular tube formation were observed.

3.6 FUBP1 knockdown accelerated the invasiveness of U-87 MG cells

The invasive properties of glioma cell line with and without FUBP1 knockdown were investigated. For this purpose, a Boyden chamber transmigration assay was performed. Matrigel was layered on the insert and incubated until it became semi-solid. 4×10^5 cells were seeded on top of the Matrigel in serum-free medium, while serum-containing medium was placed in the well below. After 48 hours of incubation, crystal violet staining of the membrane exhibited higher numbers of FUBP1-deficient U-87 MG cells which had invaded through the pores of the transwell membrane, when compared to control cells. LNT-229 *FUBP1* knockdown cells showed a significantly lower invasive capacity compared to control and U-87 MG cells lacking FUBP1 (Figure 11).

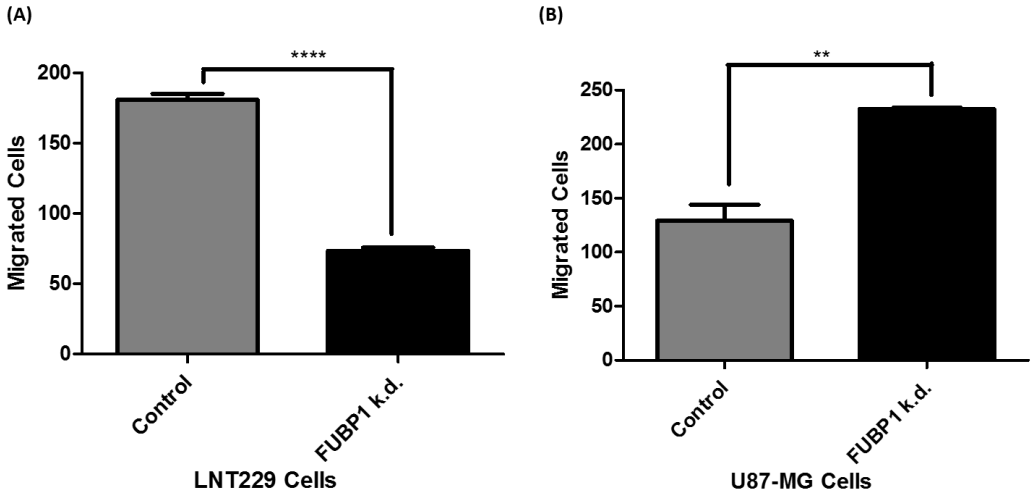

Figure 11: Influence of the *FUBP1* knockdown on cell invasion in LNT-229 and U-87 MG.

Matrigel was layered on the membrane of the transwell insert and incubated until it became semi-solid. $3x10^5$ LNT-229 (*pSEW* vector or *pSEW-FUBP1* shRNA transduced (A)) and U-87 MG (*pSEW* vector and *pSEW-FUBP1* shRNA transduced (B)) cells were seeded in a serum-free medium on top of the Matrigel. The insert was placed in a well with serum-containing medium and incubated for 48 hours. Later, the membrane was stained with crystal violet, pictures were captured with a microscope and invaded cells were counted using ImageJ software. Mean and standard deviation are shown for three independent experiments. **: $p<0.01$, ***: $p<0.001$.

3.7 FUBP1 knockdown accelerated the closure of a scratch in U-373 MG cell monolayer

Because excessive migration is one of the hall marks of glioma cells, a scratch wound assay was performed with LNT-229 and U-373 MG cells. 4×10^5 cells were seeded in serum-free medium in a well of a 24 well plate. 24 hours later a scratch was applied to the cell monolayer using a 1000 µL tip. Cells were washed twice with 1X PBS, to remove the dead or floating cells. 24 hours after scratching, FUBP1-deficeint LNT-229 cells showed a larger uncovered area (60%; Figure 12 (A) & (B)) of the scratch, compared to control LNT-229 cells (40%; Figure 12 (A) & (B)). However, in *FUBP1* knockdown U-373 MG cells, less uncovered area (60%; Figure 12 (C) & (D)) was observed compared to control U-373 MG cells (100%; Figure 12 (C) & (D)).

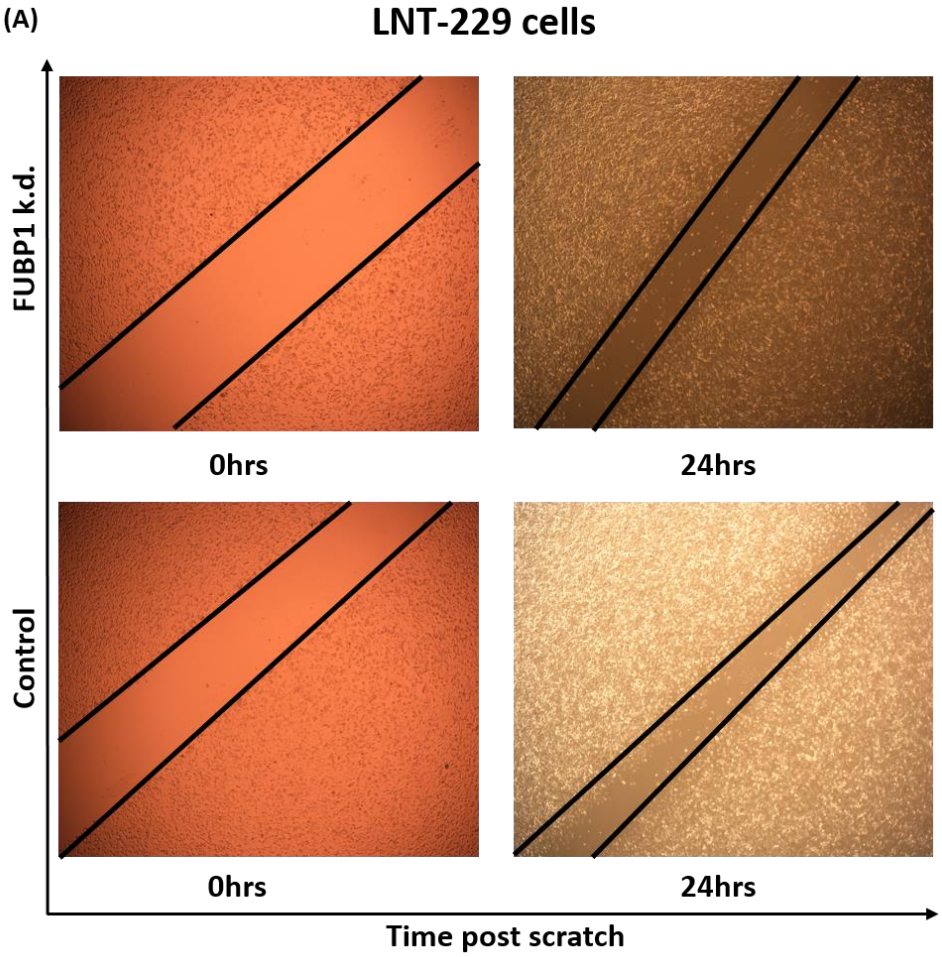
(A)
LNT-229 cells
FUBP1 k.d.
Control
0hrs
24hrs
0hrs
24hrs
Time post scratch

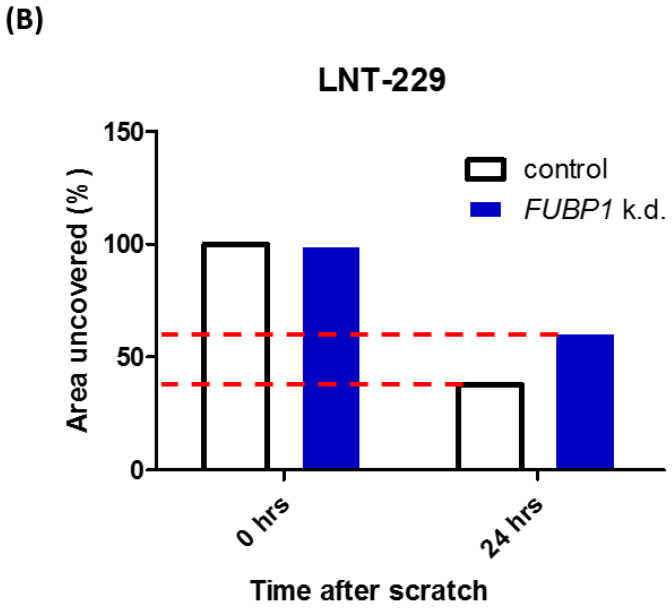
(B)
LNT-229
150
100
50
0
Area uncovered (%)
control
FUBP1 k.d.
0 hrs
24 hrs
Time after scratch

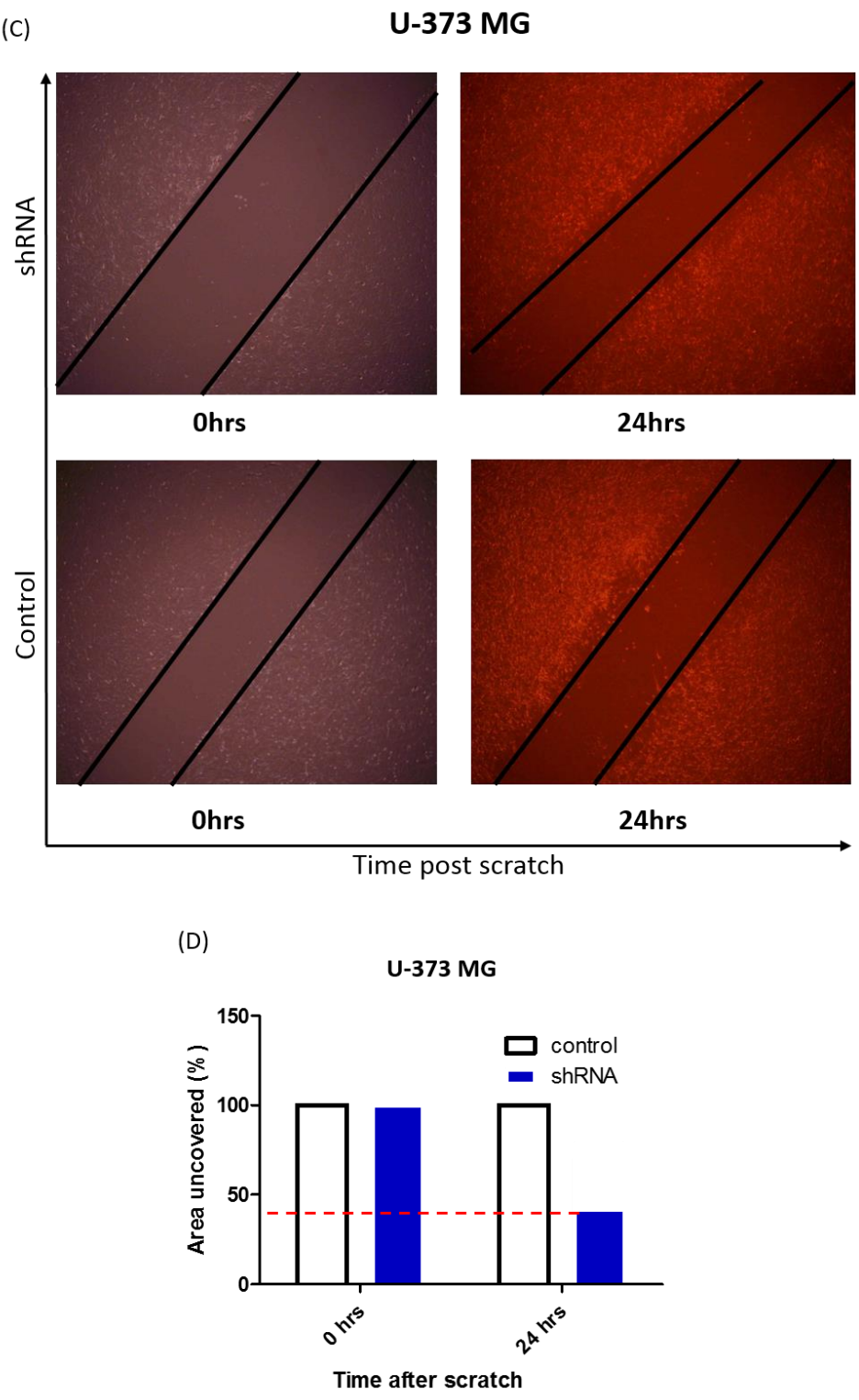

Figure 12: Influence of the *FUBP1* knockdown on the migration potential in LNT-229 and U-373 MG cells.

3x10^5 LNT-229 (*pSEW* vector or *pSEW-FUBP1* shRNA transduced (A)) and U-373 MG (*pSEW* vector or *pSEW-FUBP1* shRNA transduced (C)) cells were seeded in serum-free medium in a 24 well plate. 24 hrs later, a scratch/wound was applied using a 1 mL pipet tip. Cells were washed once with PBS to remove the detached cells; the well was filled again with serum-free media; pictures of the scratch were captured at 0 hrs time point with a microscope, and the cells were incubated. 24 hrs later, pictures were captured again with a microscope, and the area uncovered was measured using ImageJ software.

3.8 Differential functional role of FUBP1 is due to the cell type and not due to its level of expression in cell lines

To identify the key molecules responsible for the differential role of FUBP1 in glioblastoma cells, an *Affymatrix* gene expression array was performed. The analysis revealed that in FUBP1-deficient U-87 MG cells, pro-proliferative genes were up-regulated and a number of pro-apoptotic genes were downregulated. In *FUBP1* knockdown LNT-229 cells, the opposite effect was observed: pro-proliferative genes were downregulated and pro-apoptotic genes were up-regulated. Further, ingenuity pathway and cluster analysis of the array data with Hep3B, HuH7, LNT-229, U-87 MG and U-373 MG was performed. Cluster analysis revealed that the regulation of FUBP1 target genes is comparatively more significant by cell type and not by *FUBP1* knockdown. Ideally in this cluster analysis, all the cell lines in which FUBP1 behaves like an oncogene, i.e. Hep3B and HuH7 and the glioblastoma cell line LNT-229, should cluster together and the cell lines in which FUBP1 acts in an pro-proliferative and anti-apoptotic fashion, the glioblastoma cell lines U-87 MG and U-373 MG, should cluster together. However, the U-373 MG cells clustered together with LNT-229 cells, and U-87 MG cell line clustered together with Hep3B and HuH7 cells, suggesting that the clustering was not based on FUBP1 expression rather on different cell types (Figure 13).

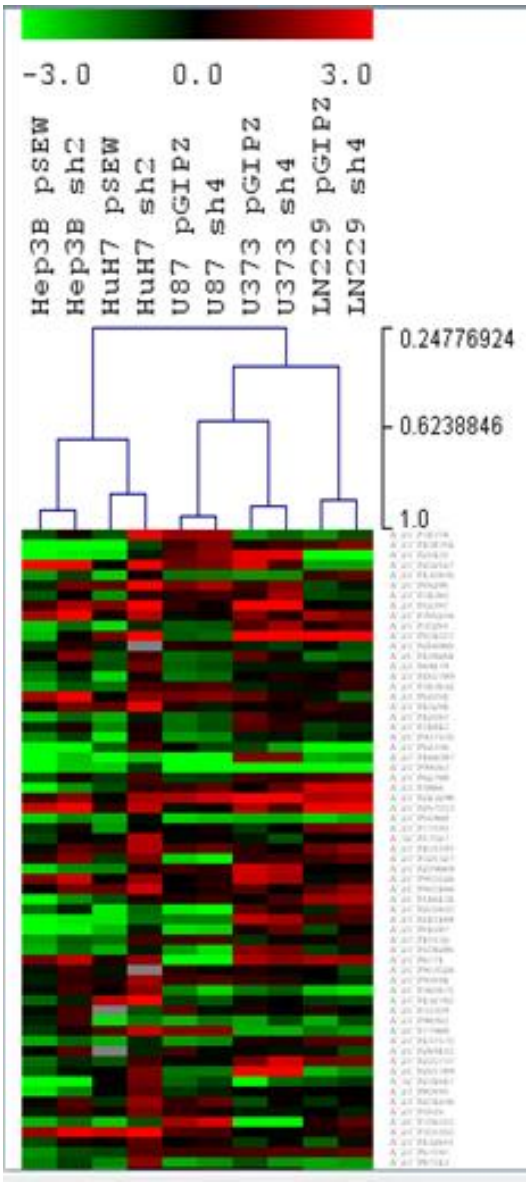

Figure 13: Affymetrix microarray analysis of gene expression profiles in *FUBP1* depleted Hep3B, HuH7, LNT-229, U-87 MG and U-373 MG cell lines.

RNA was isolated from Hep3B, HuH7, LNT-229, U-87 MG and U-138 MG cells that were stably transduced with *pSEW* empty vector or *pSEW-FUBP1 shRNA*. cDNA was transcribed, purified, labelled, fragmented, hybridised, washed and scanned with a laser. Further, clustering analysis of the FUBP1 regulated genes was performed using *Ingenuity*® software. Data from five knockdown cell lines are shown. High expression intensities are represented by red, while low expression intensities are represented by green colour. Black indicates medium intensities.

3.9 *TGFβ-1, MMP9* and *MMP2* influence the fate of FUBP1 in glioblastoma cell lines

Based on cellular proliferation and apoptosis, the highly regulated genes in Affymetrix array upon *FUBP1* knockdown (i.e. *EGR1, IGF-II, TGF-1, MMP9, MMP2* and *AKT*) were selected and further validated by qRT-PCR in LNT-229, U-138, U-

87 MG and U-373 MG cells. The analysis confirmed that the mRNA expression of *TGFβ-1, EGR1, MMP2* and *AKT* was decreased in *FUBP1* knockdown LNT-229 cells compared to control cells (Figure 14 (A)). However, *MMP9* mRNA levels was 3.5 fold upregulated upon *FUBP1* knockdown in LNT-229 cells compared to control cells. Surprisingly, *TGFβ-1* and *MMP2* mRNA expression were elevated in FUBP1-deficient U-87 MG cells compared to the control cells (Figure 14 (B)). *MMP9* mRNA levels was decreased (50%) upon *FUBP1* knockdown in U-87 MG cells compared to control cells. There was a decrease of about 40% in *FUBP1* knockdown LNT-229 cells and about 85% in *FUBP1* knockdown U-87 MG cells.

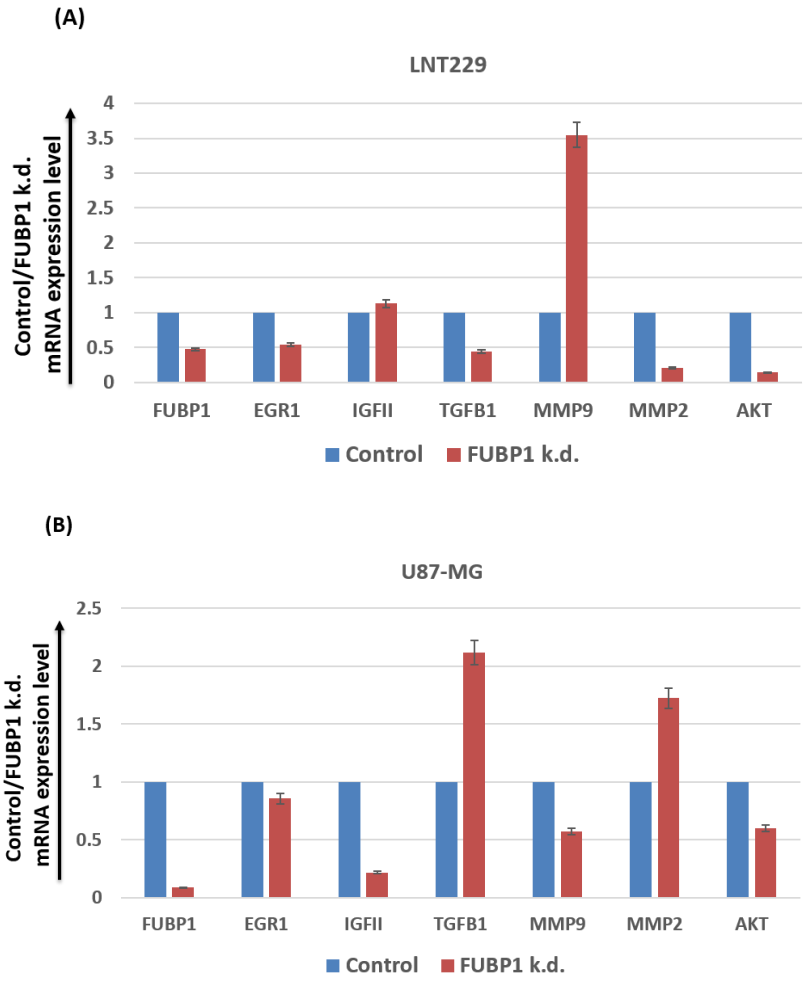

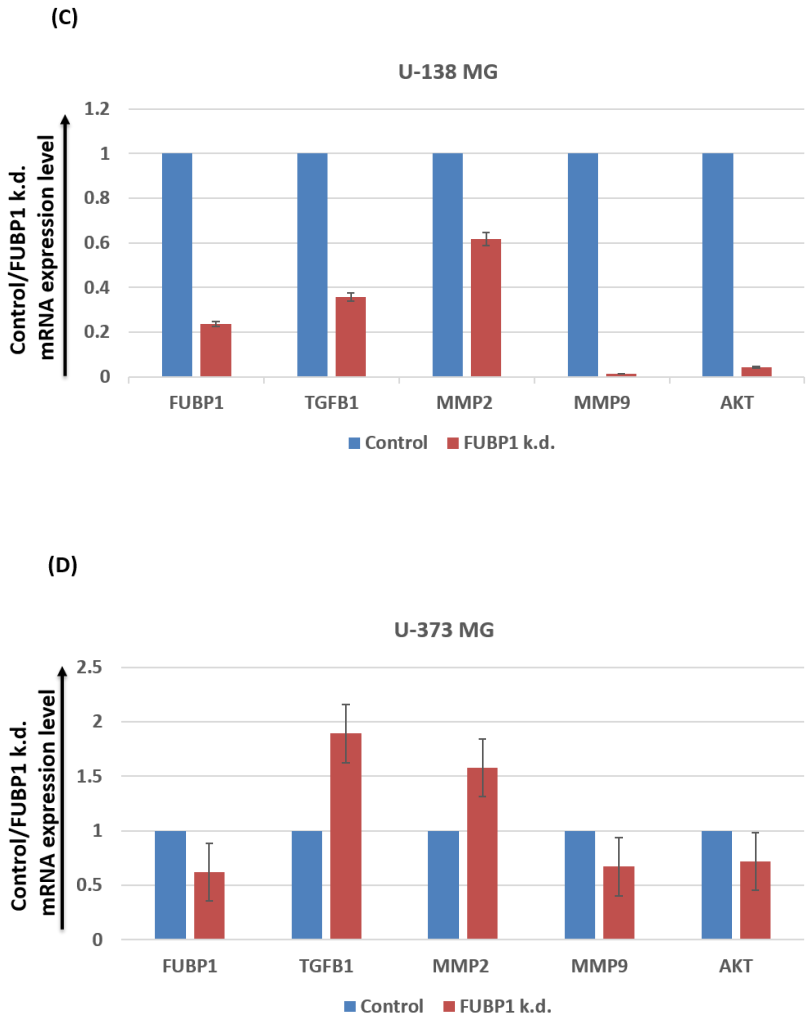

Figure 14: *FUBP1* knockdown influences the expression of TGFβ-1, MMP9 and MMP2 in LNT-229 and U-87 MG

RNA was isolated from LNT-229 (A), U-87 MG (B), U-138 MG (C) and U-373 MG (D) cells that were stably transduced with *pSEW* empty vector or *pSEW-FUBP1 shRNA*. cDNA was transcribed, and quantitative real time PCR was performed using the LightCycler®. Relative mRNA expression levels were calculated by the 2-ΔΔct method using three housekeeping genes (GAPDH, HPRT1 and SDHA) for normalization. Mean and standard deviation are shown for three independent experiments.

3.10 MMP2 is highly expressed in U-87 MG cells in contrast to LNT-229 cells

qRT-PCR results revealed that FUBP1 might have a direct or indirect effect on *MMP2* mRNA expression and might therefore contribute to the differential role of FUBP1 in LNT-229 and U-87 MG cells (Figure 14). For further analysis, *MMP2*-specific shRNAs were cloned into the lentiviral expression vector *pGIPZ.* Lentivirus was produced in HEK-293T cells and was used for stable transduction of LNT-229

and U-87 MG cells. In addition to *MMP2*-specific shRNA, the scrambled shRNA was used as a control. A zymographic assay was performed to evaluate the activity of MMP2 in LNT-229 and U-87 MG cells. MMP2 expression was analyzed using the *ImageJ* software. The analysis revealed that *MMP2*-specific shRNA led to a significant downregulation of MMP2 protein levels, corresponding to the reduction in band intensity in *MMP2* knockdown cells (Figure 15 (A)). According to the quantification, MMP2 levels were higher in U-87 MG cells compared to LNT-229 cells (Figure 15 (B)).

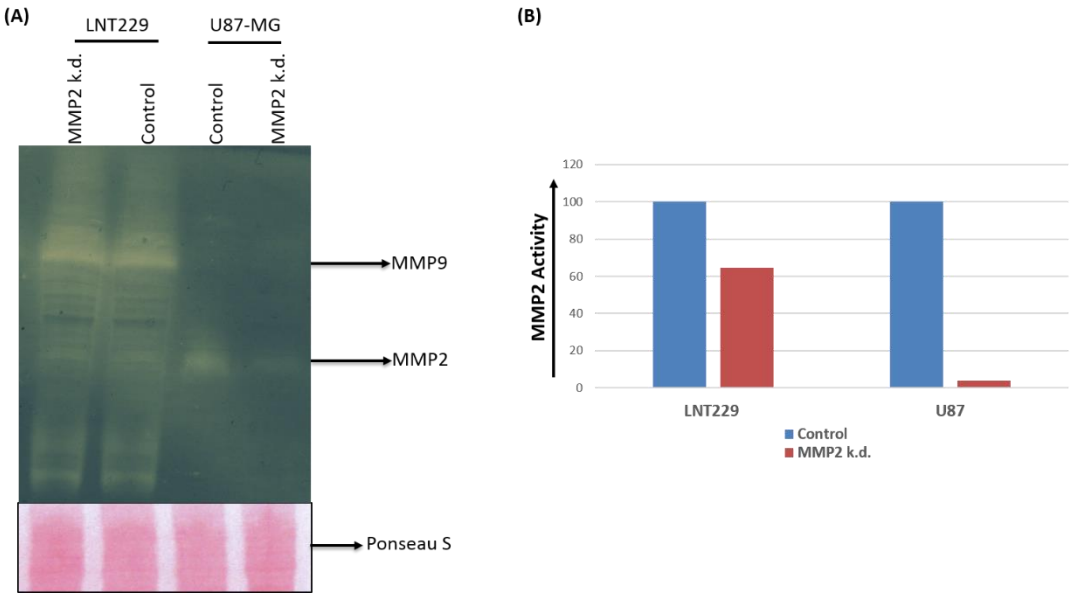

Figure 15: Knockdown of MMP2 expression in the glioblastoma cell lines LNT-229 and U-87 MG

(A) LNT-229 and U-87 MG cells were transduced with lentiviral particles containing either empty *pGIPZ* vector or *pGIPZ-MMP2* shRNA. Following two passages after transduction, knockdown efficiency was tested by zymographic assay. Transduction of *MMP2* shRNA led to a strong downregulation of the MMP2 protein. (B) MMP2 expression was quantified by measuring the band intensity using ImageJ software. 80 µg of each cell lysate were loaded for Western blot analysis. Ponseau S staining was used as a loading control. The experiment was performed once.

3.11 MMP2 acts upstream of FUBP1 and inhibits *FUBP1* mRNA expression in U-87 MG cells

Previous studies suggest that MMP2 had been involved in pro-proliferative functions and under certain conditions can also activate the proliferative signalling cascade allowing the cells to acquire more metastatic and invasive characteristics.

qRT-PCR results reveal that MMP2 might be responsible for the differential role of FUBP1 in U-87 MG and LNT-229 cells (Figure 14). In order to collect further evidence for this, *MMP2* knockdown was performed in U-87 MG cells, and *FUBP1* expression was quantified using the FUSION system. The analysis revealed that FUBP1 protein expression was increased by two fold upon *MMP2* knockdown (Figure 16). This observation led us to the assumption that MMP2 acts upstream of FUBP1 and might have an important role in regulating the expression of FUBP1 in U-87 MG cells. Whether, the inhibition of FUBP1 by MMP2 is of a direct or indirect effect is still unclear.

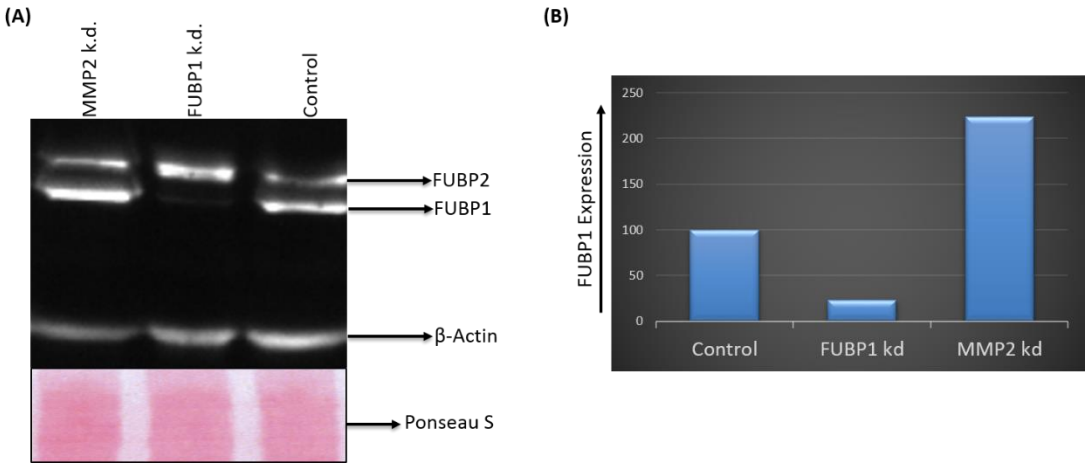

Figure 16: *MMP2* knockdown increases FUBP1 protien expression by two fold in U-87 MG cells

(A) U-87 MG cells were transduced with lentiviral particles containing either empty *pGIPZ* vector, *pGIPZ-FUBP1* shRNA or *pGIPZ-MMP2* shRNA. Following two passages after transduction, FUBP1 expression was tested by western blotting using an antibody against FUBP1. (B) FUBP1 expression was quantified by measuring the band intensity using the FUSION software. 80 µg of each cell lysate were loaded for western blot analysis. β-Actin was used as a loading control.

3.12 FUBP1 knockdown increases MMP2 levels and simultaneously inhibits MMP9 in U-87 MG-like glioblastoma cells

Western blot results (Figure 16 (A)) revealed that the knockdown of MMP2 increases FUBP1 levels in U-87 MG cells. I was interested to test the effect of a *FUBP1* knockdown on MMP2 activity in further glioblastoma cell lines. LNT-229, U-138 MG, U-87 MG and U-373 MG cells were stably transduced with empty *pSEW* vector and *pSEW-sh2FUBP1*. Cells were analyzed for *FUBP1* expression

(Figure 7 (A, B, C)) and a zymographic gel was prepared and run to quantify the activity of MMP2 and MMP9. LNT-229 and U-138 MG cells showed a decrease in *MMP2* activity and an increase in MMP9 activity upon *FUBP1* knockdown (Figure 17 (A)). FUBP1-deficient U87-MG and U-373 MG cells showed the opposite effect, i.e. an increase in MMP2 activity and a decrease in MMP9 activity (Figure 17 (B)). These results correlated with the findings obtained by qRT-PCR (Figure 14 (A, B, C, D)).

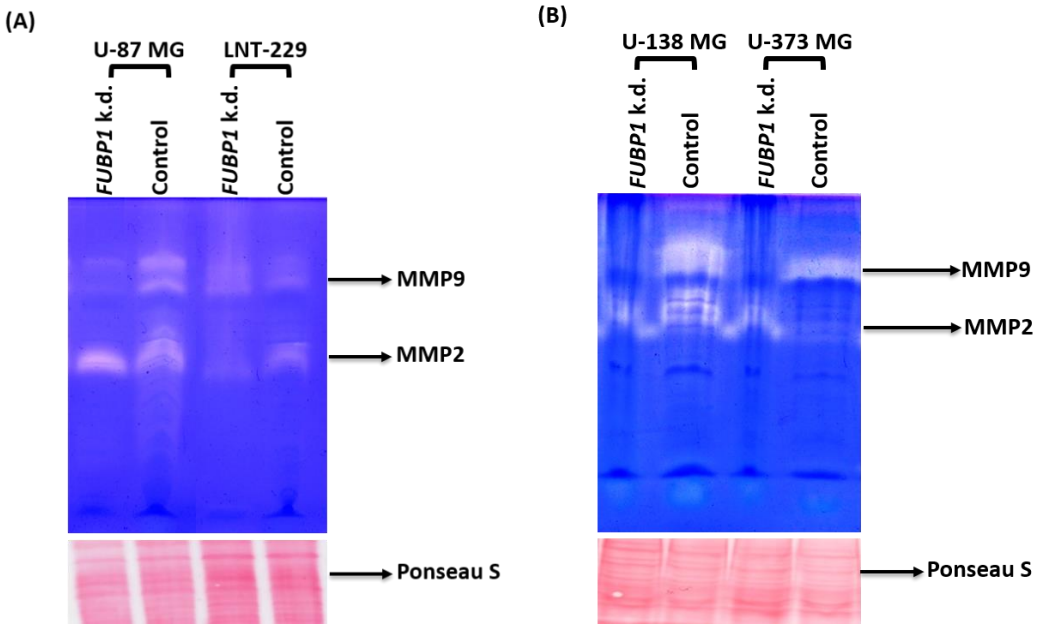

Figure 17: Influence of a *FUBP1* Knockdown on MMP2 & MMP9 expression in the glioblastoma cell lines LNT-229, U-138 MG, U-373 MG and U-87 MG

(A) LNT-229 and U-87 MG cells were transduced with lentiviral particles containing either empty *pGIPZ* vector or *pGIPZ-FUBP1* shRNA. Following two passages after transduction, MMP2 activity was tested by a zymographic assay. Transduction of *FUBP1* shRNA led to a strong downregulation of MMP2 activity and an increase in MMP9 activity in LNT-229 and U-138 MG cells (A & B). In *FUBP1* knockdown U-87 MG and U-373 MG cells, MMP2 levels were upregulated and MMP9 levels were downregulated (A and B). 80 µg of each cell lysate were loaded for Western blot analysis. Ponseau S staining was used as a loading control.

3.13 The AKT1 pathway is activated in U-87 MG cells and might be responsible for pro-proliferative properties upon *FUBP1* knockdown

qRT-PCR data suggest that the *FUBP1* knockdown decreases *AKT1* mRNA levels in LNT-229 and U-87 MG cells. However, *AKT1* was still highly expressed in *FUBP1* knockdown U-87 MG cells compared to LNT-229 cells (Figure 14 (A) & (B)). Further, I investigated the expression of AKT and that of other molecules involved in the AKT pathway in LNT-229 and U-87 MG cells with respect to *FUBP1* knockdown. Western blot results revealed that AKT pathway members i.e. PDK1, AKT, p-AKT (T308), p-AKT (s473) and p-GSK3β (s9) are active (phosphorylation of (a) tyrosine at 308 and serine at 473 in p-AKT (b) serine at 9 in p-GSK3β) and show reasonable/moderate expression in U-87 MG cells compared to LNT-229 cells (Figure 18). However, no significant difference between control U-87 MG cells and FUBP1-deficient U-87 MG cells could be detected in PDK1, AKT, p-AKT (T308), p-AKT (s473) and p-GSK3β (s9).

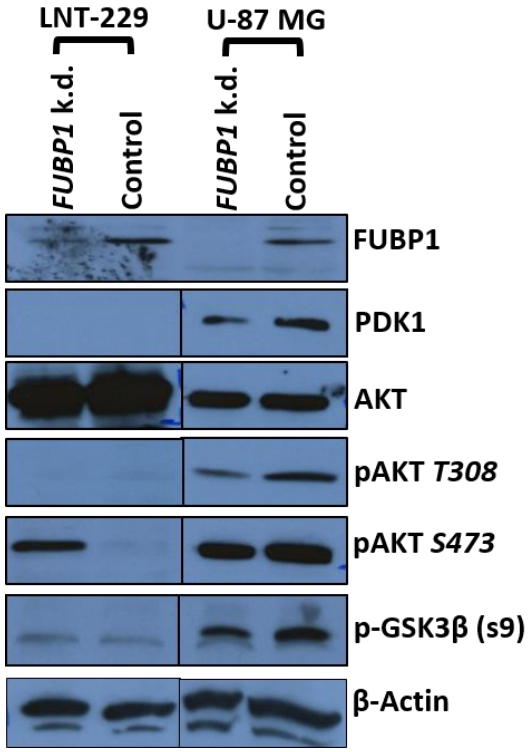

Figure 18: *FUBP1* knockdown influences AKT and that of other molecules involved in the AKT pathway expression in the glioblastoma cell line U-87 MG

LNT-229 and U-87 MG cells were transduced with lentiviral particles containing either empty *pSEW* vector (Control) or *pSEW-FUBP1* shRNA (*FUBP1* k.d.). Two passages after transduction, the expression of PDK1, AKT, p-AKT (T308), p-AKT (s473) and p-GSK3β (s9) was tested by immunoblotting with the appropriate specific antibodies. 80 µg of each cell lysate was loaded for Western blot analysis. β-Actin was visualized as a loading control.

3.14 Consequences of *FUBP1* knockdown in glioblastoma cell lines in a mouse xenograft transplantation tumour model

The *in vitro* data above suggests a functional relevance for the role of FUBP1 as an oncogene in glioblastoma. To verify this hypothesis, LNT-229 and U-87 MG cells stably transduced with empty *pSEW* vector or *pSEW-shFUBP1* were injected into the flanks of immunocompromised NOD/SCID mice. Tumor growth was monitored over a period of four weeks.

U-87 MG *FUBP1*-deficient tumors grew significantly faster than control tumors (Figure 19 (B)). Interestingly, LNT-229 *FUBP1* knockdown tumors expanded slower than control tumors (Figure 19 (A)). These findings confirmed that FUBP1 expression is required for tumor growth in LNT-229 cells and they support the cellculture data described above. The experiment with U-87 MG cells was performed by Dr. Bettina Schwamb, group of Prof. Dr. Martin Zörnig, Georg-Speyer-Haus, Frankfurt.

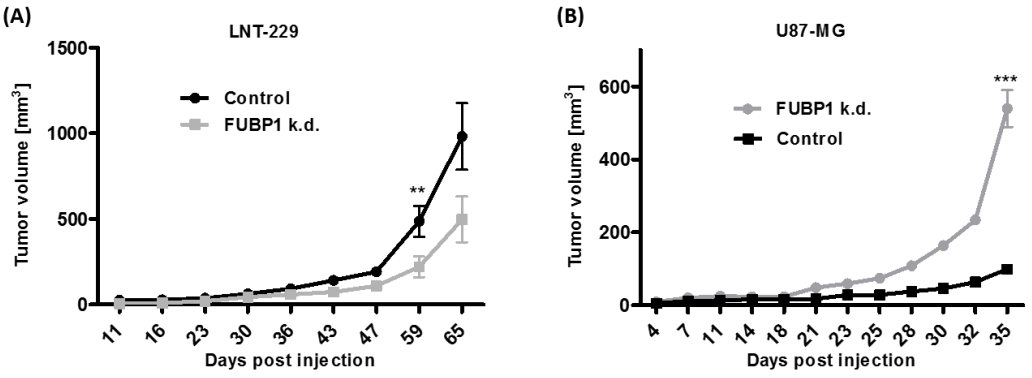

Figure 19: FUBP1 knockdown reduces/promotes tumor growth of LNT-229/U-87 MG cells in a xenograft transplantation model

$7x10^6$ stably transduced LNT-229 (A) and U-87 MG (B) cells were subcutaneously injected into the flanks of 5-6 weeks old immunodeficient NOD-SCID mice. Tumor volume was measured using callipers. 10 mice were used for each group. Data is presented as median ± standard error. On day 59 for LNT-229 and on day 35 for U-87 MG there has been significant difference.

**: $p<0.01$, ***: $p<0.001$.

3.15 Overexpression of FUBP1 in Hep3B cells

Previous studies revealed that silencing *FUBP1* mRNA expression reduced tumour growth in Hep3B cells and that FUBP1 might represent a therapeutic target for HCC. We wanted to test whether FUBP1 can be further overexpressed in Hep3B cells. In order to achieve that, Hep3B cells were infected with FLAG-tagged adenoviral vector. From the western blot and qRT-PCR results (Figure 20), we concluded that upon adenoviral infection with *FUBP1* cDNA vectors, *FUBP1* mRNA levels were significantly increased but not FUBP1 protein levels. This led us to hypothesize and investigate whether miRNAs might play an important role in repressing the expression of *FUBP1*.

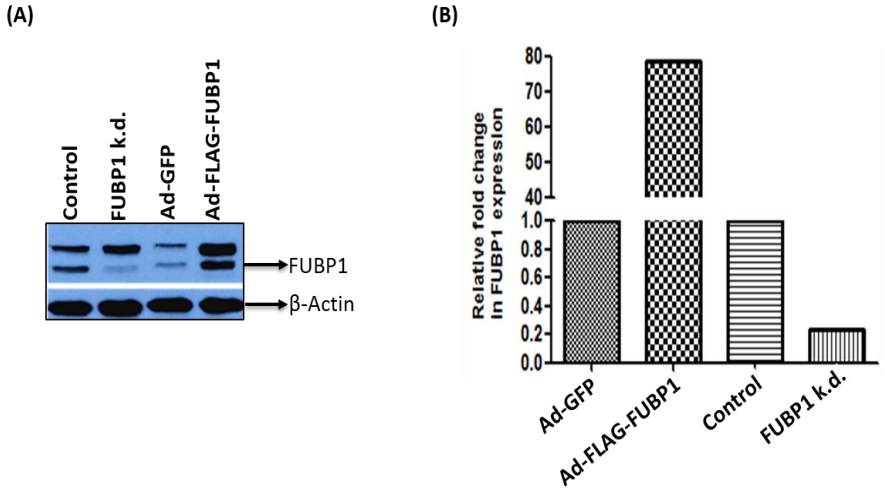

Figure 20: Overexpression and Down-regulation of endogenous FUBP1 levels in Hep3B cells

(A) Hep3B cells were infected with adenoviral particles containing either control Ad-GFP, FLAG tagged Ad-FLAG-FUBP1, empty *pSEW* vector or *pSEW-FUBP1* shRNA. Following two passages after infection, knockdown and overexpression efficiencies were tested by immunoblotting with a FUBP1-specific antibody. Transduction of *FUBP1* shRNA led to a strong downregulation of FUBP1 protein levels. However, no FUBP1 overexpression was detected in *Ad-FLAG-FUBP1*-transduced Hep3B cells. β-actin was used as a loading control. (B) qRT-PCR analysis confirmed that the *FUBP1* mRNA levels were significantly reduced in *FUBP1* shRNA-transduced Hep3B cells compared with the empty vector-transduced cells (pSEW). Surprisingly, there was a significant overexpression of *FUBP1* mRNA levels in Hep3B cells transduced with *Ad-FLAG-FUBP1*.

*The experiment was performed once. n=1

3.16 Effect of *FUBP1* knockdown on miRNA regulation in Hep3B cells

To investigate whether FUBP1 regulates miRNA expression in HCCs, a custom-made miRNA array kit (Carlo Croce's lab, The Ohio state University, USA) was hybridized to identify miRNAs deregulated in Hep3B cells. The expression of different miRNAs in *pSEW-shFUBP1* and empty *pSEW* -transduced Hep3B cells was compared. The analysis of the miRNA array data led to the identification of 62 differentially regulated miRNAs in Hep3B cells. The majority of miRNAs affected by the *FUBP1* knockdown were down-regulated in Hep3B cells, and according to the literature, several miRNAs implicated in the development of a variety of tumor entities. Based on the literature survey and their relevance to HCC, 14 miRNAs were selected for further analysis (Table 32). The data obtained with *FUBP1* knockdown Hep3B cells were further analysed.

Table 32: miRNAs which have been related to HCC and which are differentially expressed upon *FUBP1* knockdown

miRNA
hsa-miR-1
has-miR-15a
hsa-miR-17
hsa-miR-21
hsa-miR-23a
hsa-miR-26a
hsa-miR-30d
hsa-miR-100
hsa-miR-146a
hsa-miR-199b
hsa-miR-219
hsa-miR-330
hsa-miR-422a
hsa-miR-613
hsa-miR-495

3.17 Prediction of miRNA binding sites located in the 3'UTR of the *FUBP1* gene

As endogenous expression of FUBP1 appears under strict transcriptional control (Figure 20), FUBP1 overexpression is not achieved upon transfection/transduction of *FUBP1* cDNA. We hypothesised that miRNAs might play an important role in regulating the expression of FUBP1. Further, we were interested in looking for a

feedback loop mechanism by a particular miRNA which would repress FUBP1 protein. Using the *Target Scan* miRNA target prediction tool, I discovered 8 miRNAs (miR1, miR26a, miR613, miR21, miR199b, miR15a, miR17, miR26a and miR495) which might regulate *FUBP1* by binding to the 3'UTR of the *FUBP1* gene (Figure 21).

miRNA	Seed Region(s) (Nucleotide No.)
has-miR-495	51-57, 92-101, 208-215
has-miR-26a	76-82, 742-749
has-miR-199b	60-70
has-miR-613	237-245
has-miR-1	240-245
has-miR-17	292-297, 313-319
has-miR-21	447-454
has-miR-15a	701-708

Figure 21: Eight miRNAs are predicted to bind to the 3'UTR of the *FUBP1* gene

The Prediction was performed using ***miRanda*** software (http://www.microrna.org/). Only miRNAs that were deregulated in the absence of FUBP1 are shown. miR-26a has two and miR-495 has three potential binding sites, respectively.

3.18 Potential regulation of FUBP1 levels by miRNA binding in the 3'UTR region of *FUBP1* in Hep3B cells

To test whether miRNAs repress *FUBP1* mRNA expression, the *FUBP1* 3′ UTR was cloned into the 3′ UTR region of a luciferase reporter vector downstream of the firefly *luciferase* gene. The constitutively active *Renilla* reporter was co-transfected with the luciferase reporter vector containing either the wild type FUBP1 3'UTR or the FUBP1 3'UTR with mutated miRNA binding sites into Hep3B cells. Transfection of the *FUBP1* 3′UTR luciferase reporter with mutated miRNA binding sites resulted in increased luciferase activity for certain miRNAs (Figure 22) suggesting that certain miRNAs might repress *FUBP1* expression upon binding to its 3′ UTR. Mutated binding sites for miR-17, miR-15, miR-21, miR-26 and miR-495 showed an increase in luciferase activity and might be responsible for repressing *FUBP1* expression in Hep3B cells. The constructs *miR-26-I*, *miR-495 3X* (triple mutant) and *miR-21* showed a three-fold increase in luciferase activity compared to wildtype FUBP1 3'UTR (Figure 22). For miR-26, the FUBP1 3'UTR contains two and for miR-495 three potential binding sites, but only one single mutant of the miR-26 binding site (i.e. miR-26-I), one double mutant of the miR-495 binding site (miR-495-I+II), and the triple mutant (miR-495 3X) of the miR-495 binding site showed increased luciferase activity (Figure 22).

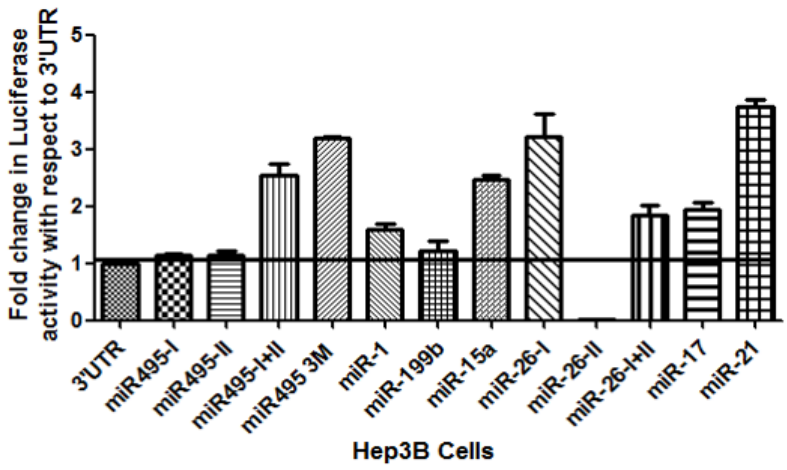

Figure 22: miRNAs regulating *FUBP1* by binding to its 3'UTR

Hep3B cells were cultured in 24-well plates. 24 hrs later, they were co-transfected with wild type or mutated *FUBP1* 3'UTR plasmids, *Renilla* normalization plasmid (*pGL 4.74*) and pcDNA using Attractene (QIAGEN, Hilden, Germany). The *Renilla* normalization plasmid was used to transfect equal amounts of DNA into the cells. Luciferase activity was measured 48 hours post transfection using the Dual-luciferase reporter assay system (Promega).

*The experiment was performed once in triplicates. n=1

4. Discussion

4.1 FUBP1 downregulation in glioblastoma cells regulates apoptosis and proliferation

As a cell culture system for the functional analysis of FUBP1 in glioblastoma cells, the glioblastoma cell lines LNT-229, SKMG-3, LN-428, U-138 MG, U-87 MG and U-373 MG were chosen, and lentiviral shRNA expression was used as a tool for the manipulation of FUBP1 activity. Downregulation of FUBP1 expression was achieved by transduction of the cells with a lentiviral *pSEW* vector construct expressing a shRNA that specifically targets the *FUBP1* mRNA. Upon identification of FUBP1 in a screen for anti-apoptotic genes and confirmation of the anti-apoptotic potential in the hepatocellular carcinoma cell line Hep3B, we could demonstrate an oncogenic function for FUBP1 in HCCs (Rabenhorst, Beinoraviciute-Kellner et al. 2009). Moreover, our group detected a low expression of FUBP1 in astrocytes and demonstrated elevated levels of FUBP1 in glioblastoma, the most common malignant brain tumor in humans. In addition, Prof. Kinzler's laboratory found that inactivating mutations in the genes *CIC* and *FUBP1* contribute to human oligodendroglioma (Bettegowda, Agrawal et al. 2011).
Thus, we suspected that the inhibition of FUBP1 might facilitate a curative gateway for glioblastoma. Therefore, the effect of FUBP1 downregulation on apoptosis sensitivity and proliferation of glioblastoma cell lines was tested. Before quantification of apoptosis, cells were treated with MG-132 (a proteosomal inhibitor) and recombinant TRAIL and they were incubated for 5-6 hours to induce apoptosis. Knockdown of *FUBP1* in the glioblastoma cell lines LNT-229, SKMG-3, LN-428 and U-138 MG led to a significantly increased rate of spontaneous apoptosis relative to control cells (Figure 8). Surprisingly, the FUBP1-deficient glioblastoma cell lines U-87 MG and U-373 MG were resistant to apoptotic stimuli and showed significant reduced apoptosis compared to control cells with normal FUBP1 expression levels.

TRAIL, a member of the tumor necrosis factor/death receptor (DR) gene superfamily can bind to 4 plasma membrane receptors and 1 soluble receptor, that is, TRAIL-R1 (DR4), TRAIL-R2 (DR5/ KILLER), TRAIL-R3 [decoy receptor (DcR)

1], TRAILR4 (DcR2), and osteoprotegerin (Kelley and Ashkenazi 2004). Oligomerisation of the DcR4 and DcR5 receptors leads to formation of the death-inducing signaling complex (DISC), which recruits the adaptor molecule, FADD, and activates Caspase-8 and -10. These activated caspases cleave and activate Caspase-3, which in turn cleaves substrates that commit cells to undergo apoptosis (Wang and El-Deiry 2003). TRAIL resistance may result from a combination of increased AKT activity (Puduvalli, Sampath et al. 2005) and deficient expression of caspases. Therefore, based on the cell type, FUBP1 downregulation increases sensitivity of the cells to apoptosis, and FUBP1 overexpression in glioblastoma cell lines might contribute to tumor formation by inhibition of cell death.

Previously, it was published that FUBP1 expression is required for the proliferation of leukemia (He, Weber et al. 2000) and Hep3B cells (Rabenhorst, Beinoraviciute-Kellner et al. 2009). Activation of *c-myc* expression might be expected in other cell types as well. Stimulation of cell proliferation could provide another mechanism by which FUBP1 overexpression contributes to the formation of glioblastoma. Cell proliferation was measured by EdU (5-ethynyl-2'-deoxyuridine) labelling. Stable transduction with *pSEW-sh2 FUBP1* shRNA led to a decreased percentage of EdU-positive cells compared to control cells in the LNT-229, SKMG-3, LN-428 and U-138 MG cell lines (Figure 9). Thus, less cells were in S-phase during the EdU incubation period. But surprisingly, FUBP1-deficient U-87 MG and U-373 MG cells showed an increased percentage of EdU-positive cells compared to control cell (Figure 9). Collectively, the result confirm that downregulation of *FUBP1* leads to reduced proliferation of glioblastoma cells (LNT-229, SKMG-3, LN-428 and U-138 MG). However, in U-87 MG and U-373 MG cells, FUBP1 might fullfill a special important function relavant for glioblastomas which differs from its role in HCC.

The *in vitro* assays demonstrated that FUBP1 overexpression inhibits apoptosis and stimulates proliferation in most glioblastoma cell lines (LNT-229, SKMG-3, LN-428 and U-138 MG), implying an oncogenic function for FUBP1 in glioblastoma.

4.2 TGFβ-1 and MMP9 regulate FUBP1 expression in glioblastoma cell lines

To test the differential role of FUBP1 in different glioblastoma cell lines, an affymetrix array was performed. Analysis of the array revealed a set of genes which were regulated upon *FUBP1* knockdown (Figure 13). Further qRT-PCR analysis confirmed four genes (i.e. *TGFβ-1, MMP9, MMP2* and *AKT1*) that were highly regulated upon *FUBP1* knockdown (Figure 14). The above-mentioned genes were selected for further analysis based on their involvement in cellular functions like proliferation, apoptosis, migration and invasion in glioblastoma.

In FUBP1-deficient LNT-229 cells, the mRNA levels of *TGFβ-1, MMP2* and *AKT1* were downregulated compared to control cells. The levels of MMP9 were highly elevated in FUBP1-deficient LNT-229 cells compared to control cells. In contrast to LNT-229 cells, *FUBP1* knockdown U-87 MG cells showed increased *TGFβ-1, MMP2* and *AKT1* mRNA levels and decreased *MMP9* mRNA levels compared to control cells.

Angiogenesis is a fundamental process during which new blood vessels are formed (Folkman and Shing 1992, Risau 1997). Highly regulated and transient angiogenesis plays a pivotal role in development, morphogenesis, wound repair, and reproduction (Folkman and Shing 1992, Salamonsen 1994, Risau 1997). Angiogenesis is mainly associated with extracellular remodelling involving different proteolytic systems among which the plasminogen system plays an important role. Plasmin is an important enzyme which degrades many blood plasma proteins including fibrin. It is highly expressed in human brain and blood. MMP7 and MMP9 convert human plasminogen to angiostatin fragments (Patterson and Sang 1997). Angiostatin (a fragment of plasminogen) and endostatin (a fragment of type XVIII collagen) are examples of endogenous inhibitors of angiogenesis (O'Reilly, Holmgren et al. 1994, O'Reilly 1997). Basing on these results we hypothesize that in FUBP1-deficient LNT-229 cells, increased *MMP9* mRNA levels lead to the formation of angiostatin by degrading plasminogen. As a result, reduced cell proliferation was observed. Similarly, in *FUBP1* knockdown U-87 MG cells, decreased *MMP9* mRNA levels lead to a malfunction in the production of angiostatin. As a result, there was an increase in cell proliferation and vascular tube formation capacity.

Transforming growth factor (TGF) - β is a member of a structurally related family of secreted growth factors, which also includes activins and bone morphogenetic proteins (BMPs). TGF-β superfamily members induce many of the biological effects in a context-dependent manner and have been shown to regulate proliferation, differentiation, migration, and apoptosis of many different cell types (Massague 1990, Roberts, Heine et al. 1990). In many cases, cellular perturbations of protein translocation have been reported to lead to alterations in gene expression that in turn leads to disease development (Dreger 2003, Bennett 2005). TGFβ-1 regulates FUBP1 localisation (Milosevic, Bulau et al. 2009). In addition, TGFβ induces p38 MAP kinase phosphorylation and nuclear translocation. Therefore, we speculate that, FUBP1 translocation might be regulated by p38 MAPK activity, as p38 is required for the regulation of FUSE-binding protein and c-myc expression. So, the increase in *TGFβ-1* mRNA levels in FUBP1-deficient U-87 MG cells might be via p38 MAPK signalling. Studies in our lab showed that FUBP1 is exclusively localised in the nucleus of HCC cells (data not shown). Hence, in FUBP1-deficient U-87 MG cells, there is an increase in *TGFβ-1* mRNA levels which further excises it's pro-proliferative and angiogenic functions.

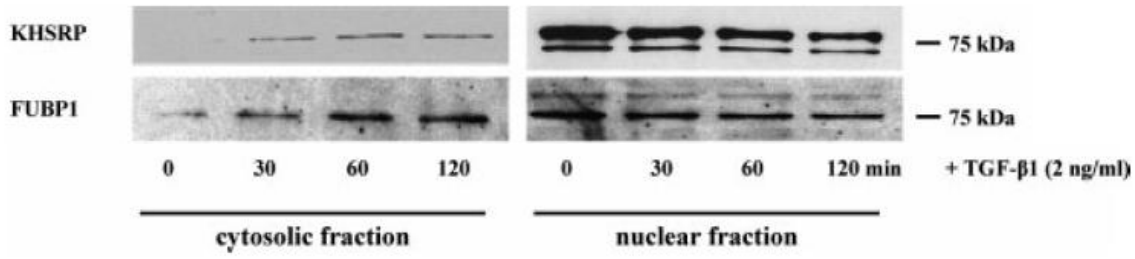

Figure 23: Translocation of FUBP1 after TGFβ-1 stimulation

A549 lung epithelial cells were stimulated with TGFβ-1 (2ng/mL) for the indicated time points. Cytosolic and nuclear fraction were prepared and western blotting was performed (Milosevic, Bulau et al. 2009).

4.3 FUBP1 expression regulates proliferation, migration and invasion in glioblastoma cell lines via MMP2

From our qRT-PCR results we know that MMP2 might be an important candidate for explaining the differential role of FUBP1 in glioblastoma cell lines. In FUBP1-deficient U-87 MG cells, there is an increase in *MMP2* mRNA levels compared to control cells. But in *FUBP1* knockdown LNT-229 cells, there is a decrease in *MMP2*

mRNA levels compared to control cells. Matrix metalloproteinases (MMPs) are a family of calcium-dependent zinc-containing endopeptidases, which are responsible for the tissue remodelling and degradation of the extracellular matrix (ECM). Degradation of the ECM by MMPs not only enhances tumour invasion, but also affects tumour cell behaviour and leads to cancer progression. Most human MMPs can be grouped into four main subclasses on the basis of substrate specificity, protein-domain structure and sequence homology (Shingleton, Hodges et al. 1996). Studies suggest strong correlations between increased MMP levels and tumour-cell invasion in human gliomas. MMPs enhance tumour-cell invasion by degrading extracellular- matrix proteins, activating signalling cascades that promote motility and solubilizing ECM-bound growth factors (McCawley and Matrisian 2001). In addition, MMPs can cleave and activate growth factors that are implicated in glioblastoma motility and proliferation, such as TGFβ (Platten, Wick et al. 2001). TGFβ-1 up-regulates these MMPs in cultured human keratinocytes (Salo, Lyons et al. 1991) and human fibroblasts (Overall, Wrana et al. 1991). Rooprai et al. have showed in their study that in glioma cells MMP2 expression is directly related to TGFβ1 levels. There is a significant increase in MMP2 levels when induced with TGFβ-1 (Figure 24).

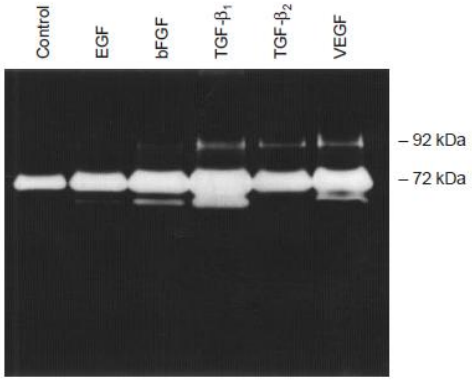

Figure 24: Zymogram gel representing MMP2 expression when induced with growth factors

A zymographic assay was performed using the glioma cell line IPAB-AO3, to investigate the effect of various growth factors on MMP2 expression. The intense band at 72 kDa represents MMP2, and the less intense band at 92 kDa represents MMP9 (Rooprai, Rucklidge et al. 2000).

To test whether MMP2 has a potential role in executing the pro-proliferative, pro-angiogenic functions of FUBP1 and whether it is involved in regulating the expression of FUBP1 in U-87 cells, a zymographic assay was performed. The zymogram gel revealed that the activity of MMP2 is higher in U-87 MG cells compared to LNT-229 cells, which correlated with the qRT-PCR data. To test the effect of *FUBP1* knockdown on the cellular invasion and migration potential, a matrigel invasion assay and a scratch wound assay were performed. In both

assays, FUBP1-deficient U-87 MG cells invaded and migrated more intensively compared to control cells. However, in LNT-229 cells, *FUBP1* knockdown cells showed a lower invasion and migration capacity compared to control cells (Figure 11, Figure 12).

In addition, the vascular tube formation capacity of the glioblastoma cell lines (LNT-229 and U-87 MG) in the presence and absence of FUBP1 was investigated. FUBP1-deficient LNT-229 cells failed to form tubular-like structures compared to control cells, whereas *FUBP1* knockdown U-87 MG cells formed clean tubular-like structures (Figure 10). The increase in MMP2 levels in the FUBP1-deficeint U-87 MG cells may be the reason for the elevated proliferation, migration and invasion.

4.4 A potential feedback loop exists between FUBP1 and MMP2

From the zymographic assay it was evident that the MMP2 activity was higher in U-87 MG cells compared to LNT-229 cells (Figure 15). In order to test and reverse the *FUBP1* knockdown phenotype in U-87 MG cells, MMP2 activity was inhibited using a shRNA targeting MMP2. Surprisingly, FUBP1 protein levels were increased two-fold upon *MMP2* knockdown in U-87 MG cells (Figure 16). Interestingly, there was no difference observed in FUBP1 protein levels in MMP2-deficient LNT-229 cells compared to control LNT-229 cells. Furthermore, MMP2 and MMP9 levels were investigated upon *FUBP1* knockdown in U-87 MG cells. FUBP1-deficient U-87 MG cells showed a higher MMP2 activity and a lower MMP9 activity compared to control U-87 MG cells (Figure 17), on the other hand, *FUBP1* knockdown LNT-229 and U-138 MG cells showed a higher MMP9 activity and lower MMP2 activity compared to control cells. These results strongly suggest that there is a feedback loop mechanism between FUBP1 and MMP2 in U-87 MG cells which might also contribute to the differential role of FUBP1 in U-87 MG and LNT-229 cells.

The results showed an increase in MMP2 levels both on mRNA and protein levels upon *FUBP1* knockdown in U-87 MG cells, which might represent an important factor for the increased proliferation, invasion, migration and the decreased apoptosis sensitivity of FUBP1-deficient U-87 MG cells. To reverse the phenotype, simultaneous knockdown of MMP2 and FUBP1 was performed in U-87 MG cells, and functional assays were investigated. Apoptosis assays revealed that a

MMP2/FUBP1 double knockdown in U-87 MG cells showed higher apoptotic rates compared to control and *FUBP1* single knockdown U-87 MG cells.

4.5 AKT1 signalling is active in U-87 MG cells but completely absent in LNT-229 cells

From qRT-PCR results we know that *AKT1* might be one important candidate to explain the differential role of FUBP1 in glioblastoma cell lines. In FUBP1-deficient U-87 MG cells, higher *AKT1* mRNA levels were observed compared to FUBP1-deficient LNT-229 cells. However, in *FUBP1* knockdown LNT-229 cells, *AKT1* mRNA levels were lower than in control cells and FUBP1-deficient U-87 MG cells. From the apoptosis assays, we could conclude that *FUBP1* knockdown U-87 MG cells were highly resistance to TRAIL and MG132. TRAIL resistance may result from a combination of increased AKT1 activity (Puduvalli, Sampath et al. 2005) and deficient expression of caspases. In order to test the involvement of AKT1 and its pathway members in the regulation of FUBP1 in different glioblastoma cell lines, we investigated the AKT-pathway in the presence and absence of *FUBP1*. Results revealed that the AKT-pathway was completely silent in LNT-229 cells, whereas in U-87 MG cells, the AKT1-pathway was active. As LNT-229 cells express a wildtype PTEN, this might be the reason for the shutdown of AKT-pathway. Since U-87 MG cells harbor mutant PTEN, this would inhibit the formation of PDK1 and the downstream members of AKT-pathway.

4.6 FUBP1 overexpression is required for tumor growth in LNT-229 cells

To test whether FUBP1 is of functional importance for the formation of solid tumors *in vivo*, LNT-229 and U-87 MG cells transduced with scrambled lentiviral *pSEW* vector or the shRNA construct *pSEW-sh2 FUBP1* were subcutaneously injected into the flanks of immunodeficient NOD/SCID mice, and tumor growth was monitored. While tumors formed by LNT-229 control cells expanded to a volume of 1 cm^3 within 65 days, tumors initiated by injection of FUBP1-deficient LNT-229 cells only grew to a size of about 650 mm^3 during the same time (Figure 19 (A)). Surprisingly, tumors formed by FUBP1-deficient U-87 MG cells expanded to a volume of 600 mm^3 within 35 days compared to U-87 MG control cells which formed tumors of a volume of 150 mm^3 during the same time period (Figure 19 (B)).

According to these results, downregulation of FUBP1 in the glioblastoma cell line LNT-229 reduces tumor cell expansion, while the same knockdown enhances expansion in U-87 MG cells in a xenograft mouse model as would have been predicted from the functional cell culture assays. Taken together, these results confirm that FUBP1 overexpression is required for growth of tumors formed by the glioblastoma cell line LNT-229 *in vivo*. Prof. Michal Mittelborn (Edinger Institute, Frankfurt) in his laboratory checked for mutational status of FUBP1 in glioblastoma cell line and primary glioblastomas. There were no mutations found in either of them (Personal Communication). This led us to conclude that in U-87 MG cells, FUBP1 might fulfill a special important function which differs from its role in LNT-229 cells.

Based on my results obtained in different glioblastoma cell lines, I conclude that FUBP1 executes its function depending on the cell line. Looking at the observed effects of TGFβ-1, MMP9 and MMP2, we put forward the following scheme to explain the molecular function of FUBP1 in different glioblastoma cell lines. In LNT-229 cells, upon *FUBP1* knockdown TGFβ-1 expression is reduced, which results in decreased MMP2 downstream activity and less cell proliferation, migration and tumor growth, while the apoptosis sensitivity in the cell is increased in the absence of FUBP1. However, in FUBP1-deficient U-87 MG cells there is increased TGFβ-1 expression which enhances MMP2 downstream activity, leading to increased proliferation, migration, enhanced tumor growth and reduced apoptosis sensitivity.

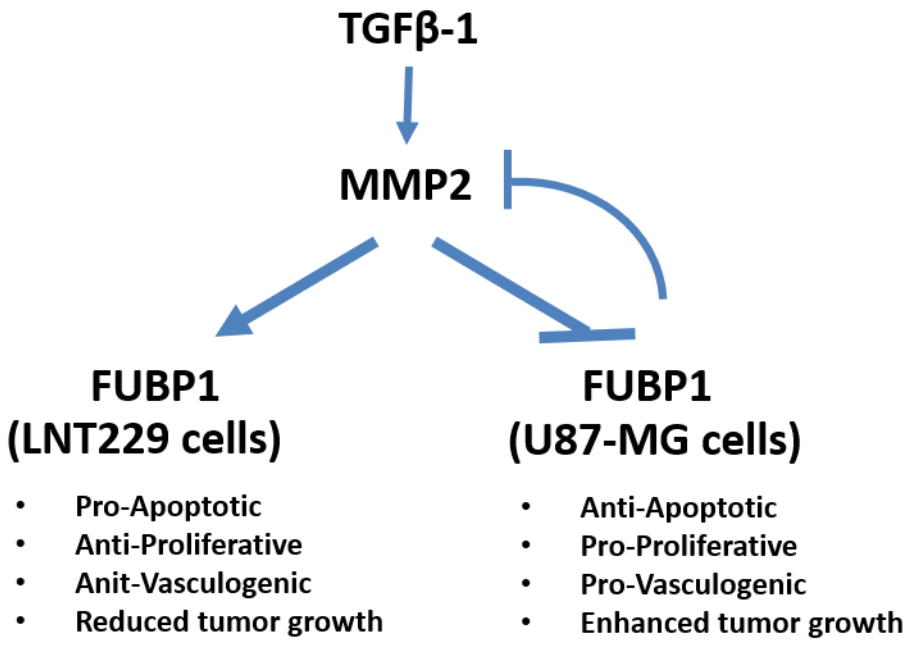

5. References

1. Adamson, C., O. O. Kanu, A. I. Mehta, C. Di, N. Lin, A. K. Mattox and D. D. Bigner (2009). "Glioblastoma multiforme: a review of where we have been and where we are going." Expert Opin Investig Drugs **18**(8): 1061-1083.
2. Ambros, V. (2004). "The functions of animal microRNAs." Nature **431**(7006): 350-355.
3. Aranapakam, V., G. T. Grosu, J. M. Davis, B. Hu, J. Ellingboe, J. L. Baker, J. S. Skotnicki, A. Zask, J. F. DiJoseph, A. Sung, M. A. Sharr, L. M. Killar, T. Walter, G. Jin and R. Cowling (2003). "Synthesis and structure-activity relationship of alpha-sulfonylhydroxamic acids as novel, orally active matrix metalloproteinase inhibitors for the treatment of osteoarthritis." J Med Chem **46**(12): 2361-2375.
4. Aravalli, R. N., C. J. Steer and E. N. Cressman (2008). "Molecular mechanisms of hepatocellular carcinoma." Hepatology **48**(6): 2047-2063.
5. Avigan, M. I., B. Strober and D. Levens (1990). "A far upstream element stimulates c-myc expression in undifferentiated leukemia cells." J Biol Chem **265**(30): 18538-18545.
6. Bader, A. G., D. Brown and M. Winkler (2010). "The promise of microRNA replacement therapy." Cancer Res **70**(18): 7027-7030.
7. Bala, S., M. Marcos and G. Szabo (2009). "Emerging role of microRNAs in liver diseases." World J Gastroenterol **15**(45): 5633-5640.
8. Bartel, D. P. (2009). "MicroRNAs: target recognition and regulatory functions." Cell **136**(2): 215-233.
9. Bellail, A. C., S. B. Hunter, D. J. Brat, C. Tan and E. G. Van Meir (2004). "Microregional extracellular matrix heterogeneity in brain modulates glioma cell invasion." Int J Biochem Cell Biol **36**(6): 1046-1069.
10. Bennett, M. C. (2005). "The role of alpha-synuclein in neurodegenerative diseases." Pharmacol Ther **105**(3): 311-331.
11. Bettegowda, C., N. Agrawal, Y. Jiao, M. Sausen, L. D. Wood, R. H. Hruban, F. J. Rodriguez, D. P. Cahill, R. McLendon, G. Riggins, V. E. Velculescu, S. M. Oba-Shinjo, S. K. Marie, B. Vogelstein, D. Bigner, H. Yan, N. Papadopoulos and K. W. Kinzler (2011). "Mutations in CIC and FUBP1 contribute to human oligodendroglioma." Science **333**(6048): 1453-1455.
12. Bouchireb, N. and M. S. Clark (1999). "Human FUSE binding protein 3 gene (FBP3). Map position 9q33-34.1." Chromosome Res **7**(7): 577.
13. Brew, K., D. Dinakarpandian and H. Nagase (2000). "Tissue inhibitors of metalloproteinases: evolution, structure and function." Biochim Biophys Acta **1477**(1-2): 267-283.
14. Bruix, J., M. Sherman and D. American Association for the Study of Liver (2011). "Management of hepatocellular carcinoma: an update." Hepatology **53**(3): 1020-1022.
15. Budhu, A., H. L. Jia, M. Forgues, C. G. Liu, D. Goldstein, A. Lam, K. A. Zanetti, Q. H. Ye, L. X. Qin, C. M. Croce, Z. Y. Tang and X. W. Wang (2008). "Identification of metastasis-related microRNAs in hepatocellular carcinoma." Hepatology **47**(3): 897-907.
16. Chen, X., Y. Ba, L. Ma, X. Cai, Y. Yin, K. Wang, J. Guo, Y. Zhang, J. Chen, X. Guo, Q. Li, X. Li, W. Wang, Y. Zhang, J. Wang, X. Jiang, Y. Xiang, C. Xu, P. Zheng, J. Zhang, R. Li, H. Zhang, X. Shang, T. Gong, G. Ning, J. Wang, K. Zen, J. Zhang and C. Y. Zhang (2008). "Characterization of microRNAs in serum: a novel class of biomarkers for diagnosis of cancer and other diseases." Cell Res **18**(10): 997-1006.

17. Chung, H. J., J. Liu, M. Dundr, Z. Nie, S. Sanford and D. Levens (2006). "FBPs are calibrated molecular tools to adjust gene expression." Mol Cell Biol **26**(17): 6584-6597.
18. Davis-Smyth, T., R. C. Duncan, T. Zheng, G. Michelotti and D. Levens (1996). "The far upstream element-binding proteins comprise an ancient family of single-strand DNA-binding transactivators." J Biol Chem **271**(49): 31679-31687.
19. Delpech, B., C. Maingonnat, N. Girard, C. Chauzy, R. Maunoury, A. Olivier, J. Tayot and P. Creissard (1993). "Hyaluronan and hyaluronectin in the extracellular matrix of human brain tumour stroma." Eur J Cancer **29A**(7): 1012-1017.
20. Dreger, M. (2003). "Emerging strategies in mass-spectrometry based proteomics." Eur J Biochem **270**(4): 569.
21. Duncan, R., L. Bazar, G. Michelotti, T. Tomonaga, H. Krutzsch, M. Avigan and D. Levens (1994). "A sequence-specific, single-strand binding protein activates the far upstream element of c-myc and defines a new DNA-binding motif." Genes Dev **8**(4): 465-480.
22. Folkman, J. and Y. Shing (1992). "Angiogenesis." J Biol Chem **267**(16): 10931-10934.
23. Forner, A., J. M. Llovet and J. Bruix (2012). "Hepatocellular carcinoma." Lancet **379**(9822): 1245-1255.
24. Fukuda, S., T. Itamoto, H. Nakahara, T. Kohashi, H. Ohdan, H. Hino, M. Ochi, H. Tashiro and T. Asahara (2005). "Clinicopathologic features and prognostic factors of resected solitary small-sized hepatocellular carcinoma." Hepatogastroenterology **52**(64): 1163-1167.
25. Gherzi, R., K. Y. Lee, P. Briata, D. Wegmuller, C. Moroni, M. Karin and C. Y. Chen (2004). "A KH domain RNA binding protein, KSRP, promotes ARE-directed mRNA turnover by recruiting the degradation machinery." Mol Cell **14**(5): 571-583.
26. Harburger, D. S. and D. A. Calderwood (2009). "Integrin signalling at a glance." J Cell Sci **122**(Pt 2): 159-163.
27. Hartmann, C., J. Meyer, J. Balss, D. Capper, W. Mueller, A. Christians, J. Felsberg, M. Wolter, C. Mawrin, W. Wick, M. Weller, C. Herold-Mende, A. Unterberg, J. W. Jeuken, P. Wesseling, G. Reifenberger and A. von Deimling (2009). "Type and frequency of IDH1 and IDH2 mutations are related to astrocytic and oligodendroglial differentiation and age: a study of 1,010 diffuse gliomas." Acta Neuropathol **118**(4): 469-474.
28. He, L., A. Weber and D. Levens (2000). "Nuclear targeting determinants of the far upstream element binding protein, a c-myc transcription factor." Nucleic Acids Res **28**(22): 4558-4565.
29. Hinsdale, I. (2010). "Primary brain and central nervous system tumors diagnosed in the united states in 2004-2006."
30. Hinsdale, I. (2011). "Primary brain and central nervous system tumors diagnosed in the United States in 2004-2007." Central Brain Tumor Registry of the United States.
31. Hoglund, A., K. Odelius, M. Hakkarainen and A. C. Albertsson (2007). "Controllable degradation product migration from cross-linked biomedical polyester-ethers through predetermined alterations in copolymer composition." Biomacromolecules **8**(6): 2025-2032.
32. Hsiao, H. H., A. Nath, C. Y. Lin, E. J. Folta-Stogniew, E. Rhoades and D. T. Braddock (2010). "Quantitative characterization of the interactions among c-myc transcriptional regulators FUSE, FBP, and FIR." Biochemistry **49**(22): 4620-4634.
33. Huang, S. and X. He (2011). "The role of microRNAs in liver cancer progression." Br J Cancer **104**(2): 235-240.

34. Hung, C. H., C. H. Chen, C. M. Lee, T. H. Hu, S. N. Lu, J. H. Wang and C. M. Huang (2013). "Role of viral genotypes and hepatitis B viral mutants in the risk of hepatocellular carcinoma associated with hepatitis B and C dual infection." Intervirology **56**(5): 316-324.
35. Jarvelainen, H., A. Sainio, M. Koulu, T. N. Wight and R. Penttinen (2009). "Extracellular matrix molecules: potential targets in pharmacotherapy." Pharmacol Rev **61**(2): 198-223.
36. Kanu, O. O., B. Hughes, C. Di, N. Lin, J. Fu, D. D. Bigner, H. Yan and C. Adamson (2009). "Glioblastoma Multiforme Oncogenomics and Signaling Pathways." Clin Med Oncol **3**: 39-52.
37. Kelley, S. K. and A. Ashkenazi (2004). "Targeting death receptors in cancer with Apo2L/TRAIL." Curr Opin Pharmacol **4**(4): 333-339.
38. Kelly, K. A., J. M. Kirkwood and D. S. Kapp (1984). "Glioblastoma multiforme: pathology, natural history and treatment." Cancer Treat Rev **11**(1): 1-26.
39. Krutzfeldt, J., S. Kuwajima, R. Braich, K. G. Rajeev, J. Pena, T. Tuschl, M. Manoharan and M. Stoffel (2007). "Specificity, duplex degradation and subcellular localization of antagomirs." Nucleic Acids Res **35**(9): 2885-2892.
40. Lasserre, J. P., F. Fack, D. Revets, S. Planchon, J. Renaut, L. Hoffmann, A. C. Gutleb, C. P. Muller and T. Bohn (2009). "Effects of the endocrine disruptors atrazine and PCB 153 on the protein expression of MCF-7 human cells." J Proteome Res **8**(12): 5485-5496.
41. Law, P. T. and N. Wong (2011). "Emerging roles of microRNA in the intracellular signaling networks of hepatocellular carcinoma." J Gastroenterol Hepatol **26**(3): 437-449.
42. Lee, R. C., R. L. Feinbaum and V. Ambros (1993). "The C. elegans heterochronic gene lin-4 encodes small RNAs with antisense complementarity to lin-14." Cell **75**(5): 843-854.
43. Leitinger, B. and E. Hohenester (2007). "Mammalian collagen receptors." Matrix Biol **26**(3): 146-155.
44. Lim, L. P., N. C. Lau, P. Garrett-Engele, A. Grimson, J. M. Schelter, J. Castle, D. P. Bartel, P. S. Linsley and J. M. Johnson (2005). "Microarray analysis shows that some microRNAs downregulate large numbers of target mRNAs." Nature **433**(7027): 769-773.
45. Liu, J., S. Akoulitchev, A. Weber, H. Ge, S. Chuikov, D. Libutti, X. W. Wang, J. W. Conaway, C. C. Harris, R. C. Conaway, D. Reinberg and D. Levens (2001). "Defective interplay of activators and repressors with TFIH in xeroderma pigmentosum." Cell **104**(3): 353-363.
46. Louis, D. N., H. Ohgaki, O. D. Wiestler, W. K. Cavenee, P. C. Burger, A. Jouvet, B. W. Scheithauer and P. Kleihues (2007). "The 2007 WHO classification of tumours of the central nervous system." Acta Neuropathol **114**(2): 97-109.
47. Maes, O. C., H. M. Chertkow, E. Wang and H. M. Schipper (2009). "MicroRNA: Implications for Alzheimer Disease and other Human CNS Disorders." Curr Genomics **10**(3): 154-168.
48. Mahesparan, R., T. A. Read, M. Lund-Johansen, K. O. Skaftnesmo, R. Bjerkvig and O. Engebraaten (2003). "Expression of extracellular matrix components in a highly infiltrative in vivo glioma model." Acta Neuropathol **105**(1): 49-57.
49. Malz, M., A. Weber, S. Singer, V. Riehmer, M. Bissinger, M. O. Riener, T. Longerich, C. Soll, A. Vogel, P. Angel, P. Schirmacher and K. Breuhahn (2009). "Overexpression of far upstream element binding proteins: a mechanism regulating proliferation and migration in liver cancer cells." Hepatology **50**(4): 1130-1139.

50. Massague, J. (1990). "The transforming growth factor-beta family." Annu Rev Cell Biol **6**: 597-641.
51. Matsushita, K., T. Kajiwara, S. Itoga, M. Satoh, K. Sogawa, H. Umemura, S. Sawai, M. Nishimura, M. Tamura, N. Tanaka, H. Shimada, T. Tomonaga and F. Nomura (2009). "[Clinical application of alternative splicing form of c-myc suppressor FUSE-binding protein-interacting repressor for cancer detection and treatment]." Rinsho Byori **57**(12): 1151-1158.
52. Matsushita, K., T. Tomonaga, H. Shimada, A. Shioya, M. Higashi, H. Matsubara, K. Harigaya, F. Nomura, D. Libutti, D. Levens and T. Ochiai (2006). "An essential role of alternative splicing of c-myc suppressor FUSE-binding protein-interacting repressor in carcinogenesis." Cancer Res **66**(3): 1409-1417.
53. Maxon, M. E., J. A. Goodrich and R. Tjian (1994). "Transcription factor IIE binds preferentially to RNA polymerase IIa and recruits TFIIH: a model for promoter clearance." Genes Dev **8**(5): 515-524.
54. McCawley, L. J. and L. M. Matrisian (2001). "Matrix metalloproteinases: they're not just for matrix anymore!" Curr Opin Cell Biol **13**(5): 534-540.
55. Michelotti, G. A., E. F. Michelotti, A. Pullner, R. C. Duncan, D. Eick and D. Levens (1996). "Multiple single-stranded cis elements are associated with activated chromatin of the human c-myc gene in vivo." Mol Cell Biol **16**(6): 2656-2669.
56. Milosevic, J., P. Bulau, E. Mortz and O. Eickelberg (2009). "Subcellular fractionation of TGF-beta1-stimulated lung epithelial cells: a novel proteomic approach for identifying signaling intermediates." Proteomics **9**(5): 1230-1240.
57. Mitchell, P. S., R. K. Parkin, E. M. Kroh, B. R. Fritz, S. K. Wyman, E. L. Pogosova-Agadjanyan, A. Peterson, J. Noteboom, K. C. O'Briant, A. Allen, D. W. Lin, N. Urban, C. W. Drescher, B. S. Knudsen, D. L. Stirewalt, R. Gentleman, R. L. Vessella, P. S. Nelson, D. B. Martin and M. Tewari (2008). "Circulating microRNAs as stable blood-based markers for cancer detection." Proc Natl Acad Sci U S A **105**(30): 10513-10518.
58. Nakasa, T., Y. Nagata, K. Yamasaki and M. Ochi (2011). "A mini-review: microRNA in arthritis." Physiol Genomics **43**(10): 566-570.
59. O'Reilly, M. S. (1997). "Angiostatin: an endogenous inhibitor of angiogenesis and of tumor growth." EXS **79**: 273-294.
60. O'Reilly, M. S., L. Holmgren, Y. Shing, C. Chen, R. A. Rosenthal, M. Moses, W. S. Lane, Y. Cao, E. H. Sage and J. Folkman (1994). "Angiostatin: a novel angiogenesis inhibitor that mediates the suppression of metastases by a Lewis lung carcinoma." Cell **79**(2): 315-328.
61. Ohgaki, H. and P. Kleihues (2007). "Genetic pathways to primary and secondary glioblastoma." Am J Pathol **170**(5): 1445-1453.
62. Otsuka, M., T. Kishikawa, T. Yoshikawa, M. Ohno, A. Takata, C. Shibata and K. Koike (2014). "The role of microRNAs in hepatocarcinogenesis: current knowledge and future prospects." J Gastroenterol **49**(2): 173-184.
63. Overall, C. M., J. L. Wrana and J. Sodek (1991). "Transcriptional and post-transcriptional regulation of 72-kDa gelatinase/type IV collagenase by transforming growth factor-beta 1 in human fibroblasts. Comparisons with collagenase and tissue inhibitor of matrix metalloproteinase gene expression." J Biol Chem **266**(21): 14064-14071.
64. Patterson, B. C. and Q. A. Sang (1997). "Angiostatin-converting enzyme activities of human matrilysin (MMP-7) and gelatinase B/type IV collagenase (MMP-9)." J Biol Chem **272**(46): 28823-28825.
65. Platten, M., W. Wick and M. Weller (2001). "Malignant glioma biology: role for TGF-beta in growth, motility, angiogenesis, and immune escape." Microsc Res Tech **52**(4): 401-410.

66. Poon, R. T. and S. T. Fan (2004). "Hepatectomy for hepatocellular carcinoma: patient selection and postoperative outcome." Liver Transpl **10**(2 Suppl 1): S39-45.
67. Puduvalli, V. K., D. Sampath, J. M. Bruner, J. Nangia, R. Xu and A. P. Kyritsis (2005). "TRAIL-induced apoptosis in gliomas is enhanced by Akt-inhibition and is independent of JNK activation." Apoptosis **10**(1): 233-243.
68. Qu, K. Z., K. Zhang, H. Li, N. H. Afdhal and M. Albitar (2011). "Circulating microRNAs as biomarkers for hepatocellular carcinoma." J Clin Gastroenterol **45**(4): 355-360.
69. Rabenhorst, U., R. Beinoraviciute-Kellner, M. L. Brezniceanu, S. Joos, F. Devens, P. Lichter, R. J. Rieker, J. Trojan, H. J. Chung, D. L. Levens and M. Zornig (2009). "Overexpression of the far upstream element binding protein 1 in hepatocellular carcinoma is required for tumor growth." Hepatology **50**(4): 1121-1129.
70. Rabenhorst U, Z. M. (2010). FUSE Binding Protein 1 as a Regulator of Tumorigenesis and Embryonic Development. PhD PhD, Goethe University.
71. Rao, J. S. (2003). "Molecular mechanisms of glioma invasiveness: the role of proteases." Nat Rev Cancer **3**(7): 489-501.
72. Rao, J. S., P. A. Steck, S. Mohanam, W. G. Stetler-Stevenson, L. A. Liotta and R. Sawaya (1993). "Elevated levels of M(r) 92,000 type IV collagenase in human brain tumors." Cancer Res **53**(10 Suppl): 2208-2211.
73. Raspollini, M. R., F. Castiglione, D. Rossi Degl'Innocenti, F. Garbini, M. E. Coccia and G. L. Taddei (2005). "Difference in expression of matrix metalloproteinase-2 and matrix metalloproteinase-9 in patients with persistent ovarian cysts." Fertil Steril **84**(4): 1049-1052.
74. Risau, W. (1997). "Mechanisms of angiogenesis." Nature **386**(6626): 671-674.
75. Roberts, A. B., U. I. Heine, K. C. Flanders and M. B. Sporn (1990). "Transforming growth factor-beta. Major role in regulation of extracellular matrix." Ann N Y Acad Sci **580**: 225-232.
76. Rooprai, H. K., G. J. Rucklidge, C. Panou and G. J. Pilkington (2000). "The effects of exogenous growth factors on matrix metalloproteinase secretion by human brain tumour cells." Br J Cancer **82**(1): 52-55.
77. Rozario, T. and D. W. DeSimone (2010). "The extracellular matrix in development and morphogenesis: a dynamic view." Dev Biol **341**(1): 126-140.
78. Ruoslahti, E. (1996). "Brain extracellular matrix." Glycobiology **6**(5): 489-492.
79. Sahm, F., C. Koelsche, J. Meyer, S. Pusch, K. Lindenberg, W. Mueller, C. Herold-Mende, A. von Deimling and C. Hartmann (2012). "CIC and FUBP1 mutations in oligodendrogliomas, oligoastrocytomas and astrocytomas." Acta Neuropathol **123**(6): 853-860.
80. Salamonsen, L. A. (1994). "Matrix metalloproteinases and endometrial remodelling." Cell Biol Int **18**(12): 1139-1144.
81. Salo, T., J. G. Lyons, F. Rahemtulla, H. Birkedal-Hansen and H. Larjava (1991). "Transforming growth factor-beta 1 up-regulates type IV collagenase expression in cultured human keratinocytes." J Biol Chem **266**(18): 11436-11441.
82. Sato, F., S. Tsuchiya, S. J. Meltzer and K. Shimizu (2011). "MicroRNAs and epigenetics." FEBS J **278**(10): 1598-1609.
83. Schmidt, S. and P. Friedl (2010). "Interstitial cell migration: integrin-dependent and alternative adhesion mechanisms." Cell Tissue Res **339**(1): 83-92.
84. Schwartz, M., S. Roayaie and M. Konstadoulakis (2007). "Strategies for the management of hepatocellular carcinoma." Nat Clin Pract Oncol **4**(7): 424-432.
85. Schwartzbaum, J. A., J. L. Fisher, K. D. Aldape and M. Wrensch (2006). "Epidemiology and molecular pathology of glioma." Nat Clin Pract Neurol **2**(9): 494-503; quiz 491 p following 516.

86. Shingleton, W. D., D. J. Hodges, P. Brick and T. E. Cawston (1996). "Collagenase: a key enzyme in collagen turnover." Biochem Cell Biol **74**(6): 759-775.
87. Singer, S., M. Malz, E. Herpel, A. Warth, M. Bissinger, M. Keith, T. Muley, M. Meister, H. Hoffmann, R. Penzel, G. Gdynia, V. Ehemann, P. A. Schnabel, R. Kuner, P. Huber, P. Schirmacher and K. Breuhahn (2009). "Coordinated expression of stathmin family members by far upstream sequence element-binding protein-1 increases motility in non-small cell lung cancer." Cancer Res **69**(6): 2234-2243.
88. Sinkkonen, L., T. Hugenschmidt, P. Berninger, D. Gaidatzis, F. Mohn, C. G. Artus-Revel, M. Zavolan, P. Svoboda and W. Filipowicz (2008). "MicroRNAs control de novo DNA methylation through regulation of transcriptional repressors in mouse embryonic stem cells." Nat Struct Mol Biol **15**(3): 259-267.
89. Stupp, R., W. P. Mason, M. J. van den Bent, M. Weller, B. Fisher, M. J. Taphoorn, K. Belanger, A. A. Brandes, C. Marosi, U. Bogdahn, J. Curschmann, R. C. Janzer, S. K. Ludwin, T. Gorlia, A. Allgeier, D. Lacombe, J. G. Cairncross, E. Eisenhauer, R. O. Mirimanoff, R. European Organisation for, T. Treatment of Cancer Brain, G. Radiotherapy and G. National Cancer Institute of Canada Clinical Trials (2005). "Radiotherapy plus concomitant and adjuvant temozolomide for glioblastoma." N Engl J Med **352**(10): 987-996.
90. Tsang, K. Y., M. C. Cheung, D. Chan and K. S. Cheah (2010). "The developmental roles of the extracellular matrix: beyond structure to regulation." Cell Tissue Res **339**(1): 93-110.
91. Tysnes, B. B., R. Mahesparan, F. Thorsen, H. K. Haugland, T. Porwol, P. O. Enger, M. Lund-Johansen and R. Bjerkvig (1999). "Laminin expression by glial fibrillary acidic protein positive cells in human gliomas." Int J Dev Neurosci **17**(5-6): 531-539.
92. Uhm, J. H., N. P. Dooley, J. G. Villemure and V. W. Yong (1997). "Mechanisms of glioma invasion: role of matrix-metalloproteinases." Can J Neurol Sci **24**(1): 3-15.
93. Ulrich, T. A., E. M. de Juan Pardo and S. Kumar (2009). "The mechanical rigidity of the extracellular matrix regulates the structure, motility, and proliferation of glioma cells." Cancer Res **69**(10): 4167-4174.
94. Valverde, R., L. Edwards and L. Regan (2008). "Structure and function of KH domains." FEBS J **275**(11): 2712-2726.
95. Venkatesan, A. M., J. M. Davis, G. T. Grosu, J. Baker, A. Zask, J. I. Levin, J. Ellingboe, J. S. Skotnicki, J. F. Dijoseph, A. Sung, G. Jin, W. Xu, D. J. McCarthy and D. Barone (2004). "Synthesis and structure-activity relationships of 4-alkynyloxy phenyl sulfanyl, sulfinyl, and sulfonyl alkyl hydroxamates as tumor necrosis factor-alpha converting enzyme and matrix metalloproteinase inhibitors." J Med Chem **47**(25): 6255-6269.
96. Wang, S. and W. S. El-Deiry (2003). "TRAIL and apoptosis induction by TNF-family death receptors." Oncogene **22**(53): 8628-8633.
97. Weber, A., I. Kristiansen, M. Johannsen, B. Oelrich, K. Scholmann, S. Gunia, M. May, H. A. Meyer, S. Behnke, H. Moch and G. Kristiansen (2008). "The FUSE binding proteins FBP1 and FBP3 are potential c-myc regulators in renal, but not in prostate and bladder cancer." BMC Cancer **8**: 369.
98. Welzel, T. M., B. I. Graubard, S. Zeuzem, H. B. El-Serag, J. A. Davila and K. A. McGlynn (2011). "Metabolic syndrome increases the risk of primary liver cancer in the United States: a study in the SEER-Medicare database." Hepatology **54**(2): 463-471.
99. Xu, S. G., P. J. Yan and Z. M. Shao (2010). "Differential proteomic analysis of a highly metastatic variant of human breast cancer cells using two-dimensional differential gel electrophoresis." J Cancer Res Clin Oncol **136**(10): 1545-1556.

100. Yu, M. W. and C. J. Chen (1994). "Hepatitis B and C viruses in the development of hepatocellular carcinoma." Crit Rev Oncol Hematol **17**(2): 71-91.
101. Yuen, M. F., C. C. Cheng, I. J. Lauder, S. K. Lam, C. G. Ooi and C. L. Lai (2000). "Early detection of hepatocellular carcinoma increases the chance of treatment: Hong Kong experience." Hepatology **31**(2): 330-335.
102. Zhang, J. and Q. M. Chen (2013). "Far upstream element binding protein 1: a commander of transcription, translation and beyond." Oncogene **32**(24): 2907-2916.
103. Zhang, Z., D. Harris and V. N. Pandey (2008). "The FUSE binding protein is a cellular factor required for efficient replication of hepatitis C virus." J Virol **82**(12): 5761-5773.
104. Zubaidah, R. M., G. S. Tan, S. B. Tan, S. G. Lim, Q. Lin and M. C. Chung (2008). "2-D DIGE profiling of hepatocellular carcinoma tissues identified isoforms of far upstream binding protein (FUBP) as novel candidates in liver carcinogenesis." Proteomics **8**(23-24): 5086-5096.

6. Ehrenwörtliche Erklärung

Ich erkläre hiermit ehrenwörtlich, dass ich die vorliegende Arbeit entsprechend den Regeln guter wissenschaftlicher Praxis selbstständig und ohne unzulässige Hilfe Dritter angefertigt habe.

Sämtliche aus fremden Quellen direkt oder indirekt übernommenen Gedanken sowie sämtliche von Anderen direkt oder indirekt übernommenen Daten, Techniken und Materialien sind als solche kenntlich gemacht. Die Arbeit wurde bisher bei keiner anderen Hochschule zu Prüfungszwecken eingereicht.

Darmstadt, den ……

.....

7. Curriculum Vitae

ADDRESS

Mr. Venkatesh Kolluru
Günther Str. 7
Frankfurt am Main
60528 Germany

TELEPHONE

+49 (0) 17631166493

EMAIL

kolluru.venkatesh1508@gmail.com

DATE OF BIRTH

September 8, 1987

VENKATESH KOLLURU

Diligent Research Scholar with 4+ Years of Experience in the field of Oncology Keen to Further Utilize His Functional and Strong Interpersonal Skills to Contribute to Science

PROFESSIONAL EXPERIENCE

09/2011- PRESENT **PhD Student** **Frankfurt am Main, Germany**
Georg Speyer Haus

- Investigated the oncogenic role of FUBP1 in Glioblastoma
- Investigated the role of miRNAs in regulating the expression of FUBP1 in Hepatocellular Carcinoma (HCC)

08/2010 - 04/2011 **Honorary Researcher** **Manchester, UK**
PRSR, The University of Manchester

- Worked on the role of Notch signalling in keloid pathogenesis (project was selected for young investigation award 2011 in wound repair and regeneration society at Texas, USA)
- Tested the effect of Xiaflex (Collagenase) drug on Dupuytren Disease in collaboration with AstraZeneca

02/2010 – 06/2010 **Research Technician** **Manchester, UK**
MIB, The University of Manchester & Lonza

- Tested the efficacy of NVoy polymer N10 in protecting the proteins and enzymes form denaturation
- Tested the folding pattern of various proteins and enzymes with NVoy polymer using CD spectroscopy

PUBLICATIONS

1. Pellegrino R, Calvisi DF, Neumann O, **Kolluru V**, Wesely J, Chen X, Wang C, Wuestefeld T, Ladu S, Elgohary N, Bermejo JL, Radlwimmer B, Zörnig M, Zender L, Dombrowski F, Evert M, Schirmacher P, Longerich T. EEF1A2 inactivates p53 via PI3K/AKT/mTOR-dependent stabilization of MDM4 in hepatocellular carcinoma. Hepatology. 2013 Nov 28. doi: 10.1002/hep.26954
2. Baumgarten P, Harter PN, Tönjes M, Capper D, Blank AE, Sahm F, von Deimling A, **Kolluru V**, Schwamb B, Rabenhorst U, Starzetz T, Kögel D, Rieker RJ, Plate KH, Ohgaki H, Radlwimmer B, Zörnig M, Mittelbronn M. Loss of FUBP1 expression in gliomas predicts FUBP1 mutation and is associated with oligodendroglial differentiation, IDH1 mutation and 1p/19q loss of heterozygosity. Neuropathol Appl Neurobiol. 2013 Oct 3. doi: 10.1111/nan.12088

COMPUTER SKILLS

Microsoft Office (Word, Excel & PowerPoint)

LANGUAGES

English: C2/Business Fluent

Deutsch: Elementary Proficiency (A1)

SKYPE ID

venki1508

PUBLIC PROFILE

de.linkedin.com/pub/venkatesh-kolluru/17/855/4a4

3. Iqbal SA, Manning C, Syed F, **Kolluru V**, Hayton M, Watson S, Bayat A. Identification of mesenchymal stem cells in perinodular fat and skin in Dupuytren's disease: a potential source of myofibroblasts with implications for pathogenesis and therapy. Stem Cells Dev. 2012 Mar 1;21(4):609-22. doi: 10.1089/scd.2011.0140. Epub 2011 Jul 19
4. Syed F, Thomas AN, Singh S, **Kolluru V**, Emeigh Hart SG, Bayat A. In vitro study of novel collagenase (XIAFLEX®) on Dupuytren's disease fibroblasts displays unique drug related properties. PLoS One. 2012;7(2):e31430. doi: 10.1371/journal.pone.0031430. Epub 2012 Feb 24

EDUCATION

2011 - PRESENT	**Technical University** PhD in Oncology	**Darmstadt, Germany**
2008 - 2009	**University of Abertay Dundee** Masters in Biotechnology	**Dundee, Scotland**
2005 - 2008	**Andhra University** Bachelors in Biotechnology	**Visakhapatnam, India**

CONFERENCES & SEMINARS

- Poster presentation at New Cancer Targets Conference 2013, Heidelberg
- Poster presentation at University-Center for Tumor Diseases Conference 2012, 2013 & 2014 Frankfurt am Main

HONORS & AWARDS

- Received DAAD-SIEMENS Scholarship in 2011 for pursuing PhD
- Research work got selected for the Young Investigation Award 2011 at wound healing society, USA

8. Acknowledgement

Completion of this doctoral dissertation was possible with the support of several people. I would like to express my sincere gratitude to all of them. First of all, I am extremely grateful to my research guide Prof. Dr. Martin Zörnig, George Speyer Haus, Frankfurt for his valuable guidance, scholarly inputs and consistent encouragement that I received throughout the research work. This achievement was possible only because of the unconditional support provided by him. With friendly and positive attitude, Dr. Zörnig has always made himself available to clarify my doubts despite his busy schedules and I consider it as a great opportunity to accomplish my doctoral programme under his guidance and to learn from his research expertise.

I would like to thank DAAD and SIEMENS for providing funding throughout my PhD and helped successfully complete my PhD on time. I would also like to thank Prof. Dr. Beatrix Süß, Department of Biology, TU Darmstadt, for her immense support in the thesis as well as for the ongoing care as a co-supervisor. I thank Prof. Dr. Michel Mittelborn, Edinger Institute, Frankfurt, for his support, collaboration and intellectual discussions during the project. A special thanks to Prof. Dr. Winfred Wels laboratory for providing the glioblastoma cell lines for my research. Also a special thanks to the current and former colleagues of AG Zörnig who always maintained a friendly atmosphere. In particular, I would like to thank Dr. Bettina Schwamb for the great help in the xenograft experiments and Sussane who has been the most important pillar of Zörnig's lab and helped me in the laboratory always these years. I thank Katha for her time, knowledge and support in analyzing results and scientific discussions every time without any hesitation since my joining. Many thanks to Marek, Josy, Dr. Sabrina Hosseini and Steffi for their support during the experiments. Above all, I would like to thank everyone for their friendship. They all made my work even easier.

The faculty members of the Institute have been very kind enough to extend their help at various phases of research, whenever I approached them and I do hereby acknowledge all of them. The thesis would not have come to a successful completion, without the help I received from the IT staff.

I owe a lot to my parents who encouraged and helped me at every stage of my life and longed to see this achievement come true. I would also like to thank my in-laws for their moral support all these years. Thanks to my sister Kiranmayee for her suggestions and fruitful discussions throughout the journey. Last but not the least, a very special thanks to my wife Leena for supporting me in every aspect of my life personally and professionally. She has been a great asset to me.